JOSEPH ROSSABI.
A FIBER OPTIC SPECTROSCOPIC ANALYSIS OF DIURON SORPTION/DESORPTION PROCESSES IN SUBSURFACE MEDIA.
UNDER THE DIRECTION OF CASS T. MILLER.

ABSTRACT

The quantitative assessment of sorption and desorption processes is vital to the complete understanding of contaminant fate and transport in the subsurface. The sorption and desorption of a synthetic organic pesticide, diuron, was studied by optical ultraviolet (UV) absorption spectroscopy in two configurations. The first utilized the "grab sample" method and a conventional laboratory benchtop UV/VIS spectrophotometer, and the second employed a fiber optic spectrophotometer.

The "grab sample" method is susceptible to systematic errors related to the removal of the sample from the subsurface system for analysis. Fiber optic spectrophotometry has the potential for noninvasive, nondestructive measurements obtained within the subsurface media.

The hypothesis of this work was that fiber optic spectrophotometry can be used to determine the fate and transport of a pesticide in laboratory systems of subsurface media, using a one dimensional column configuration.

The results of this research demonstrate that fiber optic spectroscopic methods can be used for one-dimensional subsurface media column sorption/desorption and tracer experiments under the conditions used in this study. In addition, sorption kinetic experiments indicate that equilibrium conditions are not attained after 140 days of equilibration. Data from equilibrium distribution experiments support this conclusion.

ACKNOWLEDGEMENTS

I would like to thank the members of my committee, Dr. Cass T. Miller, Dr. Michael D. Aitken, and Dr. Philip C. Singer for their helpful comments and suggestions. In addition, I would like to thank my advisor, Dr. Miller, for giving me the opportunity to perform this research. Thanks are due to Joe Pedit who was my laboratory mentor. This work was made possible by grants from the United States Geological Survey and the Water Resources Research Institute of North Carolina. Of course, thanks to Terry for everything, again.

TABLE OF CONTENTS

LIST OF TABLES

LIST OF FIGURES

I INTRODUCTION

1.1 Overview

Approximately one half of the population of the United States uses ground water for drinking (Schiffman, 1988). It is therefore important to be able to discriminate and quantify the factors affecting the quality of this resource.

Over the past century, much progress has been made in the areas of chemical synthesis and the use of these chemicals in industry and agriculture. Unfortunately, this has not been accompanied by equal progress in the knowledge of the relation between synthetic chemicals and the natural environment. As a result, some of these synthetic chemicals such as organic solvents, pesticides, and herbicides have contaminated otherwise pristine subsurface environments because of improper disposal or application practices. The health risks of some of these contaminants are just beginning to be understood. Therefore, humans are currently faced with environmental problems left to them by their forbearers.

Understanding the flow and transport of contaminants in the subsurface is vital to a complete knowledge of ground

water quality. Determining contaminant concentration requires chemical analysis. Techniques for the chemical analysis of subsurface contaminants have traditionally relied on the "grab sample" method. In this method, a solid, liquid, or vapor phase sample is obtained at a particular point in the subsurface region and brought into the laboratory for analysis. This method induces many chances for systematic errors, including: the changing of the environment to physically obtain the sample; removal of the sample from its original environment; transportation of the sample in another environment; and analysis in a different environment. All of these may affect the sample or the assessment of the contaminant concentration in that sample. The ideal measurement would accurately assess the contaminant concentration without affecting the contaminant, the sample, or its environment.

1.2 Optical Spectroscopy

Since the advent of quantum mechanics, the basic principles of atomic and molecular spectra have not changed (Patterson, 1987). Spectroscopy, the study of spectra, has been used to identify atoms, molecules, and their associated structures and environments. This is done by analyzing the wavelength and intensity of the radiation emitted, absorbed, or scattered by these atoms and molecules under known

known external electromagnetic conditions often take the form of a probe wave that is made to interact with the structure of interest.

There are various types of spectroscopic techniques commonly in use. These are categorized according to the characteristics of the probe wave used and the type of interaction between the probe wave and the analyte. Optical spectroscopy uses an electromagnetic wave in the region from the low ultraviolet (less than 200 nm) to the far infrared (greater than 10,000 nm) as the probe. The types of interactions exploited with optical spectroscopy are of three basic types: absorption, elastic and inelastic scattering, and luminescence. All three have been successfully used in chemical analysis.

1.3 In Situ Measurements

Although the use of optical spectroscopy for chemical and physical analysis has been well established over the past century it has generally lacked the mobility necessary to do analysis outside of a structured laboratory environment. This problem is not limited to optical techniques but is common to most other chemical analytical procedures as well. The problem of analysis in the natural environment, or in situ, is crucial to a more complete

understanding of real world chemical, physical, and biological processes.

Performing chemical analysis requires the isolation of a measurable parameter of interest by controlling the variables associated with that parameter. Analytical techniques achieve this by the selectivity and operational control of the probe and detector as well as by the measurement of ambient conditions such as temperature and pressure. Most analytical techniques require relatively large physical instrumentation and physically stable probes and detectors to accurately make these measurements. Because of the rigidity of the probe and detector configuration, a sample must be extracted from its natural environment and brought into the measurement field of the instrument. This changes the parameter's natural conditions and may introduce error in the measurement. In order to make accurate measurements in natural settings, an instrument's presence must minimally affect the measurement yet maintain a useful degree of accuracy. This is often very difficult to achieve because of the physical size limitations required to be noninvasive while maintaining the necessary components to maintain accuracy.

Optical spectroscopy has had the most success of the analytic techniques in making the transition from laboratory to in situ measurement for a number of reasons. One reason is that most optical spectroscopic techniques are non-

destructive, which enables relatively continuous measurements. Another reason for its success is the small size and conductivity of waveguides available for the medium. These high conductivity waveguides allow measurements to be made remotely from the probe generation and detection equipment. The small size of the waveguides allows relatively noninvasive measurements to be performed.

Since optical spectroscopy techniques operate by the modulation of a light beam, the size of the probe is limited only by the minimum diameter of light achievable. Single mode fibers have typical core diameters of 5-10 μm. With the progress made in recent years on light sources and optical fibers, probes can be made small enough to be non-intrusive to many of the measurements made of parameters in natural environments.

1.4 Pesticide Sorption/Desorption

Sorption/desorption effects have been found to be among the most significant factors affecting the fate and transport of synthetic organic contaminants in the subsurface (Weber and Miller, 1989). The mechanisms for these mass transfer processes is dependent on the contaminant's properties such as hydrophobicity (McCarty et al., 1981) and the type of media as well as other conditions such as the presence of other contaminants or natural

organic matter (NOM). Many different theoretical and mathematical formulations for quantifying the dominant factors in sorption and desorption processes have been postulated over the past years but none has been universally superior in the description of experimental data to the exclusion of the others in all cases (Brusseau and Rao, 1989b). A thorough understanding of the manifestation of sorption and desorption processes in subsurface media would allow better predictions of the spatio-temporal fate of contaminants.

1.5 Research Objectives

The main objective of this work was to investigate and evaluate a fiber optic spectroscopic technique for performing important environmental analyses. The general goal was the accurate assessment of the sorption and desorption parameters of a pesticide on a typical subsurface medium. The hypothesis of this work was that fiber optic spectrophotometry can be used to determine the fate and transport of a pesticide in laboratory subsurface media systems.

Proof of the experimental hypothesis would indicate that there is potential for in situ assessment of particular sorption/desorption behavior using a fiber optic spectrophotometric configuration. This will allow the

accurate determination of sorption/desorption effects and their contribution to contaminant fate and transport in laboratory configurations. Non-invasive techniques may also eventually aid in the clarification of the predominant theoretical driving forces of the sorption and desorption mechanisms.

II THEORY

2.1 Optical Spectroscopy

As mentioned in Section 1.2, there are three basic types of optical spectroscopies currently employed for chemical analysis. Two of these are briefly discussed in the paragraphs following. UV absorption spectroscopy was used in this work and is discussed in more detail.

2.1.1 Absorption Spectroscopy

The absorption of electromagnetic energy follows the principles of quantum electrodynamics, however, the process is often adequately described by a semi-classical mechanism (Patterson, 1987). Matter preferentially absorbs light of a particular wavelength range. The wavelength of the light absorbed corresponds to the amount of energy required by the matter to move from a lower energy state to a higher energy state. Quantum dynamic theory specifies the precise wavelength of light necessary to achieve a particular energy state in a unique substance by the Bohr model of the photon.

$$E = h\nu \qquad (2\text{-}1)$$

where E is the energy of the photon, ν is the frequency of the photon with units cm^{-1}, and h is Planck's constant.

Within an energy state there are several small vibrational levels of energy or perturbations around the energy state. These various levels have their own individual energy requirements but taken together can be thought of as a continuum around an energy state with very little loss in theoretical accuracy (Janata, 1989). The concept of a continuum allows a statistical treatment of the interaction of light and matter. This treatment leads to the well known Lambert-Beers' equation (Chen, 1987):

$$\log_{10}\frac{I_o}{I}=abC \qquad (2\text{-}2)$$

where I and I_o are the instantaneous and source intensities at a particular wavelength, a is the absorptivity constant of the matter for a given set of conditions, and b and C are the path length of the light through the matter and the concentration of the absorbing species in grams/liter (Silverstein et al., 1974). It is useful to define a quantity called the absorbance A of a species as:

$$A=abC \qquad (2\text{-}3)$$

A is known as the optical density of a material in the older literature (Silverstein et al., 1974). A plot of the absorbance with respect to wavelength is normally described as the absorbance or absorption spectrum of a chemical species. As is outlined above, the absorption spectrum is dependent on the species type and current energy state and concentration.

2.1.2 Luminescence Spectroscopy

Matter is usually in its lowest stable energy state for a given ambient condition before the energy of the photon is absorbed. After absorption, the excited matter will again seek its lowest stable energy state. This state is achieved in several ways: chemical or physical transformations of the matter that uses the excess energy, a radiative process in which the energy is lost by the emission of a photon, or a combination of the two processes (Chang, 1971). The wavelength of the radiated photon is dependent on the physical and chemical characteristics of the matter. The radiative processes give rise to the field of luminescence spectroscopy, which includes both fluorescence spectroscopy commonly used in liquid chromatography apparatus for liquid analysis, and photoluminescence spectroscopy, which is often

used to characterize crystal purity in semiconductor materials (Goldberg and Weiner, 1989).

2.1.3 Scattering Processes

The last process mentioned is scattering. Radiative scattering is a process involving the interaction of the wave and momentum vectors of the light and matter (Gilson and Hendra, 1970). This interaction gives rise to scattered radiation that is characteristically different than the incident radiation. The differences can be in wavelength, intensity, polarization, and coherence, and are dependent on the type of matter and the characteristics of the incident intensity. Scattering processes are usually probed with an incident beam of monochromatic light and are differentiated by the resultant scattered light's wavelength spectrum with respect to the incident spectrum. These processes include Rayleigh, Brillouin, and Raman scattering. Of these three, Raman scattering has been the most useful in the optical analysis of matter.

2.2 Fiber Optic Sensors

There has been a surge in the field of fiber optic sensor research over the past two decades. This surge has occurred because of progress attained in the field of fiber

optic communications research. The communications field is interested in the unadulterated transmission of light signals through plastic or glass optical fiber. However, any unwanted cause of modulation of a communications signal through a fiber has potential as a fiber optic sensing parameter.

2.2.1 Fiber Optic Waveguides

The theory behind the transmission of light down a fiber waveguide harkens back to the classical Maxwell's Equations describing electromagnetic fields and Snell's law (Olsen and Rogers, 1984). Snell's law is usually written as:

$$n_1 \sin\theta_1 - n_2 \sin\theta_2 \qquad (2\text{-}4)$$

where n_1 and n_2 are the indices of refraction of two adjoining media, and θ_1 and θ_2 are the angles of incidence and reflection measured with respect to the perpendicular to the interfacial surface of a ray of light passing from medium 1 to medium 2.

For n_1 greater than n_2, if the angle of incidence, θ_1 is greater than the critical angle defined as θ_c, where:

$$\sin\theta_c = \frac{n_2}{n_1} \qquad (2\text{-}5)$$

nearly all of the light will be reflected back into medium 1. If medium 1 is formed as a cylinder concentric to a larger cylinder of medium 2, it is easy to see that light introduced at one end of medium 1 will traverse down the length of medium 1 by multiple internal reflections. The light is therefore guided from one end to the other.

Optical fiber is usually fabricated from glass or plastic preforms and is drawn into long thin strands serving as the primary light conduit or core. These strands are normally coated with a cladding material of a different index of refraction than the core material to maintain the waveguiding properties of the core. Other layers are also coated on to improve properties such as strength and flexibility of the fiber optic cable. The transmission properties of the fiber depend on the core and cladding materials and their relation (Daly, 1984). Fiber optic materials and manufacturing methods are rich topics but are beyond the scope of this report.

2.2.2 General Sensor Configuration

The general configuration of an active fiber optic sensing system involves three regions linked by fiber optic waveguides. Passive fiber optic sensors such as those utilizing the chemiluminescent effect do not have a separate optical source and will not be discussed here. The first region consists of an optical source. This can be any source of optical electromagnetic radiation compatible with the waveguide but most often takes the form of a lamp, a light emitting diode (LED), or a laser. The radiation from this source is carried with minimal modulation down the first waveguide to a sensing region. This second region is where the actual measurement takes place. At this point, the original light signal is modulated. Modulation can be manifest in a change in intensity, frequency, polarization, propagation time, or phase. For example, if a material that characteristically absorbs light over the wavelength range 240 to 260 nm is placed in the path of the incident radiation, the resultant light will have a lower intensity over that 20 nm range than if the absorbing material were absent.

The resultant or modulated light passes from the sensing region to the detector region via another fiber optic waveguide. The detector region is the third component of the fiber optic sensor and normally consists of either a

photomultiplier, photodiode, or avalanche photodiode. The third region often includes a spectrometer ahead of the detector to separate the components of the light by wavelength.

2.2.3 Types of Fiber Optic Sensors

The sensing region of a fiber optic sensor can be either intrinsic or extrinsic. Intrinsic sensing occurs when the light is modulated directly within the fiber. This type of sensor is often used to measure changes in phase and is incorporated in fiber optic gyroscopes and other sensors utilizing the Mach-Zender effect (Butler and Ginley, 1988). Extrinsic sensing occurs when light is modulated outside of the fiber core region and then reintroduced into the fiber leading to the detection region. This type of sensing is used most often in chemical sensing. Extrinsic modulation can occur in a cell, through a membrane, in a porous region, etc.

Chemical sensing has not been the only fertile region for the application of fiber optic sensors. Fiber optic sensors have been used for a plethora of types of measurements including temperature (Conforti et al., 1989), particle counting (Chow et al., 1988), electric current (Edwards et al., 1989), humidity (Zhou et al., 1988), electrochemistry measurements (Kuhn et al., 1990; Van Dyke

and Cheng, 1988), and pH measurements (Jones and Porter, 1988; Luo and Walt, 1989a; Gabor and Walt, 1991).

Fiber optic chemical sensors have been used in many different configurations for measuring many different parameters (Seitz, 1984; Peterson, 1988). These sensors have used all three of the general optical spectroscopic methods discussed above.

Fluorescence based fiber optic sensors have been extremely popular for chemical sensing, usually in conjunction with a catalyst or reactant attached to the fiber (Kulp et al., 1987; Louch and Ingle, 1988; Fuh et al., 1988; Zung et al., 1988; Lieberman and Brown, 1988; Herron and Whitehead, 1988; Carrol et al., 1989; Bright and Litwiler, 1989; Luo and Walt, 1989b; Shakhsher and Seitz, 1990; Gunasingham et al., 1990). These types of sensors have also had success in environmental applications such as in situ ground water monitoring (Chudyk et al., 1988), gasoline sensing, hazardous waste screening (Chudyk, 1989), and column experiments to measure flow and transport (Kulp et al., 1988).

Scattering techniques have also been employed in fiber optic sensors (Laguesse, 1988). Raman scattering probes have been studied most often (Walrafen and Stone, 1972; Ross and McClain, 1981; McCreery et al., 1983; Schwab and McCreery, 1984; Reichert et al., 1987; Leugers and McLachlan, 1988; Lewis et al., 1988).

Absorption sensing techniques have also been used in fiber optic configurations for chemical sensing (Tenge et al., 1987; Carey et al., 1989; Dickert et al., 1989; Zhou et al., 1989; Renn and Synovec, 1990; Cavinato et al., 1990).

2.3 Sorption/Desorption

When discussing the effects of sorption/desorption processes on the fate and transport of nonionic organic chemicals in the subsurface it is convenient to use the one dimensional form of the transport equation for saturated conditions:

$$\frac{\partial c}{\partial t} = D\frac{\partial^2 c}{\partial x^2} - v\frac{\partial c}{\partial x} + \left(\frac{\partial c}{\partial t}\right)_{rxn} - \frac{\rho(1-\theta)}{\theta}\left(\frac{\partial q}{\partial t}\right)_{srp} + \Gamma(c) \qquad \textbf{(2-6)}$$

where c is the solute concentration in the fluid phase; t is time; D is a longitudinal dispersion coefficient, v is an average fluid-phase pore velocity in the x direction, x is distance; the terms subscripted rxn and srp are source-sink terms for chemical reaction and sorption-desorption mass transfer, respectively; ρ is the solid-phase density; θ is the porosity; q is the solute concentration in the solid phase; and $\Gamma(c)$ is a general source-sink term. In this

section the primary focus will be on the forms of the possible sorption/desorption mass transfer terms.

2.3.1 Sorption/Desorption Processes

In a system comprised of a solute, a solid, and an aqueous phase, sorption and desorption processes can be defined to be those processes causing mass transfer of the solute between the aqueous and solid phases.

Sorption and desorption processes are usually analyzed in terms of an equilibrium state and a rate state. Single solute systems will be the only systems discussed here.

2.3.2 Sorption/Desorption Equilibrium

For nonpolar hydrophobic organic compounds the literature has shown that the dominant factors in the sorption/desorption processes of aqueous and solid phase systems are the natural organic matter content of the solid phase media and the hydrophobicity of the solute (McCarty et al.,1981; Ball and Roberts, 1991a). This is analogous to a partitioning behavior often exploited in chemical extraction procedures. Karickhoff (1984) observed that a linear relation is manifest for some compounds with low water solubility in dilute solution. The equilibrium expression for the solid and liquid phases is given by:

$$q_e = K_p c_e \qquad (2\text{-}7)$$

where q_e is the equilibrium solid-phase solute concentration, K_p is the linear sorption partition coefficient, and c_e is the equilibrium fluid-phase solute concentration. The linear sorption partition coefficient contains contributions relating to both the organic content of the solid media and the hydrophobicity of the solute as is illustrated by the following two equations:

$$K_p = f_{oc} K_{oc} \qquad (2\text{-}8)$$

and

$$Log(K_{oc}) = A\,Log(K_{ow}) + B \qquad (2\text{-}9)$$

where K_{oc} is the organic carbon referenced sorption partition coefficient, f_{oc} is the organic carbon content of the natural solid material, A and B are empirical coefficients of regression and K_{ow} is the octanol-water partition coefficient. Values for the octanol-water

coefficient and A and B can be found in the literature (Sabljić, 1987).

In most situations, especially those where the solute concentration is relatively high or the solute is ionic or highly polar, nonlinear expressions are better able to fit the relation between the solid and aqueous phase concentrations of solute. Several expressions have been used in this vein (Kinniburgh, 1986). The Freundlich equation has had a great deal of success in the description of these systems. The Freundlich expression is usually written as:

$$q_e = K_f C_e^{n_f} \qquad (2\text{-}10)$$

where K_f and n_f are constants. This implies a nonlinear relationship between the sorption retardation coefficient and the aqueous concentration making it more difficult to solve the contaminant transport equation.

Non-singular effects have been observed in many sorption/desorption equilibrium experiments, in which the curves describing the equilibrium distribution of a solute in the aqueous/solid phase system are different after sorption and desorption processes (also referred to as hysteresis). Although this behavior has been observed by

researchers (Di Toro, 1985; Chang, 1989), there is no strong conviction that this is an inherent property of the sorption/desorption mechanism. Several researchers (Koskinen et al., 1979; Curl and Keoleian, 1984; Gschwend and Wu, 1985; Brusseau and Rao,1989; Chang, 1989; Ball and Roberts, 1991a) have listed a number of explanations for non-singular data. The explanations have mostly related to problems in the experimental techniques often used to study systems such as these. However, Brusseau and Rao (1989) have suggested that chemical reactions fixing the solute onto the solid phase may be occurring after sorption in hysteretic systems.

2.3.3 Sorption/Desorption Rate Models

Researchers have recently found that the equilibrium conditions for sorption and desorption processes can take months or longer to occur (Chang, 1989; Pedit and Miller, 1990; Levert, 1990; Ball and Roberts, 1991a, 1991b). Therefore in order to accurately describe contaminant fate and transport it is necessary to understand the rate of sorption and desorption processes.

Sorption/desorption rate models usually take one of three forms: the local equilibrium model, chemical site specific models, or physical diffusion models.

2.3.3.1 Local Equilibrium Models

The local equilibrium assumption (LEA) postulates that sorption/desorption occurs quickly with respect to advection. This implies that the solid and aqueous phases of solute are in equilibrium at localized points within the system. The contaminant transport equation would therefore employ one of the equilibrium expressions discussed above to describe the changes in solute with respect to time. For a system described by the Freundlich expression, the following would hold under the LEA:

$$\frac{\partial q}{\partial t} = \frac{\partial q}{\partial c}\frac{\partial c}{\partial t} = n_f K_f c^{n_f - 1}\frac{\partial c}{\partial t} \qquad \text{(2-11)}$$

For a conservative solute this results in a retardation of solute breakthrough normally observed from the contaminant transport equation with no sorption. This retardation factor can be expressed as:

$$R_f = 1 + \frac{\rho(1-\theta)}{\theta} n_f K_f C^{n_f - 1} \qquad (2\text{-}12)$$

The retardation factor is independent of solute concentration when the sorption equilibrium distribution relationship is linear (n_f=1).

The LEA model has been shown to be incorrect in experimental investigations in both the field (Goltz and Roberts, 1986) and the laboratory (Weber and Miller, 1988). However, it has been used as a reference point for comparing other types of sorption/desorption models (Weber and Miller, 1988; Goltz and Roberts, 1986; Miller and Weber, 1986, 1988).

2.3.3.2 Chemical Models

Chemical rate models assume that the sorption process is limited by kinetics rather than by mass transport limitations assumed by the physical models. Generally these models are categorized as single site rate equations or two site mechanisms in which the sorption process is depicted as a combination of fast and slow sites. Of these, the two site model has been more successful at accurately representing non-equilibrium data (Cameron and Klute, 1977; Rao et al., 1979). The two site model usually assumes that

the fast or instantaneous sites are represented by an equilibrium condition and the slow sites are controlled by a kinetic expression. This model can be represented as:

$$\frac{\partial q}{\partial t} = f\frac{\partial q}{\partial c}\frac{\partial c}{\partial t} + (1-f)\left(\frac{\theta}{\rho(1-\theta)}k_1 c - k_2 q\right) \qquad (2\text{-}13)$$

where f is the fraction of instantaneous sites, and k_1 and k_2 are the sorption and desorption rate constants, respectively. Assuming a linear sorption equilibrium distribution, the transport equation for a conservative solute is given by:

$$R_f\frac{\partial c}{\partial t} = D\frac{\partial^2 c}{\partial x^2} - v\frac{\partial c}{\partial x} - (1-f)\frac{\rho(1-\theta)}{\theta}\left(\frac{\theta}{\rho(1-\theta)}k_1 c - k_2 q\right) + \Gamma(c) \qquad (2\text{-}14)$$

where

$$R_f = 1 + \frac{\rho(1-\theta)}{\theta}fK_p \qquad (2\text{-}15)$$

2.3.3.3 Physical Models

Physical models are fundamentally different from the chemical models described above in that sorption is postulated to occur instantaneously when a solute has physically reached a sorption site. The rate limiting factor in this type of model is embedded in a diffusion parameter. There are two general categories of physical models. The first are usually called first order mass transfer models, and the second type can be described as diffusion models.

2.3.3.3.1 First Order Mass Transfer Models

First order mass transfer models usually describe two types of solid surface regions associated with a particle in a saturated system. The immobile region is defined as the surface of the solid within the pores and contacting the stagnant fluid phase within the particle. The mobile region is the surface of the solid that is in contact with the bulk fluid of the system (assuming a negligible hydrodynamic layer around the surface of the particle). The limiting step in the sorption process is the mass transfer from the bulk fluid phase to the stagnant fluid phase. Many researchers have had success using this type of model to describe experimental observations (Van Genuchten et al.,

1977; Nkedi-Kizza et al., 1982; Goltz and Roberts, 1986; Brusseau et al., 1989).

2.3.3.3.2 Physical Diffusion Models

Physical diffusion models have only recently become popular for modeling sorption/desorption effects in subsurface media although they have been used for some time in modeling activated carbon systems. In these models, diffusion into the particle characterizes the rate limiting step, and is dependent on the radial position of the solute with respect to the particle's geometry. The types of diffusion that can occur are pore diffusion, surface diffusion, intraorganic matter diffusion, or a combination of these.

In the pore diffusion process, fluid and solid phase solute concentrations at the same radial position within a pore volume are assumed to be in equilibrium. However, the concentrations are dependent upon the radial position as moderated by a diffusion process. For a particle with a spherical geometry, this concentration can be written as:

$$\frac{\partial c_p}{\partial t} = \frac{D_a}{r^2}\frac{\partial}{\partial r}\left(r^2\frac{\partial c_p}{\partial r}\right) \qquad (2\text{-}16)$$

where c_p is the solute concentration in the fluid phase within the intraparticle pore space, D_a is the apparent diffusion coefficient, and r is the radial distance from the center of the sphere. The apparent diffusion coefficient is given by:

$$D_a = \frac{D_p}{R_p} \qquad (2\text{-}17)$$

where D_p is the effective pore-diffusion coefficient and R_p is the intraparticle pore-retardation factor. The pore retardation factor is defined by an equilibrium distribution expression. When the Freundlich expression is used to describe the sorption equilibrium distribution relationship, R_p is given by:

$$R_p = 1 + \frac{\rho(1-\theta_p) n_f K_f C_p^{n_f-1}}{\theta_p} \qquad (2\text{-}18)$$

where θ_p is the intraparticle porosity. If the solute is nonsorbing, $R_p = 1$; however, often there is still an apparent sorption effect due to very small diameter, tortuous pores that might result in the steric hindrance of a solute (Ball and Roberts, 1991b; Brusseau et al., 1991;). In addition, mass transfer resistance at the hydrodynamic boundary layer surrounding the particle may impart additional constraints on solute sorption (Miller and Weber, 1986).

In the surface diffusion model, solute diffuses into the particle by concentration gradients in the solid phase along the walls of the pore. For a particle with a spherical geometry, the change in solid concentration with respect to radial position is given by:

$$\frac{\partial q_r}{\partial t} = \frac{D_s}{r^2} \frac{\partial}{\partial r}\left(r^2 \frac{\partial q_r}{\partial r}\right) \qquad (2\text{-}19)$$

where q_r is the solute concentration in the solid phase as a function of radial position and D_s is the surface diffusion

coefficient. For a Freundlich equilibrium condition, the particle boundary conditions are:

$$c_s = \left(\frac{q_r (r - R)}{K_f} \right)^{\frac{1}{n_f}} \qquad (2\text{-}20)$$

and

$$\frac{\partial q_r}{\partial r} = 0 \quad at\ r = 0 \qquad (2\text{-}21)$$

where c_s is the solute concentration at the surface of the particle.

Two problems with the pore and surface diffusion models as described above are that a uniform particle size and a spherical particle shape are usually assumed. These two assumptions are not valid in natural subsurface conditions and must be accounted for in some systems to preserve the accuracy of the model (Cooney et al., 1983; Rasmuson, 1985). However, researchers have observed excellent results using a single representative average particle size (Miller and Weber, 1986, 1988).

The intraorganic matter diffusion model assumes that solute diffuses into the natural organic matter found within

the particle's pores. This model is developed analogously to the first order mass transfer model. Here organic matter on the external surfaces of the particle are equivalent to the mobile phase and organic matter on surfaces within the particle are analogous to the immobile phase (Brusseau and Rao, 1989a, 1989b; Brusseau et al., 1991).

III MATERIALS AND METHODS

3.1 Materials

3.1.1 Solid

The subsurface media used (Wagner media), was collected from a sand and gravel pit owned by Killins Concrete Company in Ann Arbor, Michigan. The media was comprised of glacial deposits taken at a depth of 20 to 25 meters below the surface. The material was air dried, sieved to remove particles larger than 2 mm in diameter, and prewashed to remove easily dissolved natural organic matter and to eliminate nonsettling particles (Levert, 1990). The characteristics of the media are given in Table 3-1.

Table 3-1	Solid Properties
Washed Wagner Subsurface Media	
Median Grain Size Diameter (mm)	0.50
Grain Size Uniformity Coefficient (d_{60}/d_{10})	2.98
Solid Density (g/cm^3)	2.67
pH (aqueous slurry)	8.80
Organic Carbon Content (%)	1.20

3.1.2 Solutes

Diuron, (3-(3,4-dichlorophenol)-1,1-dimethylurea), a herbicide used in a variety of agricultural applications (Mustafa and Gamar, 1972), was chosen as the solute to be investigated . The general characteristics of this moderately hydrophobic, nonvolatile, nonionic, organic chemical are given in Table 3-2.

Table 3-2	Solute Properties	
Diuron	3-(3,4-dichlorophenyl)-1,1-dimethylurea	
CAS #	330-54-1	Mercer et al, 1990
Molecular Wt. (g/mol)	233.10	
Melting Pt. (°C)	158-159	Worthing and Walker, 1983
Aqueous Solubility (mg/l)	42 @ 25° C	Worthing and Walker, 1983
Vapor Pressure (mm Hg)	3.1×10^{-6} @ 50° C	Worthing and Walker, 1983
log K_{ow}	2.81	Mercer et al, 1990

Chemical and biological transformations which can be extremely important factors in the fate and transport of organic chemicals are only briefly discussed in this work.

The transformation of organic chemicals in the subsurface can occur by several different processes including biological degradation and chemical transformation

(Weber and Miller, 1989). Researchers have found that diuron is biodegradeable under both aerobic and anaerobic conditions (Khan et al., 1976; Attaway et al., 1982). Under aerobic conditions, diuron was found to be transformed to 3,4-dichloroaniline by two N-demethylations followed by a hydrolysis reaction. Diuron was found to be transformed to 3-(3-chlorophenyl)-1,1-dimethylurea by reductive dehalogenation under anaerobic conditions. Researchers have also found that chemical transformations of diuron under ordinary temperatures and neutral pH ranges were negligible (Hill et al., 1955; Worthing and Walker, 1983). This was confirmed by Chang (1989). The biological contribution to diuron degradation was found to be negligible for this work. The minimal contributions of chemical and biological transformation allowed easier analysis of sorption/desorption processes in the experimental configurations of this work.

Sodium azide (NaN_3) is often used as an inhibitor of biological activity in experiments like these, however, because of its strong and broad UV absorption peak at 210 nm sodium azide was not used in conjunction with diuron in four of the six experiments. The characteristically prominent UV absorption mode of sodium azide was exploited in the column tracer experiments. A buffer solution spiked with sodium azide was used in these conservative tracer experiments to determine the dispersion of the subsurface media columns.

Methanol (CH_3OH) was used in extraction experiments as a solvent for diuron and was obtained from EM Science (Gibbstown, NJ).

3.1.3 Solutions

There were primarily three solutions used in these experiments: diuron in buffer, diuron in methanol, and sodium azide in buffer.

The buffer solution consisted of 0.005 M sodium tetraborate ($Na_2B_4O_7 \cdot 10H_2O$) and 0.005 M calcium chloride dihydrate ($CaCl_2 \cdot 2H_2O$) in distilled, de-ionized (DDI) water. This water was obtained from a Corning Model AG-11 Still and Corning Mega-Pure System Model D1 Deionizer (Corning Glass Works, Corning, NY). The sodium tetraborate was used as a buffer to help control the pH of the solutions and the calcium chloride dihydrate was used to improve particle settling during centrifugation of samples in the bottle point experiments.

The pH of the buffer solution was adjusted to approximately 8.40 by the addition of small amounts of hydrochloric acid (HCl). Extractions of selected sample bottles were done using methanol to confirm that no transformation was occurring. This was accomplished using mass balance considerations with the known influent solute concentration and the measurement of solute concentrations

in solution and extracted solid phases. All of the inorganic chemicals were obtained from Fisher Scientific Company (Norcross, GA) and were used as received.

Diuron solutions were obtained by dissolving diuron (reported 98% pure) from E.I. duPont de Nemours Co.,Inc. (Wilmington, DE) into either the buffer solution or methanol. The diuron was used as received and the aqueous solutions of diuron were filtered to remove undissolved impurities before using. Filtering was accomplished with a vacuum filter apparatus and 8-μm particle retention filter paper (Whatman, grade 40, Fisher Scientific Company, Norcross, GA).

3.2 Experimental Methods

This work involved three basic types of experiments: batch kinetic, batch equilibrium, and column experiments. The two batch experiment types can be grouped under the title bottle point experiments. The experiments were designed to obtain the sorption and desorption parameters of diuron on typical subsurface media.

UV absorption spectroscopy was chosen for this work. It was used because of the relative ease of performing the measurement with the chemicals chosen. The method of UV absorption spectroscopy has been criticized for its lack of specificity in most chemical analysis situations. This

criticism is a valid one in many instances due to the characteristically broad and overlapping absorption bands of many complex molecules. The broadness of the band results from the large number of available energy transition levels from the normal ground state and an even larger number of vibrational and rotational sublevels giving rise to the broad apparent continuum around the energy transition level. Despite these problems, UV absorption can be very useful in the analysis of simpler molecules and those with widely spaced energy transition levels. In addition modulation spectroscopy methods such as derivative absorption spectroscopy have been employed to further resolve complex, overlapping spectra (Hawthorne et al., 1984; Cavinato et al., 1990; Karstang and Kvalheim, 1991). Such techniques would be required in field analyses of organic contamination because of the presence of spectrally interfering natural organic materials.

Ultraviolet absorption spectroscopy was chosen as the appropriate technique for the analyses of diuron in the aqueous phase because of the pesticide's relatively strong absorbance peak at approximately 248 nm. Preliminary studies were performed to confirm that this peak occurred at approximately 248 nm with several different molar concentrations of diuron. The UV absorbance spectrum of diuron from 230 nm to 300 nm is given in Figure 3-1. A conventional UV/VIS spectrophotometer was used in all three

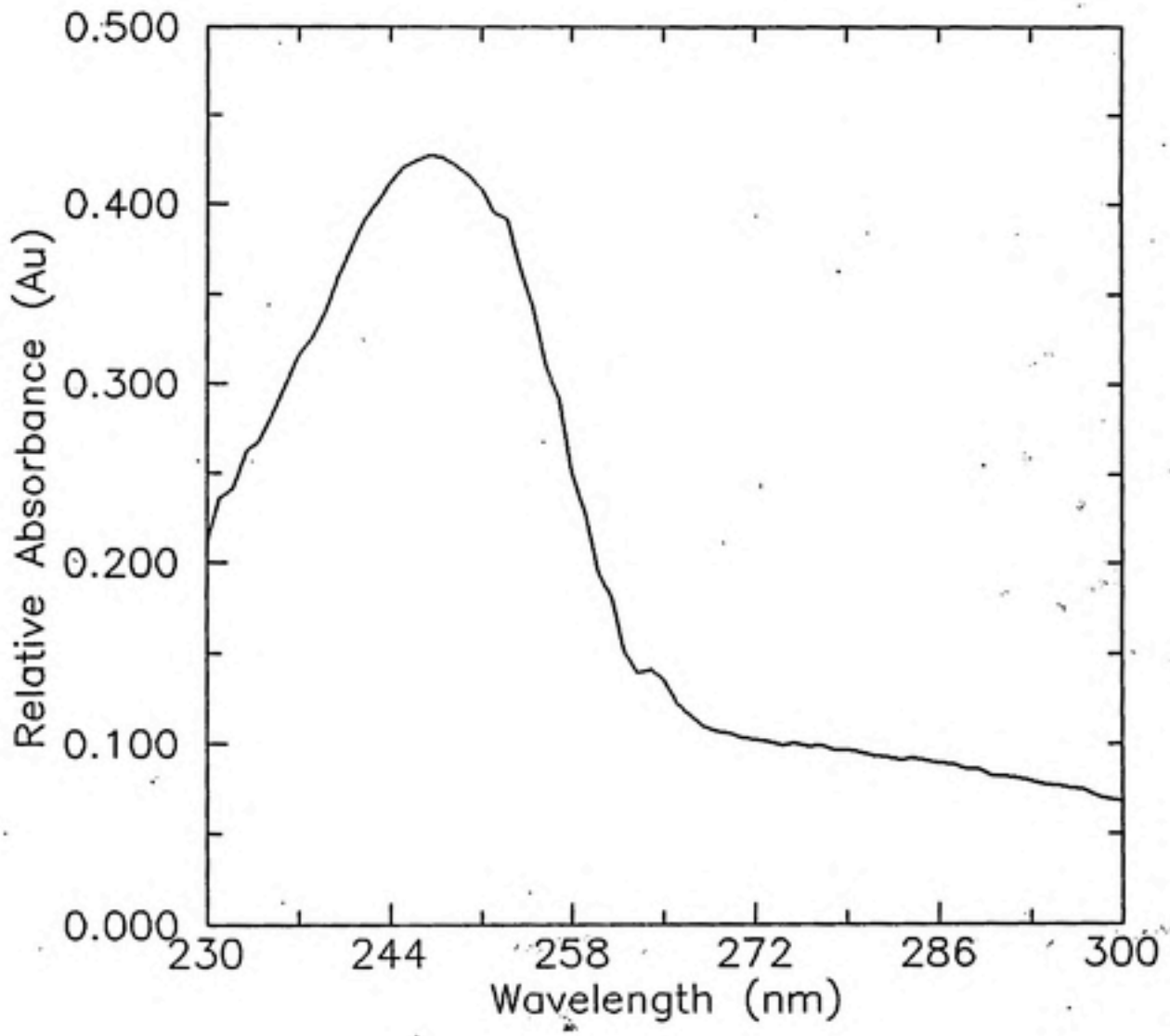

Figure 3-1 UV absorbance spectrum of diuron.

types of experiments and a fiber optic spectrophotometer was used for a batch kinetic study and several subsurface media column experiments. The general methods for both the conventional and fiber optic spectrophotometers are described in Section 3.3.

3.2.1 Control Experiment

A short term bottle point sorption kinetic experiment was carried out using sodium azide in buffer to confirm that sodium azide did not exhibit significant sorption effects with the Wagner soil. These experiments allowed the use of sodium azide as a conservative tracer for use in the subsurface media column experiments. The procedure for this experiment was the same as that for the diuron sorption experiments, which is described in detail below. The UV absorbance spectrum of sodium azide from 230 nm to 300 nm is given in Figure 3-2.

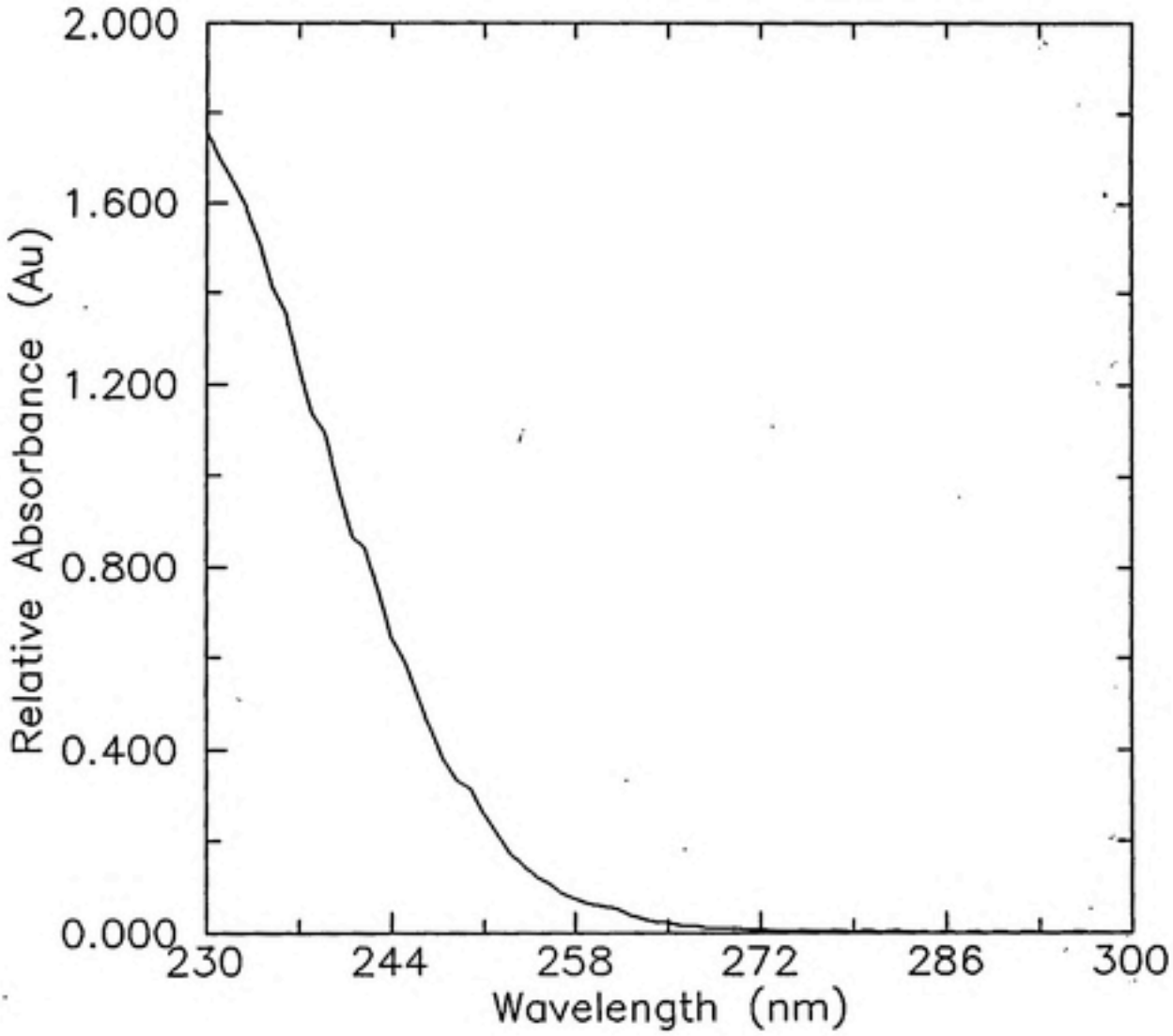

Figure 3-2 UV absorbance spectrum of sodium azide.

3.2.2 Sorption/Desorption Batch Kinetic Experiments

These experiments were designed to approximate the behavior of completely mixed batch reactors and were carried out in two experimental configurations. The first configuration used conventional 40-ml Kimax™, round bottom, borosilicate glass, centrifuge bottles as the individual batch reactors. The second configuration used custom fabricated 39-ml Suprasil™ centrifuge bottles, which allowed UV spectroscopic analysis directly in the bottle.

3.2.2.1 Conventional Configuration

The general procedure for sorption kinetic experiments consisted of the following steps:

1. A predetermined mass of Wagner subsurface media (usually 5.0 grams) was weighed and placed in each of a set of the borosilicate centrifuge bottles.

2. A predetermined volume of buffer solution without diuron (usually 12.5 ml) was pipetted into each of the bottles. The bottles were then sealed with Teflon™ lined caps and allowed to set overnight in order to completely wet the soil.

3. The following day, the caps were removed and a predetermined volume of a known concentration of diuron in

buffer solution (usually 12.5 ml) was added to each sample bottle to attain the desired subsurface media to solution ratio (grams of solid to ml of solution). The initial concentration (C_o) was determined from the known concentration of delivered diuron in buffer and the total volume of buffer solution in the centrifuge bottle. C_o was also measured by UV spectroscopy. Each bottle was considered a separate data point and a blank bottle was carried for each data point. Blank bottles were made using the same procedure as the sample bottles except when the diuron in buffer solution was added to the sample bottles, a pure buffer solution of the same volume was added to the blank bottles instead. These blank bottles were used to account for any noise in the measured UV absorption spectra contributed by desorption of natural organic matter from the Wagner soil.

4. All of the bottles were then re-sealed and packed in a plastic tub which in turn was placed on a tumbler. Using this arrangement, the bottles were turned end-over-end at 4.05 rpm.

5. Two samples and their corresponding blanks were removed from the tumbler at specific time intervals. The time intervals were chosen to best characterize the sorption rate behavior of diuron on the Wagner soil. The two samples and two blanks were immediately centrifuged at 1565 times the force of gravity (g's) for 30 minutes in order to

separate the liquid and solid portions of the sample. Approximately 10 ml of the supernatant was then removed from each of the bottles, placed in four 25-ml borosilicate sample vials (Pierce Chemical Company, Rockford, IL), and saved for spectroscopic analysis performed at a later date. Mass balance measurements performed on some of the samples indicated that diuron sorption onto the glass vials was minimal.

3.2.2.2 Suprasil™ Configuration

The Suprasil™ bottle procedure was slightly different than the borosilicate glass procedure described above. Suprasil™ is a type of fused quartz that has high transmission properties in the UV wavelength range. Centrifuge bottles (eight) were made out of 24-mm diameter Suprasil™ tubing by University Research Glassware Corp. (Carrboro, NC). Six bottles were used in the experiment: two bottles contained the diuron solution and soil; two bottles contained buffer solution and soil; one bottle contained no subsurface media and the diuron solution; and one bottle contained no subsurface media and the buffer solution. The two sample and two blank bottles were prepared in the same manner as the conventional borosilicate bottles, and the two remaining bottles without subsurface media were simply filled with the same volume of buffer or

diuron solution and sealed at the same time as the sample and buffer bottles. The six bottles were sealed with Teflon™ caps and comprised the batch reactor set. They were tumbled as in the other batch kinetic experiments until the prescribed measurement time. The bottles were then carefully centrifuged at 1565 g's for 30 minutes and the supernatant absorbance was measured directly through the Suprasil™ bottle by both the Perkin Elmer and the Guided Wave spectrophotometric instruments described below. The bottles were then replaced on the tumbler until the next measurement. This technique permitted non-destructive, repetitive analysis of each sample. Measurements were made weekly for the first 8 weeks and biweekly for the final two sets. At no time were the seals on the bottles broken.

3.2.2.3 Desorption Experiments

Desorption rate experiments were configured with the borosilicate centrifuge bottles only. The procedure for performing a desorption experiment was the same as that for the sorption experiment described above through step four. Once all the bottles were tumbling, they were all allowed to sorb for a determined length of time (2 weeks). The following procedure was then used to continue the experiment:

1. All of the bottles were taken off of the tumbler simultaneously and immediately centrifuged at 1565 g's for 30 minutes.

2. The bottles were then uncapped and a known volume (22 ml) of supernatant was removed from each bottle and saved for spectroscopic analysis.

3. A known volume (22 ml) of pure buffer solution was then delivered to each bottle and the bottles were recapped and replaced on the tumbler.

4. Two samples and their corresponding blanks were removed from the tumbler at specific time intervals. The time intervals were chosen to best characterize the desorption rate behavior of diuron on the Wagner soil. The two samples and two blanks were immediately centrifuged at 1565 g's for 30 minutes in order to separate the liquid and solid portions of the sample. Approximately 10 ml of the supernatant were then removed from each of the bottles, placed in four 25-ml borosilicate sample vials, and saved for spectroscopic analysis performed at a later date.

3.2.3 Sorption/Desorption Batch Equilibrium Experiments

These experiments were set up in the same manner as the batch kinetic experiments, but, the initial diuron in buffer concentrations delivered to the samples was varied. This was done to obtain several points on the equilibrium

isotherm curve. At least two replicates of each fluid phase concentration were carried and each sample had a corresponding blank bottle with pure buffer, as in the rate experiments. The results of the sorption rate experiments gave the necessary time for the approach of the sorption process to equilibrium. However, true equilibrium conditions were not achieved. All of the bottles were tumbled for this time and then removed from the tumbler and spectroscopically analyzed similarly to the kinetic experiments. The solid phase concentration was determined from mass balance considerations. Since diuron is conservative under these experimental conditions, the solid phase concentration was found from the difference between the initial and final fluid phase concentrations, as follows:

$$q_e = \frac{V}{M}(C_o - C_e) \qquad (3\text{-}1)$$

where q_e is the solid phase solute concentration at equilibrium, V is the volume of fluid, M is the mass of solid, C_o is the initial solute concentration in the aqueous phase, and C_e is the solute concentration in the aqueous phase at equilibrium. Mass balance for this method was

checked by performing solid phase extractions of selected samples.

3.2.4 Solid-phase Extraction

The solid phase diuron extraction procedure was as follows:

1. A known volume of the supernatant (20 ml) was removed from the sample and blank after centrifugation. This supernatant was spectroscopically analyzed and the diuron content determined. A known volume of methanol (10 ml) was immediately added to the bottles containing the mostly drained solid phase. The bottles were then resealed and replaced on the tumbler. The diuron on the solid phase desorbs into the liquid phase because of the large partitioning driving force of the diuron from the solid phase to the methanol.

2. After three days, the bottles were centrifuged and the same volume of methanol that was added previously was removed and stored in a volumetric flask. The same volume of fresh methanol was then added to the bottles. The bottles were then resealed and replaced on the tumbler as in step 1. This step was repeated for a total of five methanol additions and subsequent removals.

3. After the fifth removal of methanol from the subsurface media bottle to the volumetric flask, a small

amount of additional pure methanol was added to the flask to bring it to a known volume if necessary. The diuron in methanol solution was assumed to contain all of the diuron that was in the solid phase of the sample. This solution was spectroscopically analyzed and mass balance was checked based on a comparison with initial concentrations (C_o) and the measured aqueous phase concentrations prior to the addition of methanol.

3.2.5 Column Experiments

A diagram of the column experimental apparatus is given in Figure 3-3. Two reservoir flasks are shown in the figure. One flask contained pure buffer solution, and the other contained the buffer solution with diuron (or sodium azide). The volume of the flasks chosen was dependent on the flow rate and cumulative flow time chosen. A miniPump™ positive displacement pump (LDC Analytical, Riviera Beach, FL) was used to maintain a constant flow of solution through the column. All of the tubing in the set up was made of regular grade 304 stainless steel (Supelco,Inc., Bellefonte, PA). All of the materials in the apparatus were chosen to minimize spurious sorption to the apparatus. The glass columns were approximately 7.5-cm long, 2.4-cm internal diameter; and equipped with threaded Teflon™ end caps. The column assemblies were fabricated by University Research

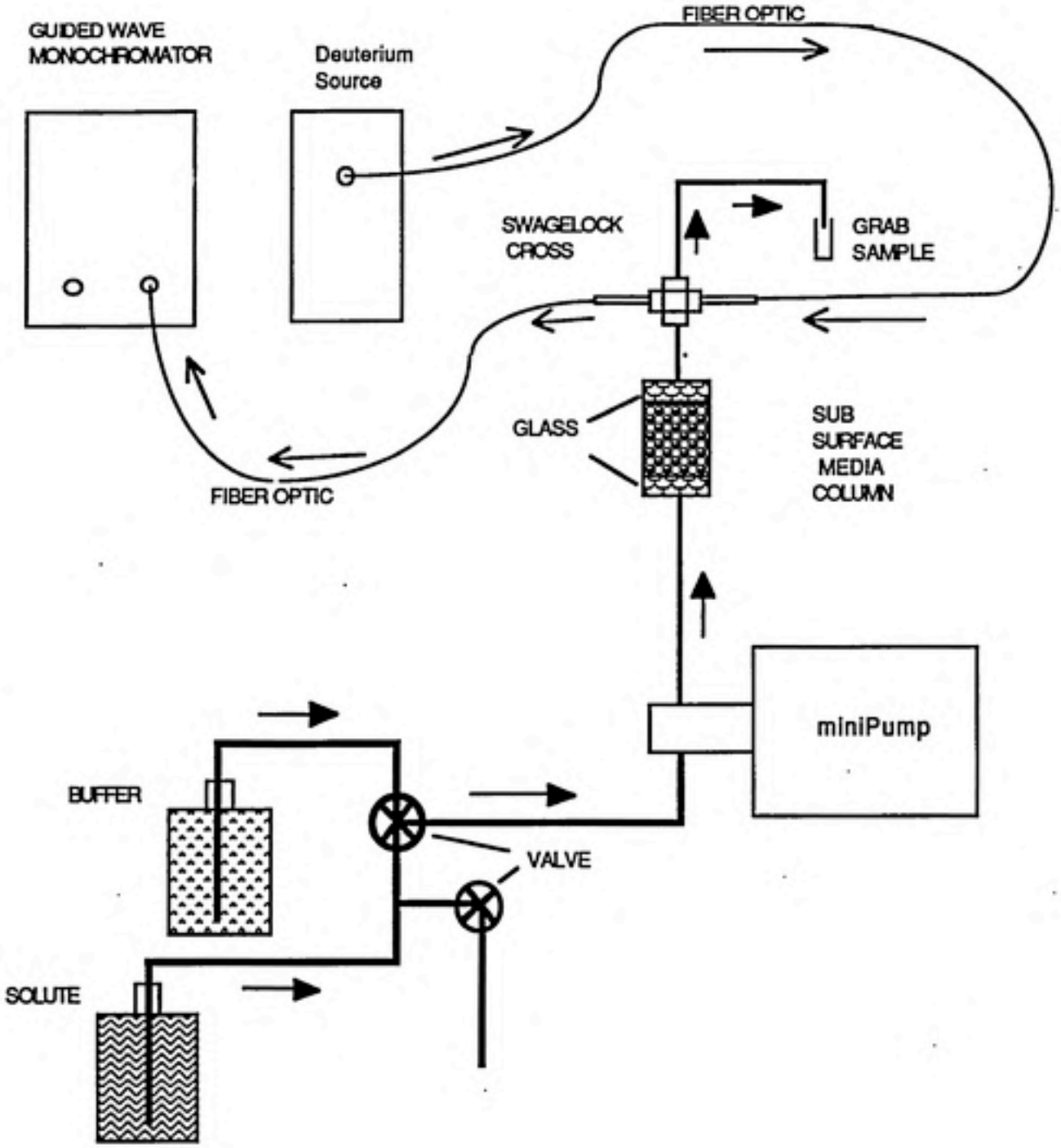

Figure 3-3 Diagram of Column Apparatus.

Glassware Corp. (Carrboro, NC).

The columns were packed with the subsurface media in the following procedure:

1. The buffer solution was pumped through the system and slightly into the bottom Teflon™ endcap orifice at the bottom of the column. A thin piece of silane treated glass wool was placed over the orifice and a preweighed amount of glass beads (McMaster-Carr Supply Company, Dayton, OH) was carefully poured into the column over the wool. The beads had a mean diameter of 0.38 mm and were included to disperse the solution more evenly before it entered the Wagner subsurface media. The sorption of diuron onto the glass beads was assumed to be negligible in comparison to that of the subsurface media. A preweighed amount of Wagner subsurface media was then carefully poured on top of the glass beads. The pouring of the glass beads and the subsequent pouring of the subsurface media into the column was done incrementally to enable the experimenter to pack the media in the column by manually vibrating the column. Sufficient fluid was allowed into the column to facilitate this packing. A top layer of preweighed glass beads was then carefully poured on top of the subsurface media and the Teflon™ endcap screwed on. The top orifice of the end cap was also covered by a piece of silanized glass wool. The top and bottom pieces of wool were placed to prevent the packed column media from escaping.

The fiber optic spectrophotometer sensing element was placed directly downstream of the column. Grab samples were taken approximately 20 cm after that.

Buffer solution was pumped through the column for at least 24 hours prior to the beginning of the experiment. This was done for two primary reasons: to adjust and stabilize the flow velocity through the system, and to flush out easily removed NOM in the subsurface media and stabilize its release during the experiment. NOM contributes to the absorption measured at the diuron peak wavelength and interferes with the accurate assessment of the diuron concentration. It was found that flushing the system minimized this effect.

The experiment was initiated by switching the feed to the pump from the buffer reservoir to the diuron solution reservoir. Care was taken prior to this point to clear all fluid lines of air.

The diuron solution was pumped for 36 hours. During this time, grab samples were taken at appropriate intervals to describe the behavior of the sorption. Grab samples were taken every 15 minutes for the first four hours, every hour for the next eight hours and every two hours for the rest of the sorption period. These grab samples were later analyzed by a conventional UV-VIS absorption spectrophotometer. At a flow rate of approximately 12 ml/hr, the minimum allowable time between samples allowable was 15 minutes. This is

constrained by the volume requirements of the conventional spectrophotometer and cuvette chosen. Wavelength scanned samples were also acquired at 15 minute intervals during the sorption period by the fiber optic spectrophotometer. The minimum time between samples allowed here is the time for a sample scan to be acquired. For the wavelength interval chosen for the first column, Col-1, (230 nm to 265 nm, .5 nm step), a scan was taken in approximately 30 seconds. The second column's (Col-2) wavelength interval was slightly different (230 nm to 300 nm, 1.0 nm step), and the scanning time was approximately 40 seconds.

At the end of the 36 hour sorption period, desorption was initiated by pumping buffer solution through the column. The desorption period was at least 36 hours. The same sampling procedures described above were used for the desorption period.

After a relative equilibrium was attained for the desorption portion of the experiment a conservative tracer study was begun. This was achieved by replacing the diuron solution with a solution of sodium azide. Switching the pump feed to the sodium azide reservoir initiated the step-up tracer test. A step-down tracer test was performed by switching back to the pure buffer solution. The step-up portion of the tracer test was run for 4 hours, and the step-down portion was run for at least 4 hours.

The fiber optic spectrophotometer sampled and stored data every 15 minutes for the diuron experiments and every five minutes for the tracer experiments. The sample consisted of the average of three continuous scans of a wavelength range chosen to include the full absorption peak.

Grab samples of the effluent of the system were also taken throughout the experiment and analyzed by conventional absorption spectroscopy. Samples were collected in pre and post weighed 25-ml borosilicate glass sample vials with Teflon™ lined screw caps (Pierce Chemical Company, Rockford, IL). The time interval of these samples was limited by the amount needed to perform spectroscopy (4 ml). These samples were taken to verify the performance of the fiber optic spectrophotometer and to verify the flow rate of the experiment. Influent samples of both reservoirs were taken periodically and spectroscopically analyzed later.

The tracer tests were performed to determine the dispersion in the column. Fiber optic scans were performed every 5 minutes during both the step-up and step-down periods. Sodium azide was chosen because it was determined that an anionic inorganic solute would have little sorption or ion exchange effects with subsurface media. This was confirmed by a sodium azide batch sorption kinetic study performed earlier.

Influent samples of the diuron, sodium azide, and buffer solutions were taken at various points in the column

experiments and analyzed by conventional absorption spectroscopy.

3.3 Instrument Description and Measurement Procedure

Conventional UV absorption spectrophotometry was performed with one of two comparably performing spectrophotometers. The first used was a Perkin Elmer Lambda 3 UV/VIS Spectrophotometer (The Perkin-Elmer Corporation, Oak Brook, IL). This spectrophotometer was used until its source lamp output intensity had decreased to the point at which the instrument's dynamic range was significantly diminished. A Hitachi Model U 2000 (Hitachi Inc.) was then used for the remainder of the experiments. The Hitachi was found to perform with equal or better resolution than the Perkin Elmer. A Guided Wave Model 200 Optical Waveguide Spectrum Analyzer (Guided Wave, Inc., El Dorado Hills, CA) was used for a batch kinetic study and several subsurface media column studies.

3.3.1 Conventional Spectrophotometry

The Perkin Elmer Lambda 3 UV/VIS and Hitachi instruments are dual beam UV/VIS spectrophotometers, which utilize a constant reference cell holding a cuvette that can contain a reference liquid of the experimenter's choice.

For nearly all experiments that were conducted here, distilled, de-ionized (DDI) water was used in the reference cell. Methanol obtained from Fisher Scientific Company (Norcross, GA) was used as received as the reference liquid for the remaining experiments. Both instruments have two available light sources: a tungsten bulb for visible and near infrared, and a deuterium lamp for UV. The UV source was used for all the experiments that were performed, the visible light source was used to initially align the cell holders for the experiments. Both instruments perform a series of diagnostic self-checks on startup and constantly correct for probe light variations by monitoring the output of the source lamp through the reference cell. The instruments have a zeroing function that along with the previously mentioned features sets the dynamic range of the instrument for a particular experiment. Both instruments have a reported accuracy below 0.001 absorbance units (Au).

The sample cuvette was filled with the reference liquid and the wavelength set for 248 nm in order to zero the instrument for all of the experiments. Both instruments had a very stable and repeatable baseline for all of the experiments performed.

Two cell holders were designed and fabricated by the UNC shop in addition to the standard 1-cm pathlength cuvette holders that came with the instruments. These cell holders were designed to hold the 24-mm pathlength custom fabricated

Suprasil™ bottles used in one of the batch kinetic experiments. In addition, the cell holders were designed so that light from either instrument would pass orthogonally through the sample bottle and supernatant, traversing the bottle's entire diameter. This would provide two surfaces perpendicular to the probe beam and minimize reflective and refractive losses. The cell holders were also designed to allow the bottle to be rotated on its longitudinal axis and clamped at a particular angular orientation. Because the bottles had slight variations in their diameter, the cell holders had a set screw to maintain the angular position of the bottles from one measurement to the next.

The spectrophotometer was turned on approximately one hour before any measurements were taken in order to give the machine a chance to perform self-diagnostic checks and stabilize. The UV source was turned on approximately 10 seconds after the spectrophotometer.

3.3.1.1 Cuvette Method

Two 1-cm path length Suprasil™ quartz cuvettes (Fisher Scientific Company, Norcross, GA) were used. These cuvettes were frosted on two sides. The cuvettes were rinsed several times with DDI water, then filled with DDI water and placed in the reference and sample cell holders. The cuvettes were always held by the frosted sides and were wiped with a

clean, dry paper cloth if they were wet. Care was taken not to let the cuvette windows get any dirt or grease on them. After the two cuvettes filled with DDI water were placed in the cell holders, the instrument was zeroed at 248 nm and left to stabilize.

After the machine had stabilized, the sample cuvette was rinsed and drained 2-3 times with DDI water, then rinsed once with the sample to be measured, and finally refilled with the rest of the sample to be measured. The sample cuvette was then wiped and placed in the cell holder. The spectrophotometer was allowed to stabilize for 5-10 seconds before a measurement was recorded. This procedure was repeated beginning with the DDI water rinses for all samples. For measurements of extractions obtained using methanol, methanol replaced DDI water as the reference and rinsing solution.

The only deviation from this procedure occurred when the samples were too small to allow for the single sample pre-rinse. In this case, the sample cuvette was vigorously shaken empty after the DDI rinses and simply filled with the sample to be measured. Procedures were kept constant throughout a given experiment.

Each set of measurements began and ended with a set of standard measurements. The set of standards consisted of 6-10 standard concentrations of the analyte in the dilution solution (e.g. diuron in buffer), beginning with pure

dilution and ending with the stock concentration of analyte in buffer. After a set of standards had been measured, a number of samples were measured and the standard measurements were repeated. The number of samples measured between standards was dependent on the stability of the spectrophotometer: 16-20 samples were measured between standards on the Perkin-Elmer, and 25-50 samples were measured between standards on the Hitachi. Several sets of standard measurements were taken to account for any instrument variations that might have been missed by the self- diagnostics of the spectrophotometers. When the data were analyzed, the standards were fit to a second order polynomial and the data interpreted by the fit. Each sample was linearly weighted depending on its temporal proximity to the two standard curves it fell between as in

$$C_x = \frac{(N-n_x)}{N} F_1 + \frac{n_x}{N} F_2 \qquad (3\text{-}2)$$

where C_x is the sample concentration, N is the number of samples measured between standard curves plus 1, n_x is the number of the sample in terms of its temporal order between standards measurements, F_1 is the concentration of the sample as determined by the second order fit to the first standards measurements, and F_2 is the concentration of the

sample as determined by the second order fit to the second standards measurements. The closer in time a data point was to a standard curve, the more it was weighted to that curve in the interpolation of its concentration.

For each time period, there were four data points. They consisted of two diuron solution with subsurface media (replicates), and two buffer solution with subsurface media (replicates). Four bottles were removed from the tumbling set at their prescribed measurement time and centrifuged at 1565 g's for 30 minutes. Approximately 10 ml of the supernatant was pipetted from the sample bottles (standard borosilicate centrifuge bottles with Teflon™-lined caps) into four clean sample vials, which were sealed with Teflon™-lined caps and stored in a refrigerator. The samples were individually analyzed after several measurement times had accumulated. The samples were discarded after measurement unless they were chosen to be extracted. This method is destructive as opposed to the Suprasil™ bottle method described below. The two buffer solution replicates were averaged and this average was subtracted from the two diuron samples. The result was then used in conjunction with the standard curves to determine the concentration of each of the two replicate samples.

Experiments with the sodium azide buffer solution required a preliminary step before accurate spectrophotometric analysis was possible. The samples'

supernatant was extracted with hexane in order to separate the diuron from the sodium azide in the buffer solution. Methanol provides a better extraction efficiency of diuron from water than hexane, however, methanol also extracts sodium azide and therefore could not be used. The extractions were performed because sodium azide has a characteristic UV absorbance peak in the vicinity of the characteristic peak of diuron. The sodium azide absorbance mode interfered with the diuron mode at the concentrations used in this experiment and prevented accurate assessment of the equilibrium concentrations of diuron in the samples.

3.3.1.2 Suprasil™ Bottle Method

As described in Section 3.2.2.2, six of the eight bottles fabricated were used for data. One of the two remaining bottles was used as a reference bottle for the Perkin Elmer spectrophotometer, the other was used similarly to the cuvette method for standard measurements i.e. rinsed with DDI water before and between standard measurements. All of the bottles were labeled and ruled in 30 degree divisions around the circumference of the bottles with white label tape and indelible ink markers. The bottles were then roughly measured over each angular division at 248 nm using air, DDI water, and a diuron solution. The bottles with the most consistent absorbances (least variation) over several

different angles were used as the reference and standard bottles. The reference bottle was filled with DDI water and placed in the reference cell holder of the custom made bottle holders at a particular angular orientation. This orientation (90 degrees) was used throughout the experiment. Four to six of the most consistent angular orientations of each of the rest of the seven bottles were picked out and these were used as data points throughout the experiment. Consistency in measurement for a given angular orientation was determined using multiple measurements of DDI water, buffer water, and a solution of diuron in buffer. Angular orientation was fixed by lining up the ruled markings on the bottles with a reference line on the bottle holder. Before the experiment began, the bottles were rinsed with acetone and DDI water. As with the cuvettes, each bottle was carefully handled so that oils and dirt would not get on them, and wiped clean before each measurement. All measurements were made at each designated angle point beginning with the lowest (nearest 0 degrees) progressing to the highest until a total of three measurements were made at each angle point (12 -18 measurements per bottle). The three measurements were averaged and a standard deviation and coefficient of variance determined for each angle point.

A characteristic offset absorbance was measured for each bottle in order to be able to relate the measurements

obtained from each bottle. The procedure for determining this offset was as follows:

1. Use DDI water as the fluid in all bottles and use the reference bottle chosen from earlier experiments to be the most consistent.

2. Measure the absorbances at five angular positions determined to be the most consistent in earlier experiments.

3. Repeat step 2 three times.

4. Average all the measurements for a particular bottle.

5. The average value of absorbance obtained is the offset absorbance for that particular bottle.

To obtain a data point from a bottle during the experiment, a similar procedure to the method of obtaining an offset was used:

1. Measure the absorbance at the most consistent angular positions.

2. Repeat step 1 three times.

3. Average all of the measurements for the bottle.

4. Subtract the characteristic offset of the particular bottle.

5. Treat the data as in the conventional bottle point experiment using the cuvette method from this point on.

Standards were measured before the sample bottles were centrifuged in order to minimize the time the sample bottles were not tumbling. The standard bottle was used similarly

to the cuvette method (DDI rinses between standards), however only one set of standards was measured per measurement time to minimize the time that the samples were not tumbling. Because of the large error measured between the three angle point measurements and the typically small error encountered between successive standard measurements, one standard set was considered sufficient.

3.3.2 Column Measurements

Samples from column experiments were collected at predetermined time intervals directly into sample vials which were sealed with Teflon™ lined caps and stored in the refrigerator. When the column experiment was completed, a set of standards was made and all the samples were measured using the cuvette method described above. A similar procedure was used for tracer studies using a solution of sodium azide in buffer.

3.3.3 Fiber Optic Spectrophotometry

The Guided Wave Model 200 spectrophotometer (Guided Wave,Inc., El Dorado Hills, CA) is a single grating monochromator (1200 lines/mm) with one internal source (tungsten) and one external source (deuterium), two detectors (silicon and photomultiplier tube), and is

designed with SMA™ type fiber optic connectors at the source and monochromator ports. Both the column and the batch kinetic (Suprasil™ bottles) experimental data were measured using direct transmission measurements over a range of UV wavelengths. Two probes with sapphire windows were aligned and samples were placed between them. The transmission probe was attached to the port of the deuterium lamp source via a 1-meter optical cable. The detector probe was connected to the monochromator port via a 30-cm optical cable. Both cables had 300 μm core, multimode fibers with good transmission properties in the UV range. The two sapphire probes limited the working UV range to 220 nm. Solarization of the transmission fiber was monitored by baseline measurements conducted before and after the experiments. The Model 200 was calibrated using the tungsten source and a short fiber optic jumper cable between the source and the monochromator. Reference scans were taken and stored in the appropriate experimental configuration using the deuterium source before each experiment and kept throughout the complete experiment. These scans were also used to monitor source variation over time. The Model 200 and source were turned on approximately 2 hours before a data set was taken. Scans normally covered a wavelength range of 30-50 nm with a resolution of 0.5 nm. Each stored measurement scan was the average of three scans performed automatically by the Guided Wave. Each stored measurement

took about 30 seconds. A high pass optical filter was used as a shutter between scans to inhibit fiber solarization.

3.3.3.1 Column Experiment

For the column experiments, probe cells were constructed by the UNC shop out of model 400-4 Swagelock Union Crosses (Swagelock Co., Solon, OH). The crosses were drilled out on parallel branches to accommodate a flush fit of the sapphire probes. The cross was then placed in the column line immediately after the subsurface media column. Therefore, transmission was measured perpendicular to the flow. Dead flow space was minimized by using proper fittings between the subsurface media column and the cross. A grab sample was collected 20 cm after the cross and analyzed on the Perkin Elmer Spectrophotometer to confirm the Guided Wave results. Measurements were normally taken every 15 minutes automatically over the course of a subsurface media column experiment. Measurements were taken every 5 minutes during tracer studies.

Several computer programs were written to analyze the raw data. Both differential wavelength absorbance at individual wavelengths and full width, half maximum (FWHM) peak area were used in the analysis. The FWHM area is often used in spectroscopic measurements and is defined as the area under the curve bounded above by the horizontal line

drawn at one half of the peak's maximum value covering the full width of the peak.

The most significant source of error encountered was introduced as a result of the decrease in output intensity of the deuterium source. This error was successfully dealt with and is described in more detail in Section 4.2.

3.3.3.2 Suprasil™ Bottle Batch Experiment

For the batch kinetic experiments, the UNC shop constructed an apparatus that enabled a Suprasil™ bottle to be placed securely between two aligned probes. The apparatus allowed the bottle to be turned on its longitudinal axis with good repeatability. An initial calibration of the bottles was performed similarly to the Suprasil™ experiments done on the Perkin Elmer Spectrophotometer and confirmed each bottle's most consistent angle points as determined by the Perkin Elmer Lambda 3. The measurement procedure for the Guided Wave fiber optic spectrophotometer was nearly identical to the procedure used for the Suprasil™ bottles on the Perkin Elmer. The only differences were that a wavelength scan from 230 to 265 nm was taken rather than a single measurement at 248 nm, and the standard set was measured after the six samples were measured. This was done to minimize the time that the samples were not tumbling.

As in the column experiments above, several computer programs were written to analyze the raw data. The programs involved: determining the average, standard deviation, and coefficient of variance of each point in the three scans for a given angular measure; correcting for source intensity decrease and other variations; determining a fit for the standard measurements; and finally interpolating the concentrations of the samples for a given measurement.

IV EXPERIMENTAL RESULTS AND DISCUSSION

4.1 Experimental Results

4.1.1 Batch Experiments

Six batch experiments were performed. These include two equilibrium distribution experiments, two sorption kinetic experiments, and two desorption kinetic experiments. Table 4-1 lists the experiments and their relevant parameters. Equilibrium distribution experiment, Eql-1, used a buffer solution that contained 0.005 M sodium azide after Chang (1989). The second equilibrium distribution experiment, Eql-2, used the normal buffer solution described in the methods Section (no sodium azide). The first desorption experiment, Dsrp-1, also used a buffer solution including sodium azide while the second desorption experiment, Dsrp-2, did not.

An additional sorption kinetic study was performed with sodium azide as the solute to confirm that the sodium azide solution could be used as a conservative tracer in the column experiments. All batch experiments were maintained at a pH of 8.4.

Table 4-1 List of Experiments					
Type/Name	C_o (mg/l)	Time (hrs)	Buffer	Solid Mass (g)	Liquid Volume (ml)
Batch Experiments					
Equilibrium Distribution					
Eql-1	7.05, 14.83, 22.87, 28.84	2016	Azide	3.0, 6.0, 15.0, 30.0	30.0
Eql-2	1.23, 2.52, 3.80, 5.42, 7.53, 11.75, 14.90, 23.42, 24.81	2016	No Azide	5.0, 2.5	24.9
Sorption					
Srp-1	11.33	2184	No Azide	5.0	25.2
Srp-2	3.08	3355	No Azide	5.0	25.0
Srp-1S	11.33	2184	No Azide	5.0	25.2
Srp-Az	326.35	168	Azide = Solute	40.0	20.0
Desorption					
Dsrp-1	13.11	1772	Azide	5.0	25.0
Dsrp-2	14.42	2032	No Azide	5.0	25.0
Column Experiments					
Diuron					
Col-1	2.80	73.25	No Azide	35.0	N.A.
Col-2	10.28	121.125	No Azide	35.0	N.A.
Tracer					
Trc-1	100.09	8.0	Azide = Solute	35.0	N.A.
Trc-2	575.21	9.5	Azide = Solute	35.0	N.A.

4.1.1.1 Equilibrium Distribution Experiments

The equilibration time for both equilibrium distribution experiments was 84 days. At the end of this time period, solution phase concentrations of diuron were measured and solid phase concentrations were determined by the difference method described in the methods section. The results obtained from Eql-1 are not shown here because the implications of the inclusion of sodium azide into the diuron/buffer solution were not investigated.

After solution phase concentrations of diuron were determined, the data were plotted and three types of equilibrium distribution models were fit to the data. Figure 4-1 shows the plot of Eql-2 along with linear, Langmuir and Freundlich model fits. It was found through error analysis that the Freundlich model provided the best fit. This was determined through a non-linear regression analysis using the statistical software package Systat™ (Wilkinson, 1988). The statistical parameters are given in Table 4-2. The criteria for the best fit was the determination of the least, normalized sum of the squared errors (NSSE) for each equilibrium distribution model. The equation for determining this is as follows:

$$NSSE = \sum_{n=1}^{N} \frac{(q_{e,n} - est_n)^2}{est_n} \qquad (4\text{-}1)$$

where N is the number of measurements made, $q_{e,n}$ is the solid phase solute equilibrium concentration measurement at n, and est_n is the model estimate of the solid phase solute equilibrium concentration at n.

Desorption points were obtained for Eql-2. Two desorption points were obtained after successive desorption equilibration periods of 56 days each for the data set. The method used to obtain desorption points for the set was consecutive centrifugation. The desorption data from this set are plotted on a log/log scale along with the Freundlich equilibrium model fit in Figure 4-2. It can be seen that significant apparent nonsingular sorption behavior occurred suggesting that equilibrium conditions were not reached. This conclusion is supported by the batch kinetic data described below.

Solid phase extractions were performed on selected sample bottles and desorption bottles. On average, greater than 96% of the diuron could be accounted for in solution measurements and subsurface media extractions. This validates the use of the difference method for determining solid phase concentrations. This also indicates that the

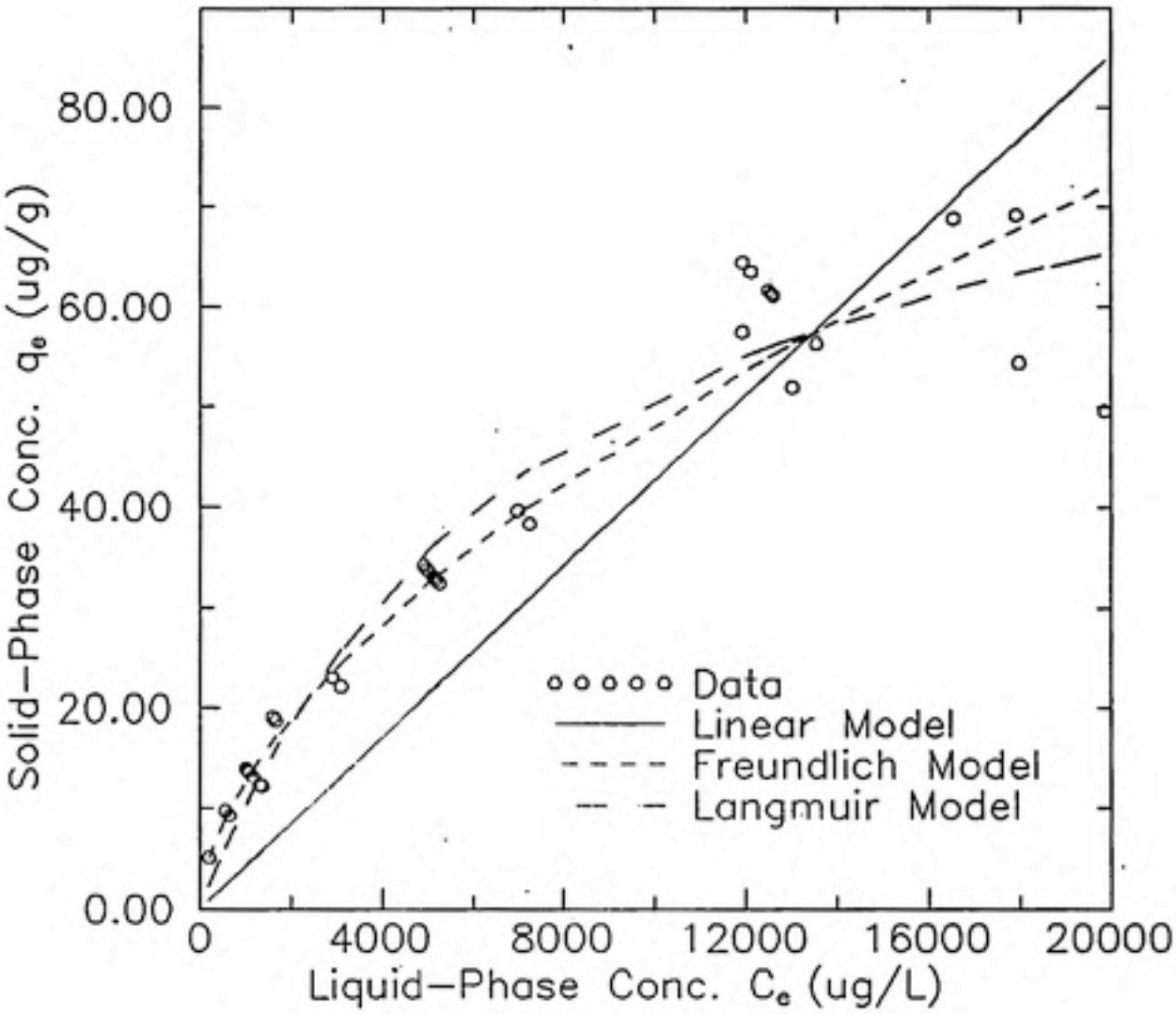

Figure 4-1 Equilibrium Distribution data with model fits.

Table 4-2	Eql-2 Statistics	
Linear Model	NSSE = 2.99E-04	
Constant	Estimate	95% Confidence
K_p (l/mg)	4.266	3.830,4.703
Freundlich Model	NSSE = 1.89E-05	
Constant	Estimate	95% Confidence
n_f (-)	0.5787	0.5465,0.6109
K_f $(ml/g)^{nf}$	0.0436	0.0333,0.1191
Langmuir Model	NSSE = 7.26E-05	
Constant	Estimate	95% Confidence
Q_o (mg/mg)	90.863	9.3024,14.0493
b (l/mg)	0.1285	0.0846,0.1724

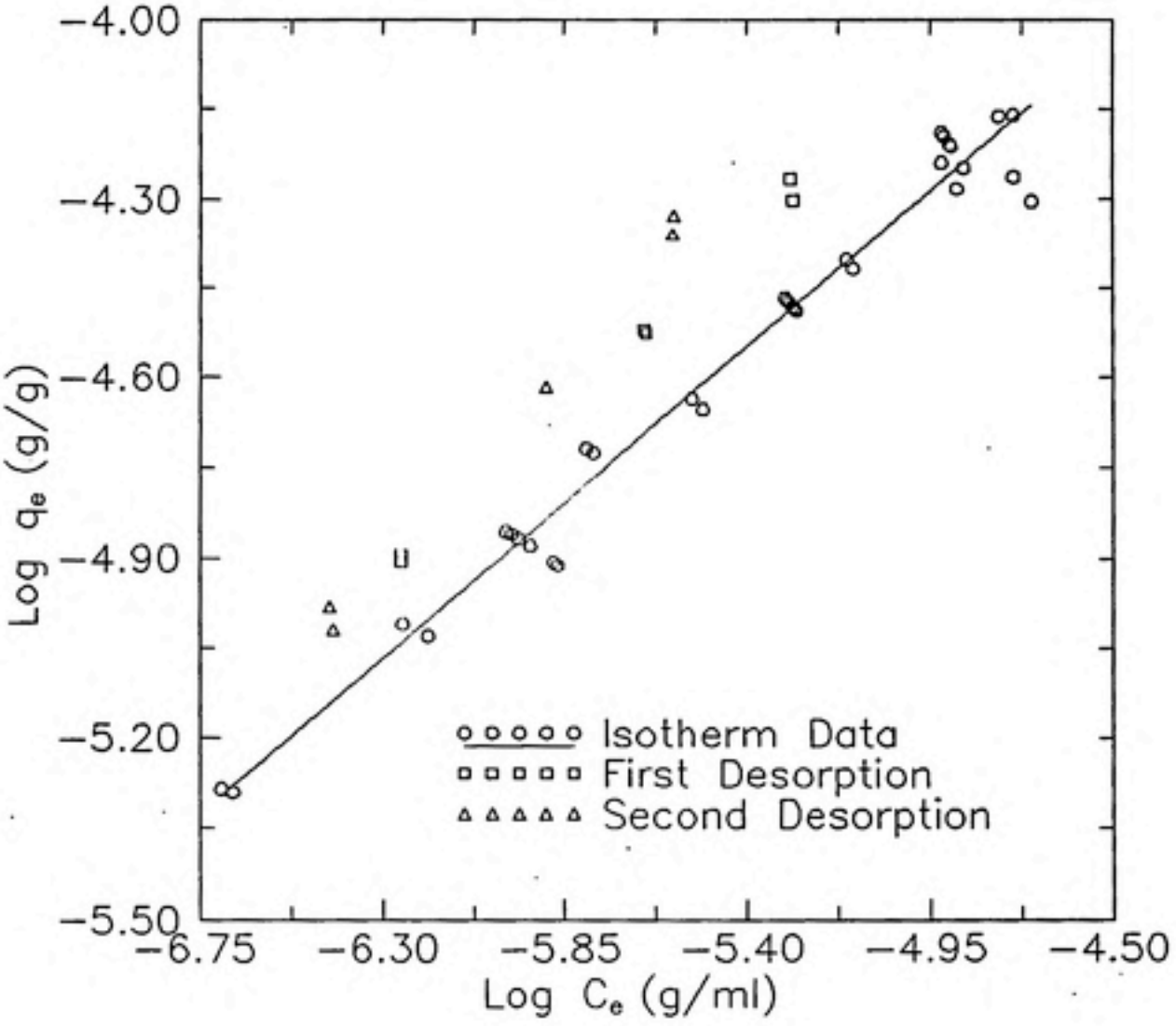

Figure 4-2 Equilibrium Distribution data, Desorption data with Freundlich fit.

samples were not subject to biodegradation over the experimental time frame.

4.1.1.2 Kinetic Experiments

Two types of kinetic experiments were performed, sorption and desorption. The experiments were performed using diuron as the solute. In addition, a sorption kinetic experiment was performed using sodium azide as a solute to determine its suitability as a conservative tracer for column dispersion studies.

4.1.1.2.1 Sorption Kinetic Experiments

The diuron sorption kinetic experiments were designed to be run over a longer period of time than had been done by previous experiments with diuron (Chang, 1989). The methodology for collecting samples was described in Section 3.2.2.

Both sample sets were analyzed by optical spectroscopy. Experiment Srp-1 was analyzed using the Perkin Elmer spectrophotometer. Experiment Srp-2, performed at a later date, used the Hitachi spectrophotometer. A comparison of the performance of the two instruments is illustrated in Figure 4-3. This plot compares data obtained from the measurements of standard concentrations of diuron. Although

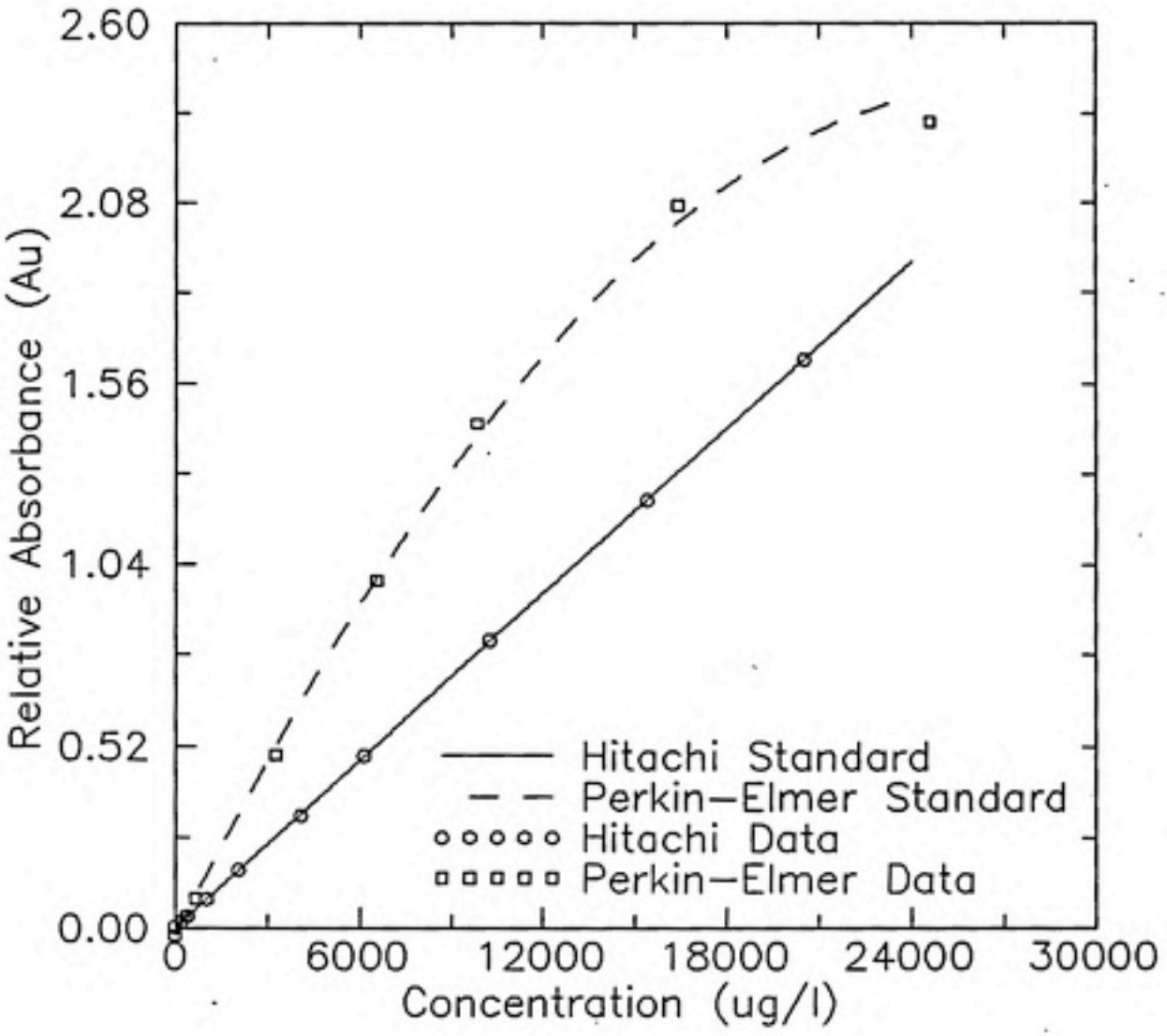

Figure 4-3 Comparison of standards data.

the two instruments were comparable in their repeatability, it is obvious that there is a discrepancy in their sensitivities. Much of this can be accounted for by source intensity problems encountered with the Perkin Elmer. This will be discussed in greater detail in Section 4.3.

Experiment Srp-1 was carried out in two parts. The first used the conventional bottle point method as described in Section 3.2.2.1. This method is limited by the initial number of bottles prepared because the sample is removed from its bottle for analysis by conventional spectroscopy using cuvettes. The number of data points that can be collected is therefore limited by the initial number of bottles prepared.

The second mode for this experiment used specially fabricated sample bottles made of Suprasil™, which allowed the sample to be analyzed by UV spectroscopy without removing it from the original sample bottle. This method allows for the potential of unlimited data points, therefore experimental times because the sample is not destroyed when it is analyzed. It also reduces the problem of inter-bottle variability found in the conventional bottle point method. The method was described in detail in Section 3.2.2.2.

Solid phase extractions were performed on selected sorption and desorption samples. On average, greater than

90% of the diuron could be accounted for in solution measurements and solid phase extractions.

The results of the conventional bottle experiment, Srp-1 are shown in Figure 4-4. It may be observed that apparent equilibrium was not reached after approximately 2200 hours. Figure 4-5 shows the results of the experiment Srp-2. Apparent equilibrium was not attained after approximately 3400 hours in this experiment. The criteria for equilibrium was assigned to be a slope change of less than 1 E-06 between data points on the normalized concentration plots given in Figures 4-4 and 4-5.

To validate the choice of sodium azide as a conservative tracer to be used for column dispersion tests, a relatively short term sorption kinetic study was performed using sodium azide as the solute. The kinetic study was carried out using the same procedure as the diuron sorption kinetic experiments described in Section 3.2.2.1, except sodium azide was the solute. Figure 4-6 is a plot of the relative sodium azide concentration as a function of time. This plot demonstrates that the aqueous phase sodium azide concentration remains relatively constant over a period of approximately 175 hours. Tracer studies for these experiments were performed in less than 5 hours. Therefore sodium azide can be used as a conservative tracer. The reason for the choice of sodium azide as a tracer as opposed to a more typically used solute such as chloride was that

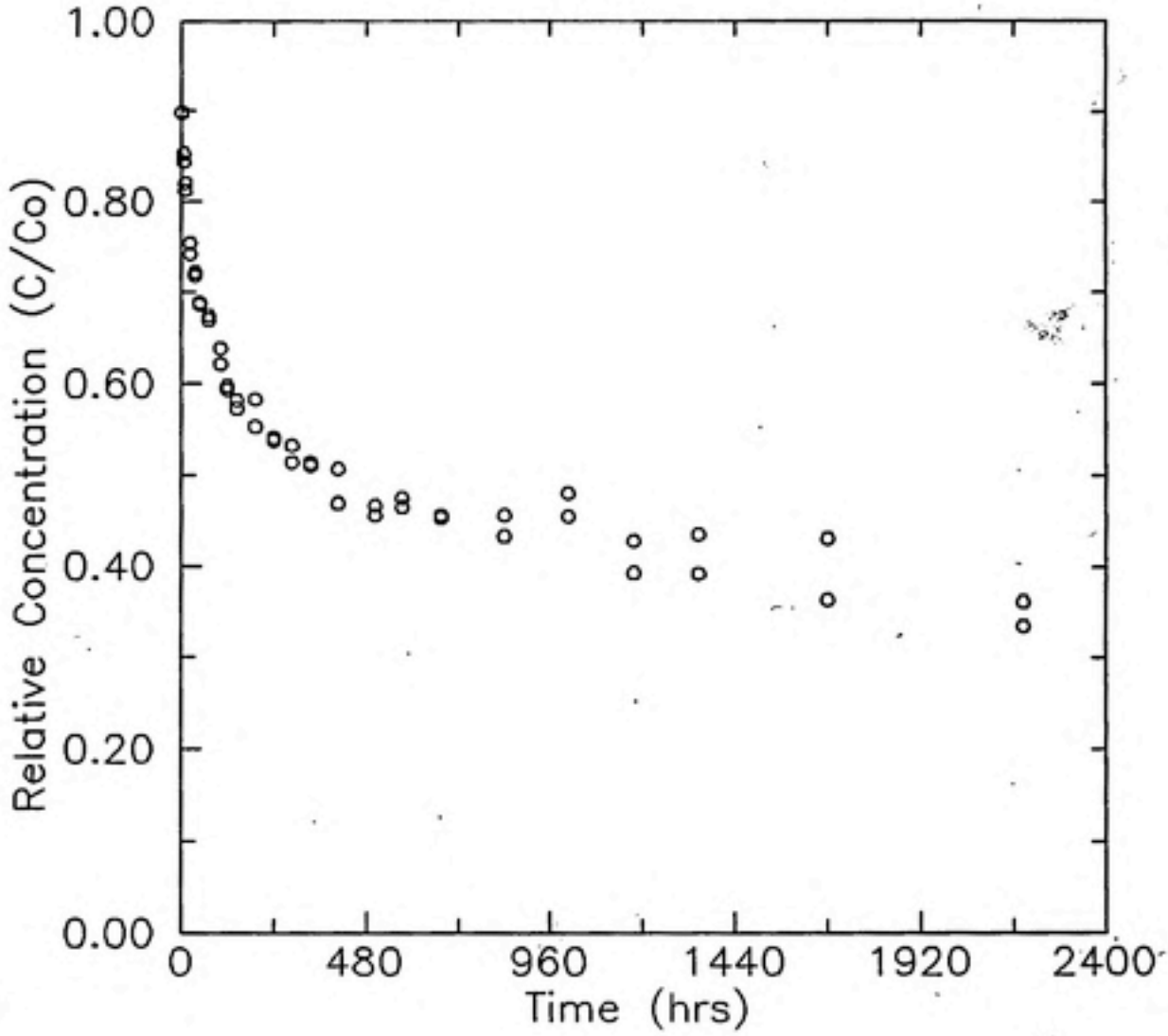

Figure 4-4 Sorption kinetic data for Srp-1.

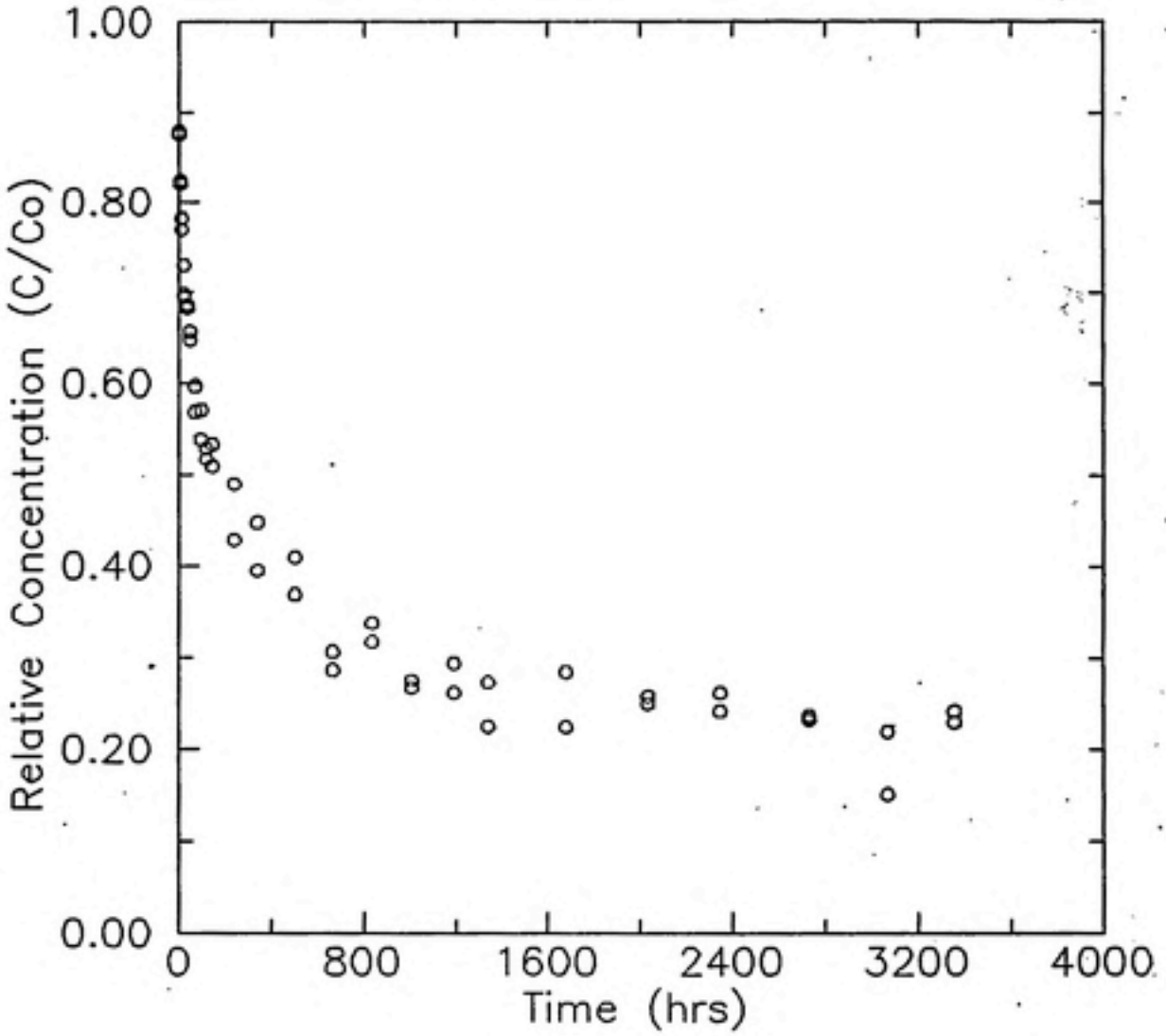

Figure 4-5 Sorption kinetic data for Srp-2.

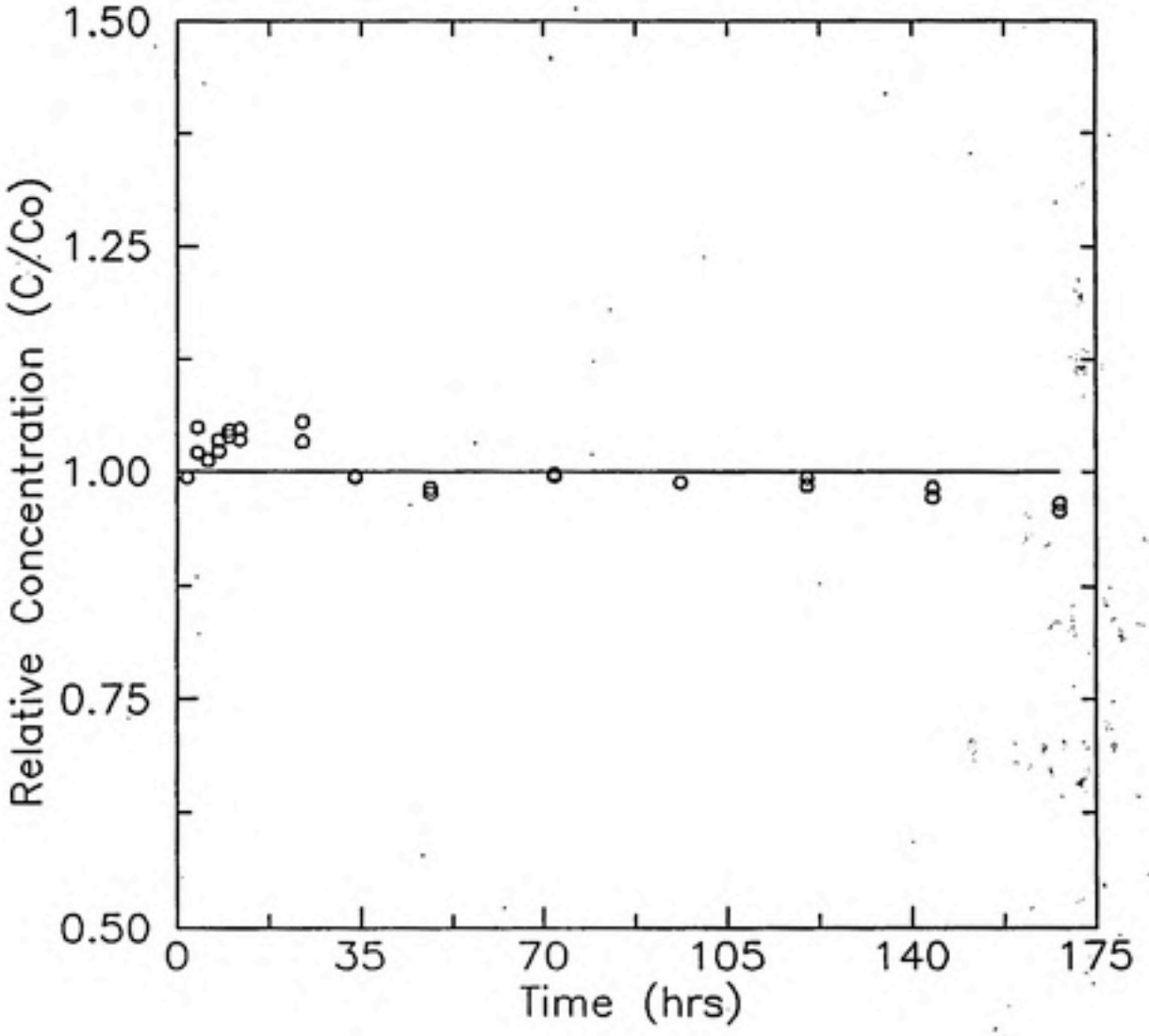

Figure 4-6 Sorption kinetic data for sodium azide.

the analysis of sodium azide can be done by UV absorption spectroscopy.

4.1.1.2.2 Suprasil™ Bottle Experiments

As mentioned in the previous section, two experimental modes were used in the high concentration sorption kinetic study, Srp-1 and Srp-1S. This section describes the results from the non-conventional mode in which analysis of samples was performed without removal of the sample from its original sample bottle. The procedure for analysis was described in detail in Section 3.2.2.2 and Section 3.3.1.2. The samples were analyzed using both a conventional UV-VIS spectrophotometer and a fiber optic spectrophotometer.

The extensive sampling procedure described in Section 3.2.2.2 and Section 3.3.1.2 was done because it was anticipated that the outer and inner diameters of the bottle would not be uniform and multiple data points for different angular orientations would need to be taken and averaged to increase the accuracy of the measurement.

Figure 4-7 shows the discrepancy in absorbance values between different angular orientations for a particular bottle. This wavelength scan of DDI water was taken with the fiber optic spectrophotometer. Similar behavior occurred with the conventional spectrophotometer.

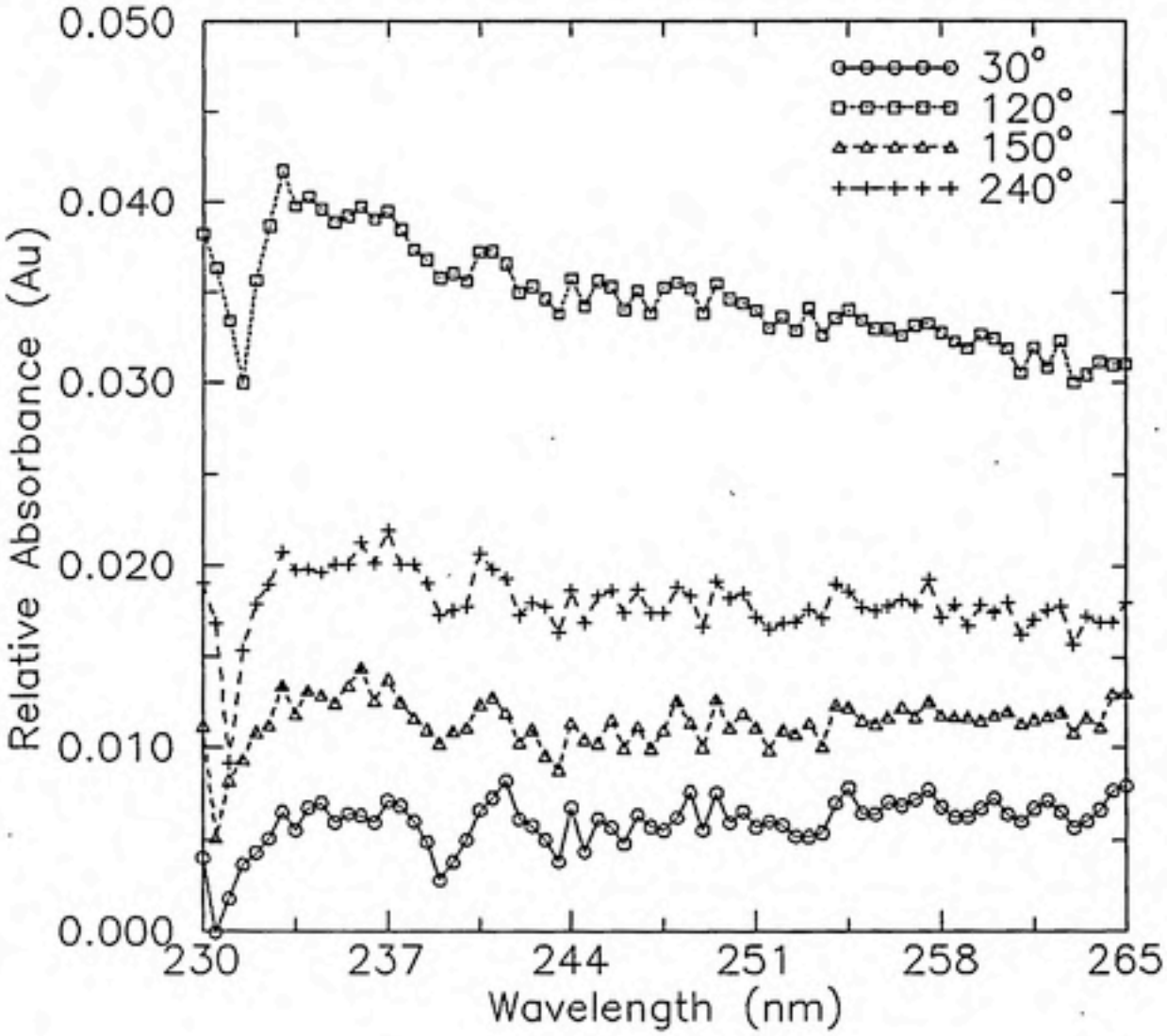

Figure 4-7 Variability of absorbance for Suprasil™ bottle.

Figure 4-8 is a comparison plot of the data obtained from the conventional method, Srp-1, and the averaged data obtained by the Suprasil™ bottle method, Srp-1S. It can be seen that there is substantially more variability in the Suprasil™ bottle method although the data does seem to be in good agreement with the rate data from the conventional experiment.

4.1.1.2.3 Desorption Kinetic Experiments

Two desorption kinetic experiments were performed. Experiment Dsrp-1 was performed using a buffer solution which included sodium azide similar to the equilibrium distribution experiment described in Section 4.1.1.1. The sorption period was four days before desorption was initiated.

Experiment Dsrp-2 was performed in a buffer solution without sodium azide. This experiment used a sorption period of 14 days. Figure 4-9 is a plot of the relative supernatant concentration versus time. It can be seen that an equilibrium condition was not reached after approximately 1700 hours of desorption. At 1700 hours, the aqueous phase solute is still resorbing onto the solid phase.

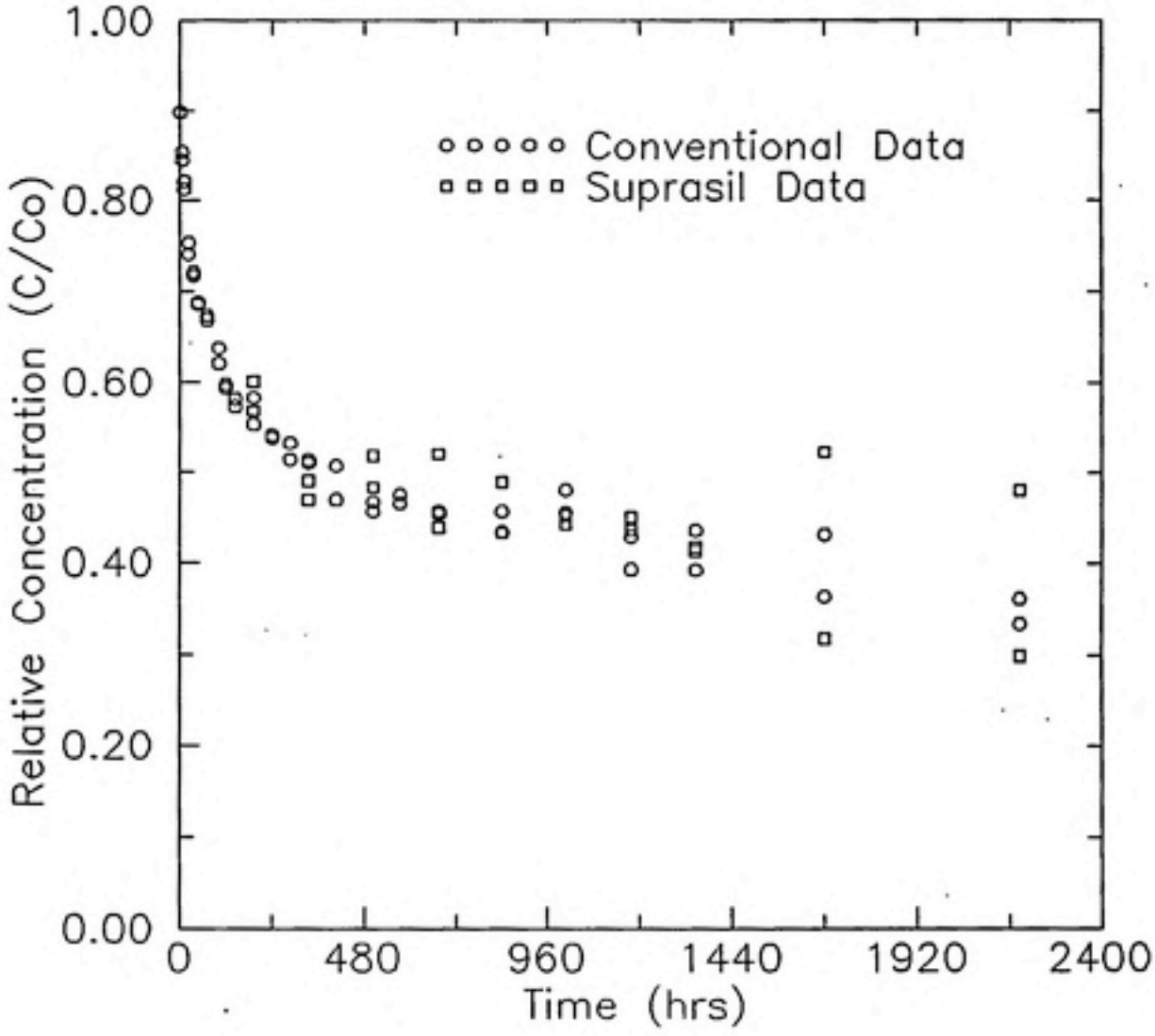

Figure 4-8 Sorption kinetic data for Srp-1 using conventional and Suprasil™ methods.

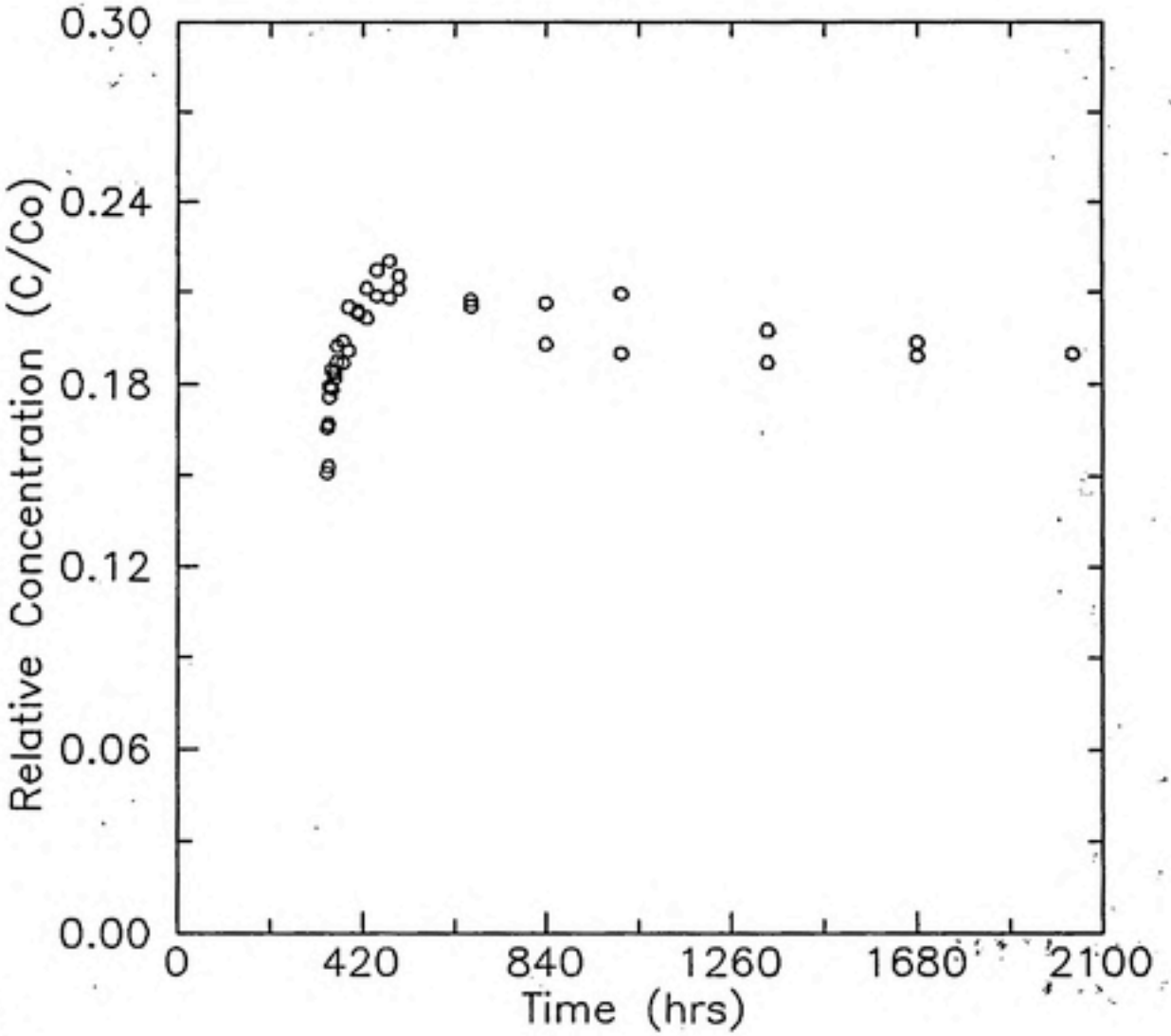

Figure 4-9 Desorption kinetic data of Dsrp-2.

4.1.2 Column Experiments

Two sorption/desorption column experiments were performed. These experiments each consisted of a step-up sorption experiment, a step-down desorption experiment, and a tracer test to determine the column dispersion. For each column experiment data was taken using both the conventional grab sample method and the fiber optic sampling method. The time for the grab sample data point was assigned to be the median time between samples. Both of the methods were described in detail in Section 3.2.5 and 3.3.3.1. The pertinent parameters for the two experiments are listed in Table 4-3.

4.1.2.1 First Column Experiment: Col-1, Trc-1

Figure 4-10 is a plot of the relative concentration of diuron through time during the sorption and desorption experiments as obtained by grab sample data. The raw absorbance was corrected for interfering humic absorbances as described in Section 3.2.5. The figure shows that equilibrium conditions have not been reached on the step-up portion of the experiment because the relative concentration is still changing with respect to time at approximately 2000 minutes and is not yet equal to 1.0. The step-down portion is also not at equilibrium because there is still a residual concentration of diuron in the system. However, the relative

concentration of diuron is changing only slightly with respect to time over this time scale.

Table 4-3 Column Parameters	Column-1 Parameters	Column-2 Parameters
Col-1, Trc-1		
Average Diameter (cm)	2.4	2.4
Average Length (cm)	7.65	7.65
Density of Wagner Material (g/ml)	2.673	2.673
Density of Glass Beads (g/ml)	2.477	2.477
Top Layer Average Length (cm)	1.65	1.63
Top Layer Mass (g)	10.835	11.615
Wagner Layer Average Length (cm)	4.3	4.35
Wagner Layer Mass (g)	35.0	35.0
Bottom Layer Average Length (cm)	1.7	1.67
Bottom Layer Mass (g)	11.75	11.75
Total Average Porosity	.358	.357
Column		
Tubing Volume in System (ml)	8.741	8.200
Pore Volume in System (ml)	6.359	6.585
Average Flow (ml/hr)	12.183	11.804
Tracer		
Tubing Volume in System (ml)	2.704	2.704
Pore Volume in System (ml)	12.396	12.081
Average Flow (ml/hr)	12.274	12.274

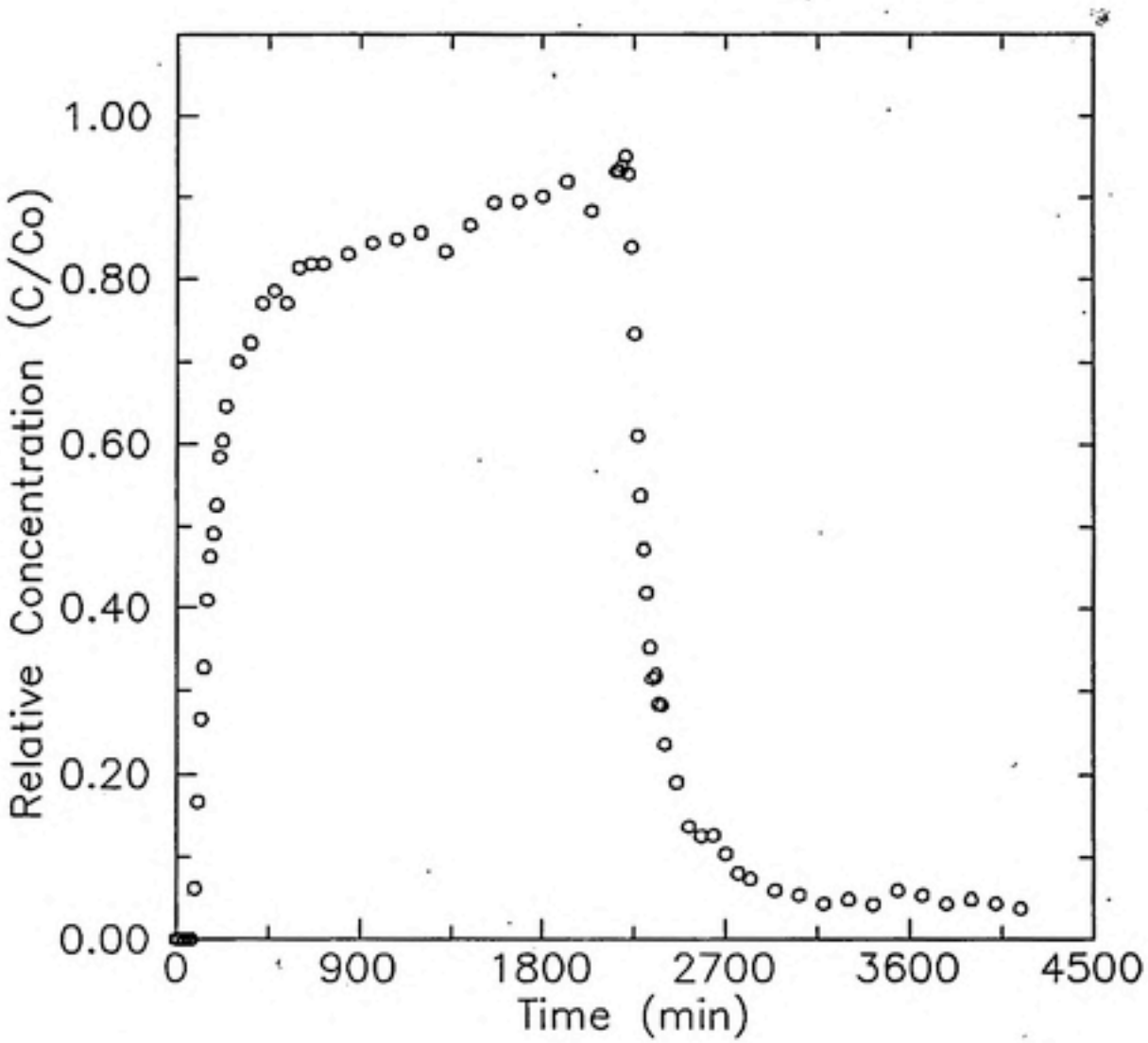

Figure 4-10 Column-1 grab sample diuron data.

Figure 4-11 is a plot of the relative concentration of sodium azide through time for the step-up tracer experiment. It was assumed that the amount of leachable NOM in the system was small in comparison with sodium azide by this time, and the residual diuron concentration would not change over the time frame of this experiment. Therefore, the absorbance data was simply calibrated to sodium azide standard concentrations. It can be seen that equilibrium is reached by the conservative tracer in this experiment.

Figure 4-12 is a plot of the raw absorbance data at 248 nm through time obtained from the fiber optic spectrophotometer. By looking at the end of the desorption part of the experiment it can be seen that absorbance values are increasing. It was determined that this behavior was due to error induced by the instrumentation. This error and the signal analysis techniques used to correct the data are discussed at length in Section 4.2.

After the signal analysis techniques were applied to the fiber optic data, this data could be compared to the data obtained from the grab sample/conventional UV-VIS spectrophotometer method. Figure 4-13 is a plot comparing the two spectroscopic methods after signal analysis and systematic instrument error treatment.

Figure 4-14 is a comparison of the signal processed fiber optic data and the grab sample data for the tracer test. Grab sample data were only taken for the step up

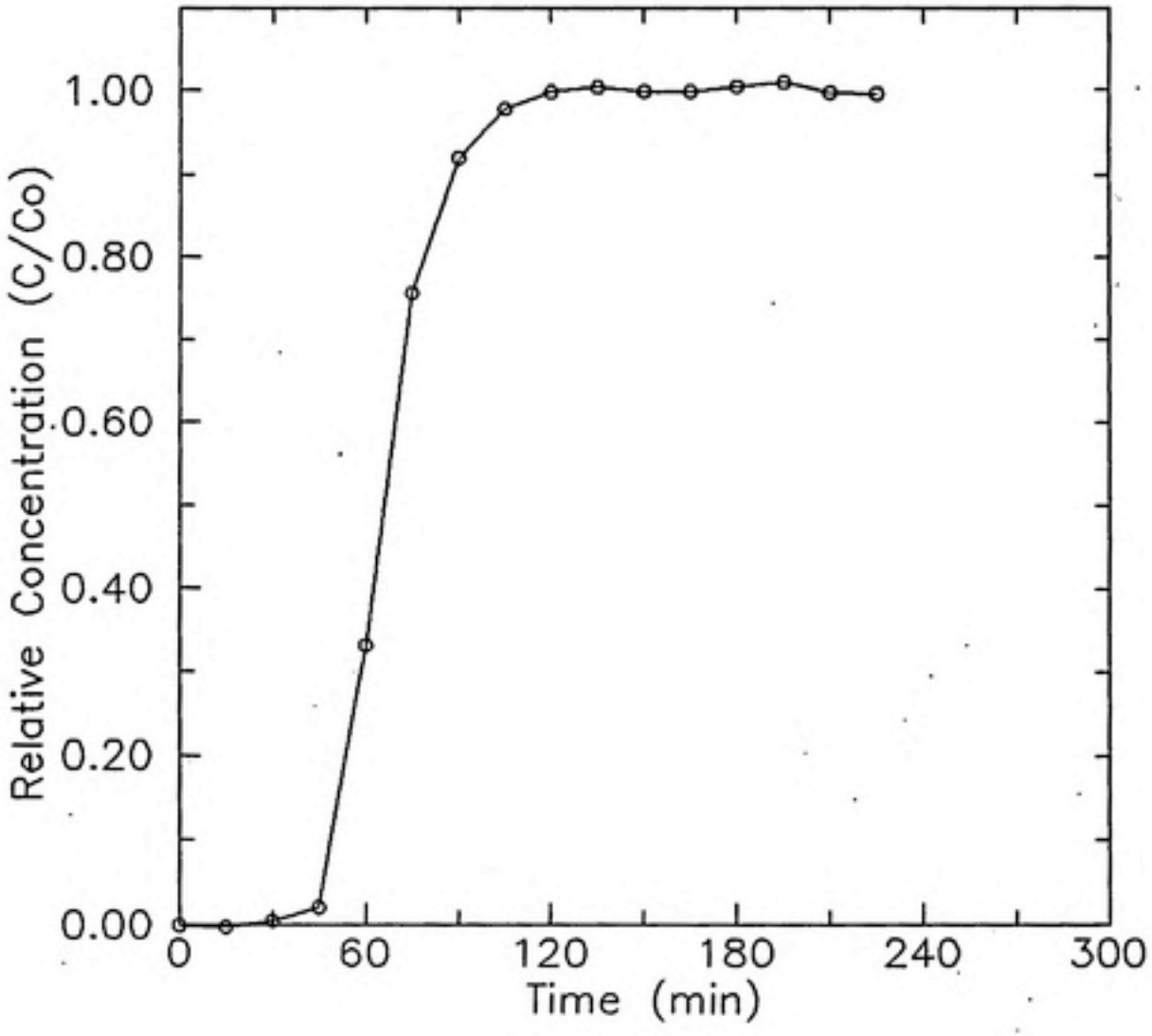

Figure 4-11 Column-1 grab sample tracer data.

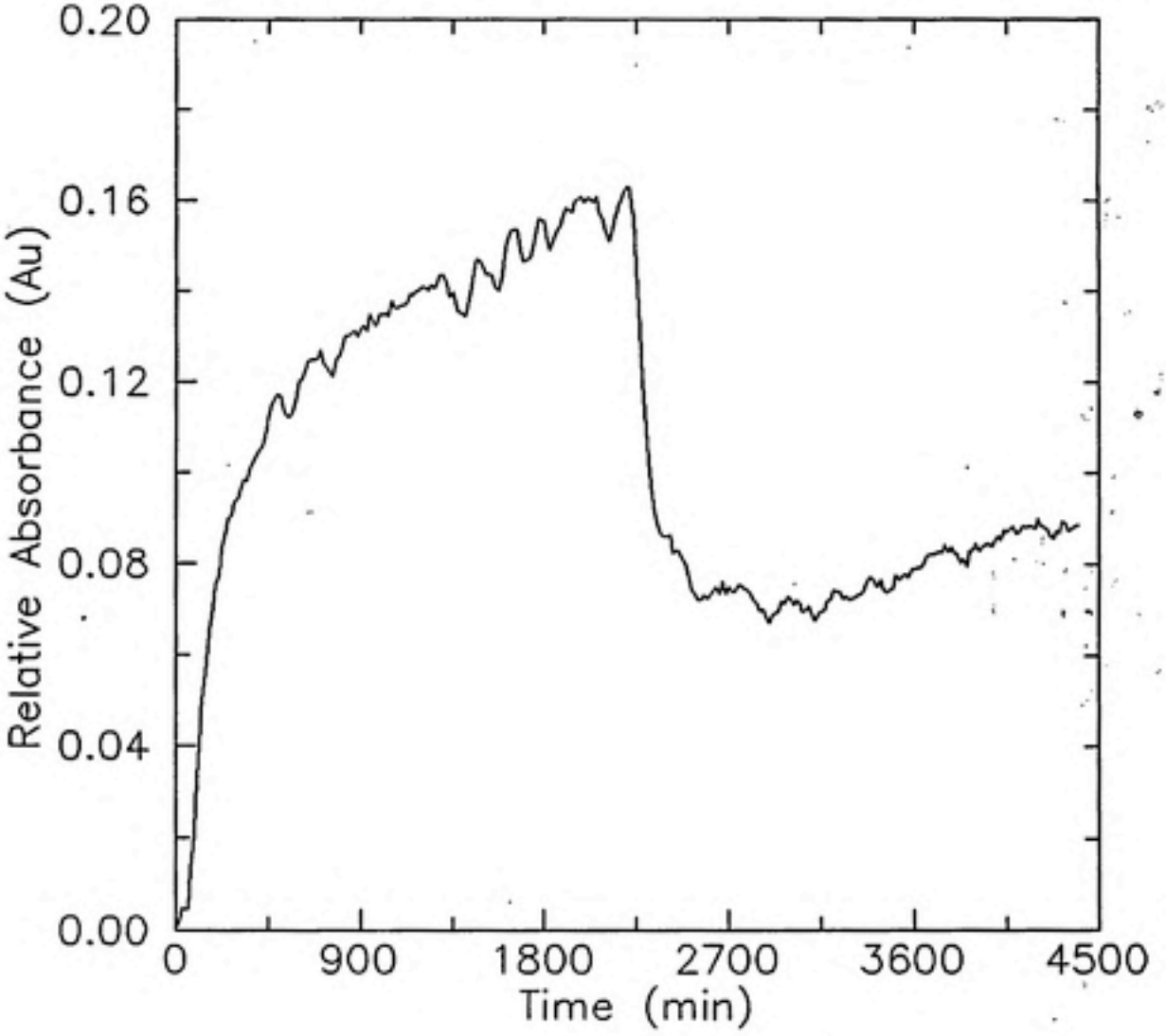

Figure 4-12 Column-1 raw fiber optic diuron data.

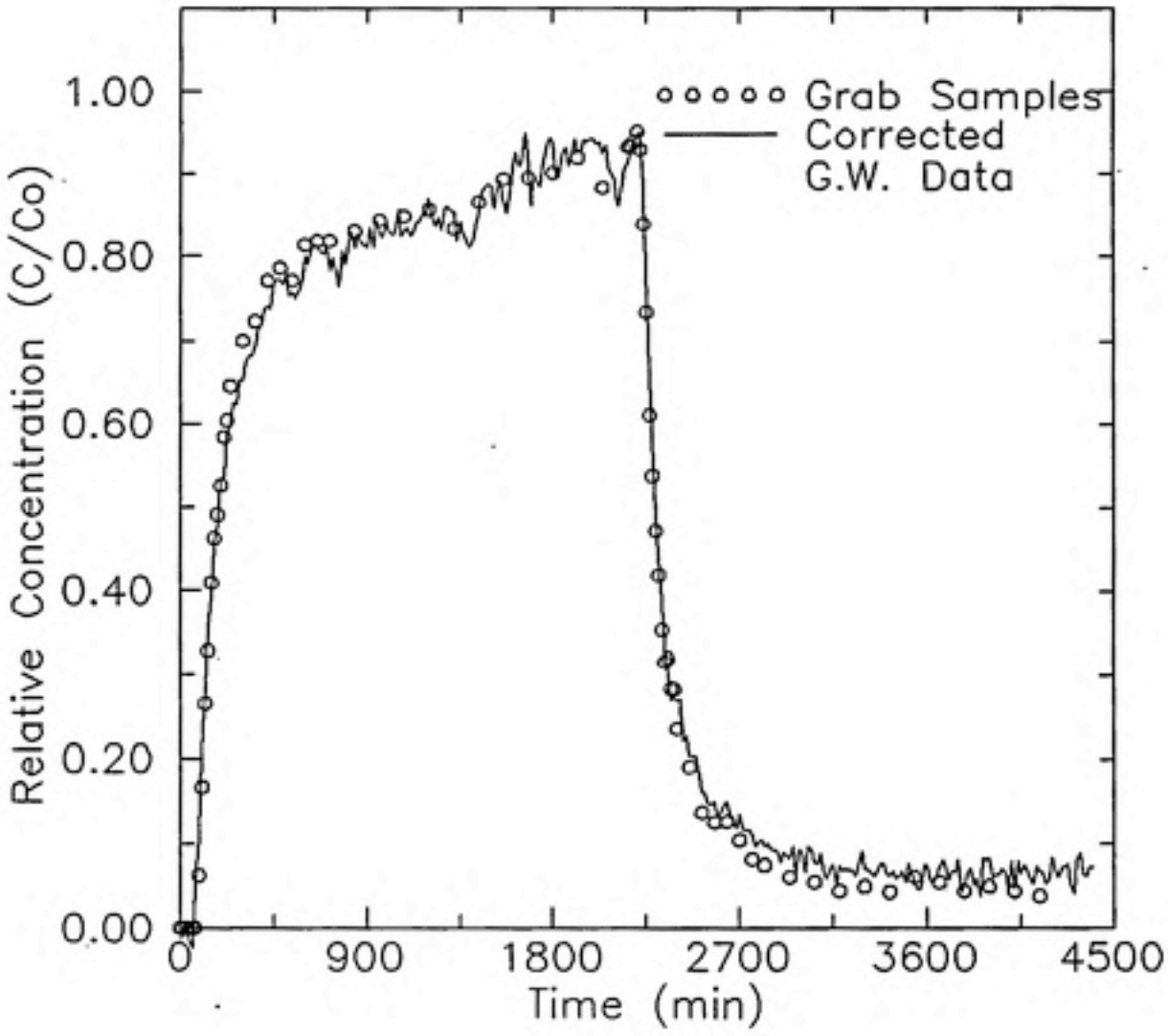

Figure 4-13 Column-1 comparison of grab sample diuron data with corrected fiber optic diuron data.

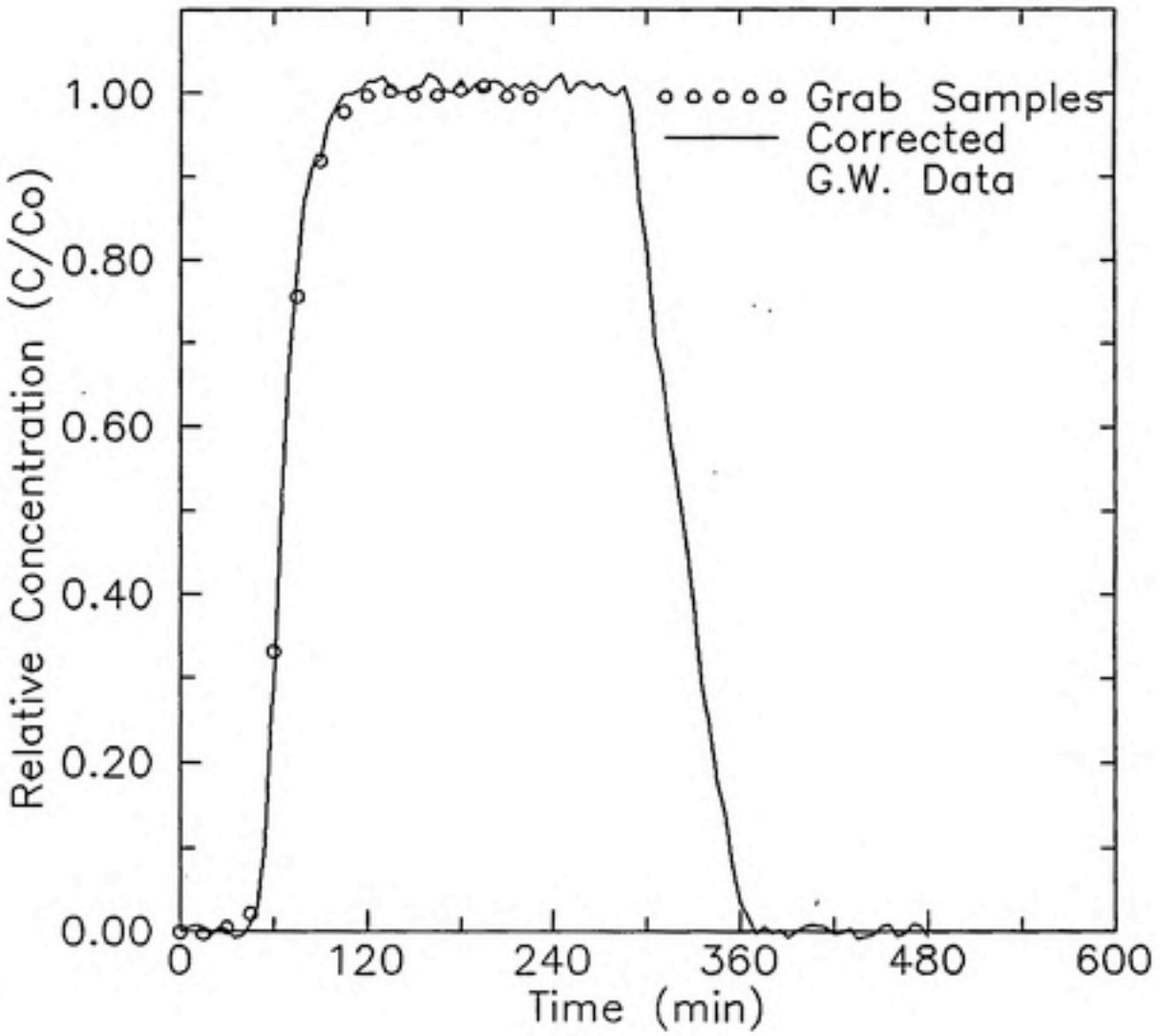

Figure 4-14 Column-1 comparison of grab sample tracer data with corrected fiber optic tracer data.

portion of the test. This plot shows good correlation of the two methods. A dispersion value for the column was obtained from the tracer data by comparing an analytical solution to a one dimensional column (Bear, 1976) with this data. Figure 4-15 is a plot of the analytical solution compared to the fiber optic and grab sample data. A dispersion value of 0.020 cm^2/min was found for this column and these flow conditions.

4.1.2.2 Second Column: Col-2, Trc-2

The second column experiment was performed after the deuterium light source on the fiber optic spectrophotometer was replaced. Some signal processing of the data was still required but the instrument error was much smaller in this experiment than in the first column experiment. A linear fit was satisfactorily used to adjust for this instrument error. In this experiment only three grab samples were evaluated before the fiber optic data were processed. The three samples were the first sorption sample, the first sample after the desorption experiment was started, and the last desorption sample. Since the sorption and desorption experiments were consecutive, the first desorption sample was assumed to be representative of the peak concentration of the system during the step up portion of the experiment. The fiber optic data were then processed as described in

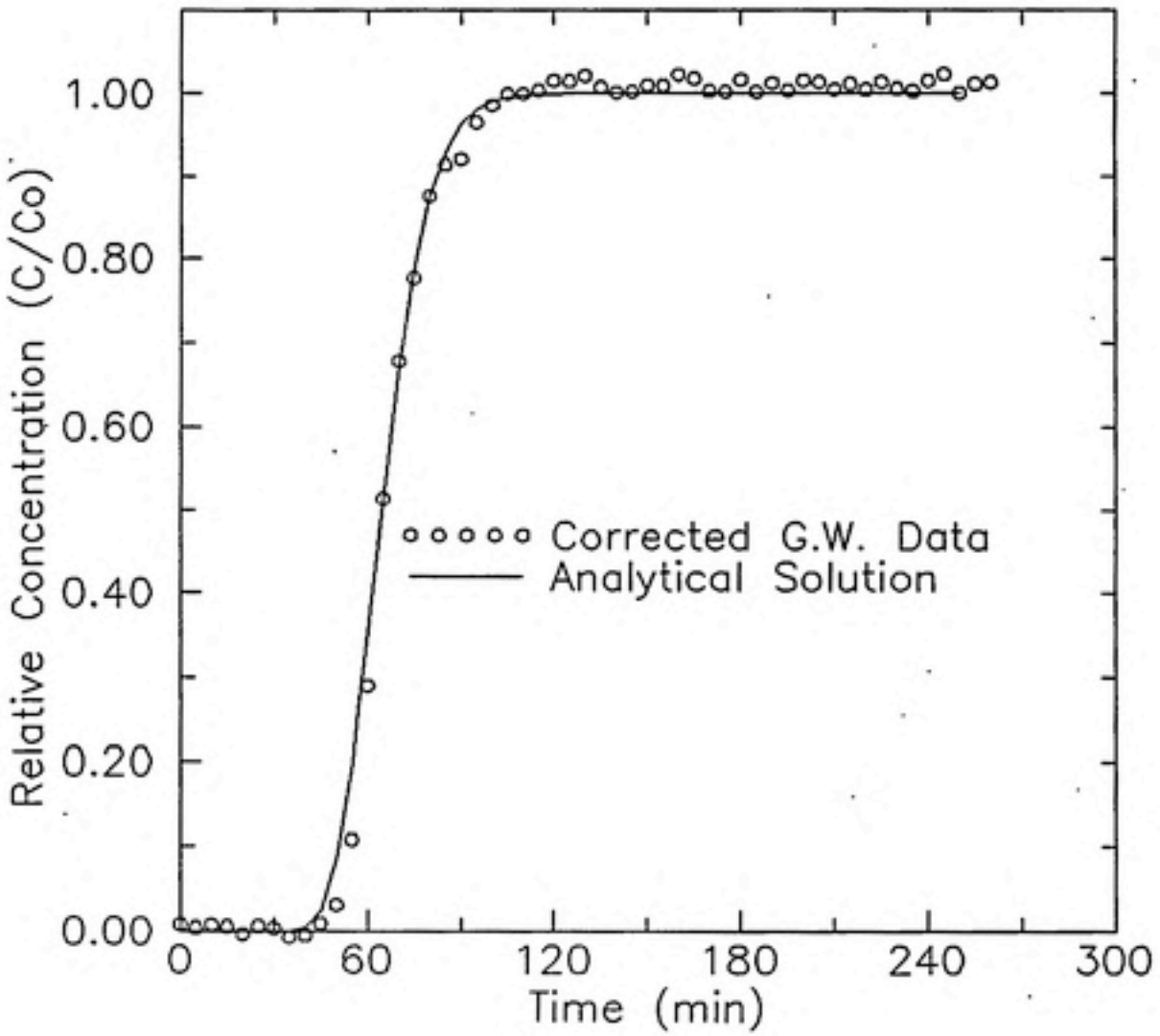

Figure 4-15 Column-1 comparison of analytic solution of tracer and corrected fiber optic data.

Section 4.3 and referenced to the peak grab sample. The rest of the grab samples were then analyzed by the conventional spectrophotometer and compared with the processed fiber optic data. This was done to eliminate human bias from the data analysis. Figure 4-16 is a comparison plot of the fiber optic data and the grab sample data.

Figure 4-17 is a plot comparing the two methods for the tracer test. The time scale shows the slight discrepancies between the two methods more distinctly in this plot. These differences are discussed in greater detail in Section 4.3.4.

4.2 Instrument Variation and Signal Processing

4.2.1 Instrument Variation

As discussed in Section 2.1, UV absorption spectroscopy requires an ultraviolet source, a sampling region and a detector. In these experiments problems with source variation were encountered with both the conventional UV-VIS spectrophotometer and the fiber optic spectrophotometer.

The conventional spectrophotometers used for these experiments are described in Section 3.3.1. The Perkin Elmer instrument was used initially for roughly half of the experiments and the Hitachi was used for the rest. The

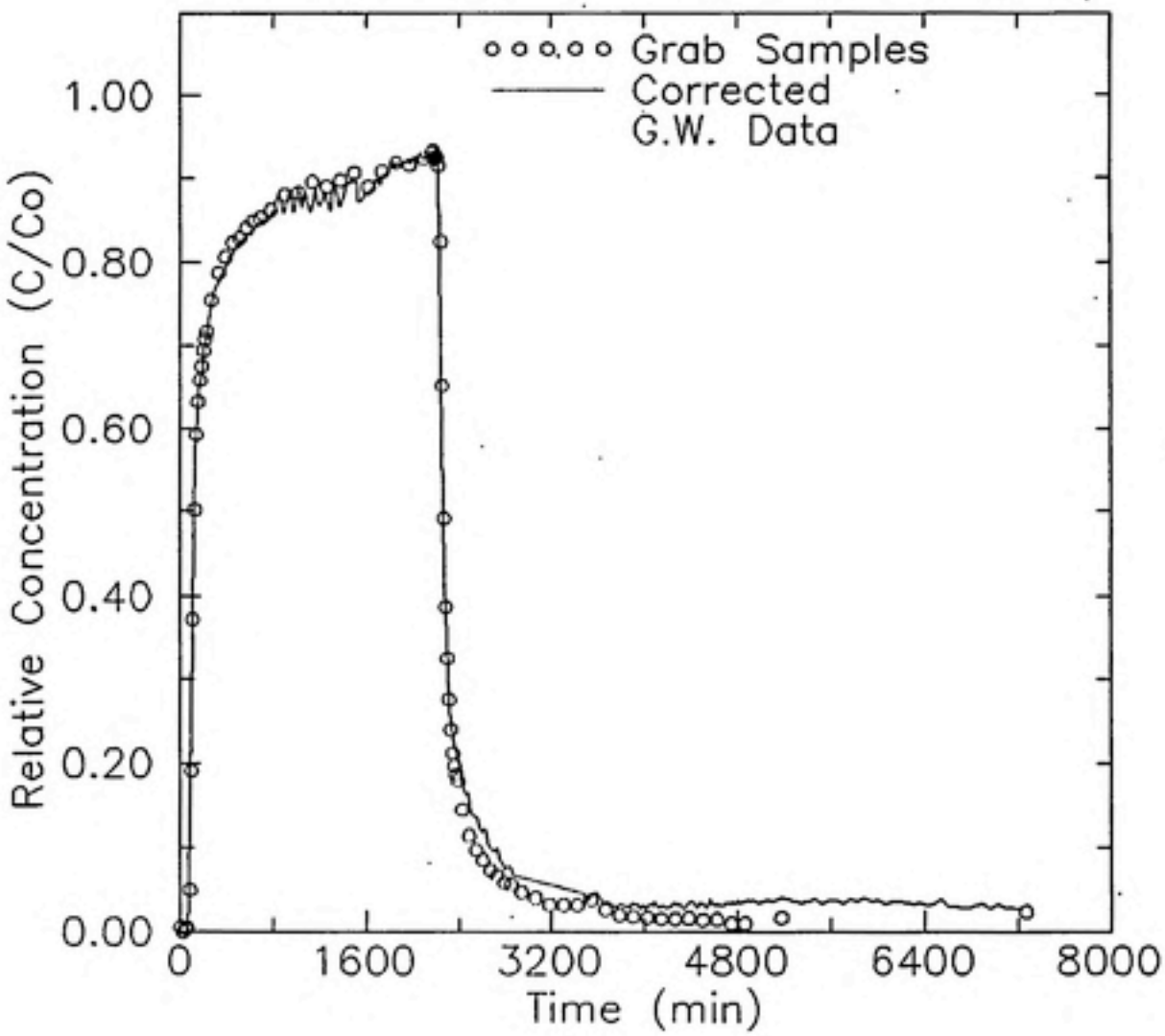

Figure 4-16 Column-2 comparison of grab sample diuron data with corrected fiber optic data.

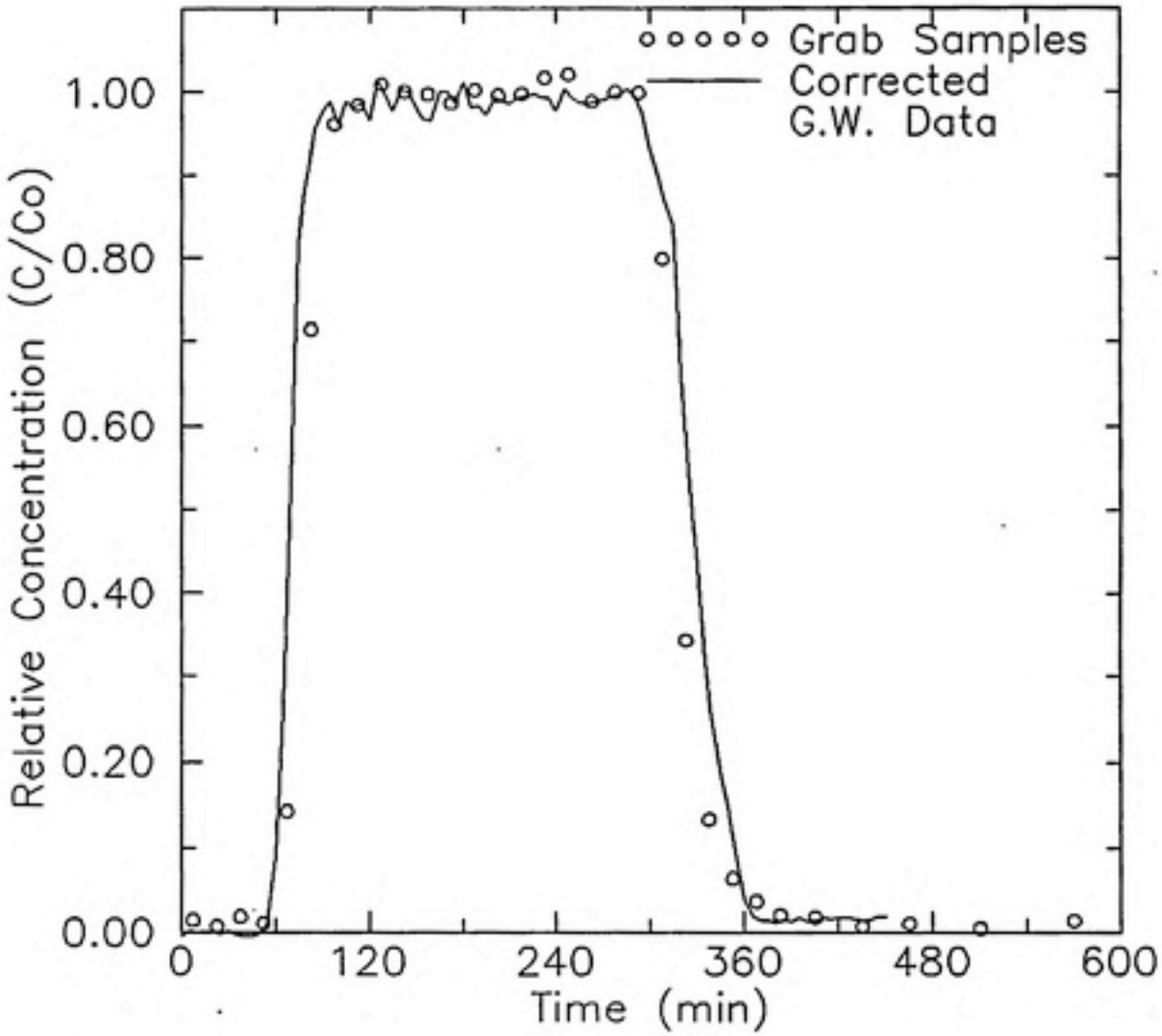

Figure 4-17 Column-2 comparison of grab sample tracer data with corrected fiber optic tracer data.

Perkin Elmer instrument was abandoned because it began to show problems distinguished by a diminished sensitivity for low absorbance measurements. The reason for this lack of sensitivity became apparent after research was performed to determine the causes of source intensity variation in the fiber optic spectrophotometer. All three instruments use deuterium sources to provide the probe beam for the spectral region used in this work (190-350 nm). From the literature of one of the leading manufacturer's of the these lamps, Hamamatsu (Hamamatsu Corporation, Bridgewater, NJ), deuterium lamps have a limited useful lifetime. This lifetime is defined as the time during which the lamp's output intensity remains greater than 60% of its original output power for a representative wavelength. The decrease in intensity during the useful lifetime period is usually roughly linear but unique for all wavelengths. Average lifetimes for lamps used in these experiments is on the order of 2000 hours. After the useful lifetime period, the output intensity usually decreases exponentially.

The predominant cause of the output intensity decrease has been determined by Hamamatsu to be solarization of the fused silica or quartz envelope surrounding the electrodes and the deuterium gas (conversation with Earl Hergert, Hamamatsu Corp., 5/22/91). Solarization is a process by which metal impurities in materials such as silica or quartz react with incident ultraviolet light and cause a clouding

of the otherwise optically clear material. The degree of solarization has been correlated to the time of the exposure, and to the intensity and wavelength of the ultraviolet light. The theoretical mechanisms of this process are not well understood and are beyond the scope of this work.

The two conventional spectrophotometers correct for the variation in source output intensity by splitting the source beam into two paths. One of the paths provides a cuvette holder for a sample containing a reference material such as DDI water or the solvent used in the experiment. The absorbance of experimental samples are then measured with respect to the reference cell. The absorbance value read by the operator of these two instruments is actually a reference corrected absorbance. The dynamic range of the instrument is usually defined by the low sensitivity limits of the detector, and the source intensity, as seen with respect to the reference cell. The reference cell is defined as having absorbance equal to zero. Although the low intensity limits of the detector rarely change, the source intensity can decrease as described above. This decreases the dynamic range of the instrument and therefore the range of measurements possible. One of the effects of the decreased dynamic range is a shift into the detector's non-linear response region. Because of the instruments'

data from the first column experiment indicated that fiber optic solarization was not the only source of error. This is illustrated in Figure 4-12 by the increase in absorbance in the tail of the desorption period. It was finally determined through component by component testing that the deuterium lamp was the major source of intensity decrease. A new lamp was ordered and this was used for the second column experiment.

4.2.2 Signal Processing

Raw data correction was required for all of the experiments. These corrections were either accomplished experimentally, by including blank samples along with data samples in an experimental set, or mathematically, by making assumptions about a data set. The use of the blanks in correcting measurements is described in Section 3.2.2. The mathematical methods used for correcting the column grab sample data where blanks could not be used and the data acquired from the fiber optic spectrophotometer are described below.

4.2.2.1 Grab Sample Corrections

The column grab sample absorbance data was corrected by subtracting the absorbance due to a decreasing NOM

concentration as the experiment progressed and NOM from the solid material was flushed out of the system. This decrease in NOM concentration was assumed to be linear with respect to time. It was assumed that the diuron concentration for the first grab sample was 0.0 mg/l so that any absorbance measured was due to NOM. At the end of the desorption experiment, it was assumed that the NOM was completely flushed from the system and the only absorbance source present was residual diuron. The absence of NOM at the end of the desorption period was confirmed by gas chromatography. Using these two conditions, and assuming a linear removal of NOM, the grab sample absorbances were corrected by:

$$Abs_{c,t} = Abs_t + Abs_0\left(\frac{t}{\tau} - 1\right) \qquad (4\text{-}2)$$

where $Abs_{c,t}$ is the corrected absorbance at a given time for a given wavelength, t is the time of the measurement, τ is the total time of the sorption/desorption experiment, and Abs_0 is the absorbance measured at time 0 (only NOM). The corrected absorbance was calibrated to diuron standard concentrations. The concentration values were then normalized and plotted.

4.2.2.2 Fiber Optic Data Corrections

There are three major contributors to the systematic error of the system. The first and main source of error was attributable to a deterioration of the deuterium light source. The output intensity of these sources decrease as a function of time and wavelength. Unlike the conventional UV-VIS spectrophotometers used in these experiments, the fiber optic spectrophotometer has no internal correction mechanism for calibrating for this decrease in intensity. The instrument is calibrated before an experiment by taking a reference scan over the wavelength region of interest. The absorbance values from this scan are used as the zero reference points for subsequent scanned absorbance values. Therefore any absorbance changes due to instrument variations following the reference scan are not accounted for.

The second source of error was an increased absorbance due to fiber optic solarization. This source of error was anticipated and was of much less concern in comparison with the deuterium lamp deterioration. The lamp and the fiber problems were discussed in Section 4.2.1.

The third source of error was actually a conglomeration of any electronic effects that produced instrument fluctuations outside of the first two sources of error. All three sources of error were corrected for by signal analysis

techniques. The computer programs written for this are included with this report in a 5.25 inch floppy disk. The techniques are described below.

To correct the data from the first column experiment two methods were used. The first assumed a simple linear decrease in intensity seen at the sample over time with respect to wavelength. The measured increase in absorbance due to these instrument effects is given by:

$$\varepsilon_t = m * t \qquad (4\text{-}3)$$

where ε_t is the increased absorbance in Au at time t, m is the general coefficient of output intensity loss, and t is the time that the equipment is on.

The second method assumed a linear decrease in lamp intensity and a non-linear increase in absorbance due to fiber optic solarization. Both of these effects were determined with respect to wavelength and time. The fiber optic time variable was the cumulative time that the fiber was exposed to the UV light (when the shutter was open). The increase in absorbance is then given by:

$$\varepsilon^{1}{}_{c} - (m^{1} * t) + \alpha * (I_{o} - m^{1} * t) * \tau \qquad (4\text{-}4)$$

where m^1 is the coefficient of output intensity loss due to deuterium lamp solarization, t is the time the equipment is on, α is the coefficient of intensity loss due to fiber solarization, I_o is the initial deuterium lamp output intensity at the beginning of the experiment, and τ is the cumulative time that the fiber has been exposed to the UV light since the beginning of the experiment.

The end portion of the desorption experiment was used to determine the instrument's contribution to absorbance. It was assumed that during this portion of the experiment, there was no change in absorbance. This assumption is a fairly good one because of the extremely small changes in solute desorption at this point. Figure 4-18 shows the time region used and the change in concentration as measured by the grab samples method.

Both correction equations were applied to the fiber optic data from this time region and a nonlinear statistical analysis was performed using Systat™. From a comparison of the fits it was determined that the correction described by equation 4-4 provided a slightly more accurate fit to the data. This was based on a comparison of the mean squared errors (MSE) of the two fits. Table 4-4 gives the statistical parameters obtained using the two fits.

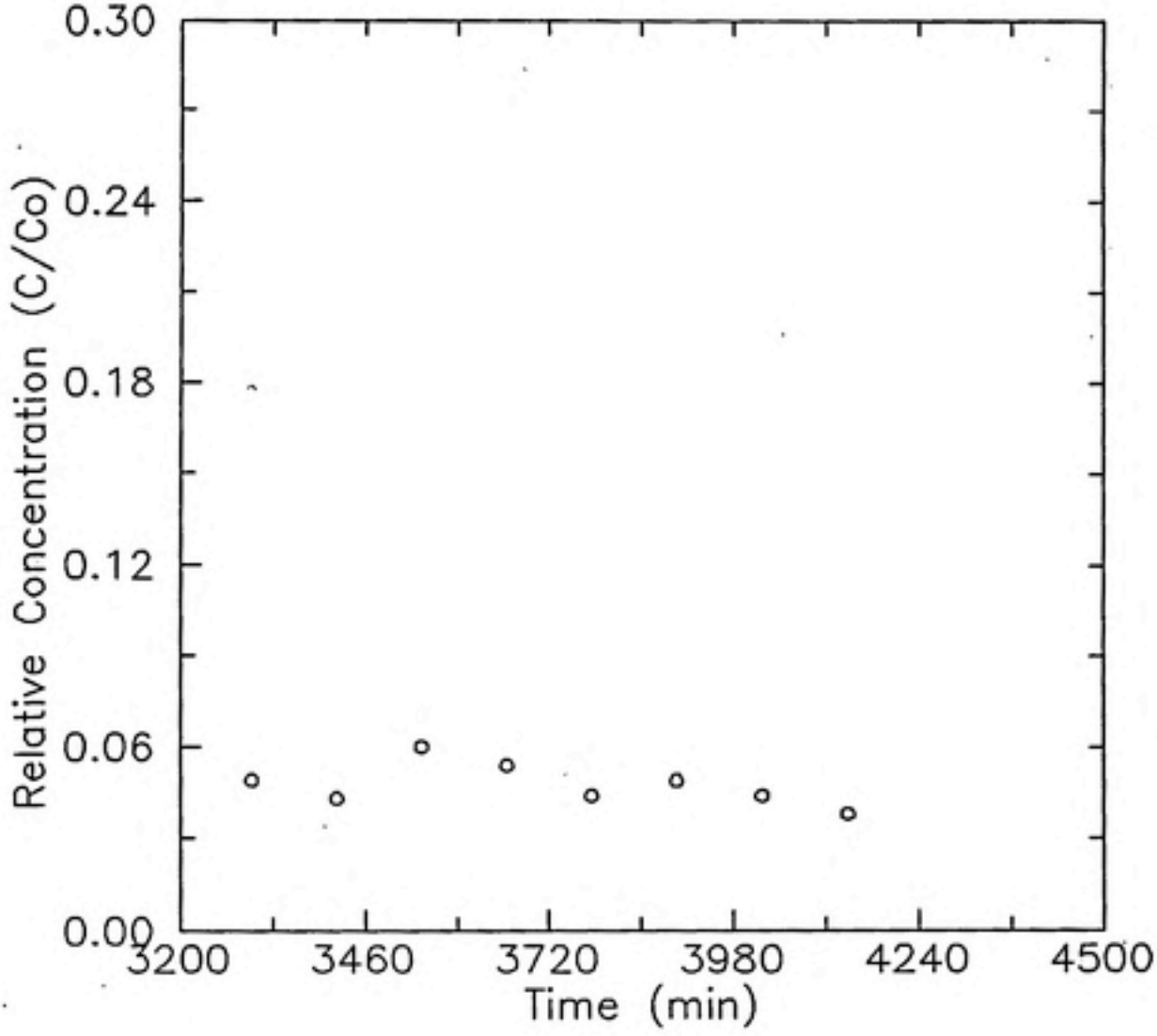

Figure 4-18 Portion of Column-1 experiment used for correction.

Table 4-4	Statistics for Column Error Correction	
Linear Fit		
248 nm	Residual MSE = 2.447E-06	
Constant	Estimate	95% Confidence
m	1.476E-05	1.376E-05,1.577E-05
265 nm	Residual MSE = 2.907E-06	
Constant	Estimate	95% Confidence
m	1.762E-05	1.652E-05,1.871E-05
Non-linear Fit		
248 nm	Residual MSE = 2.443E-06	
Constant	Estimate	95% Confidence
m	-5.021E-05	-2.255E-04,1.251E-03
alpha	-2.592E-05	-9.608E-05,4.424E-05
265 nm	Residual MSE = 2.901E-06	
Constant	Estimate	95% Confidence
m	-5.739E-05	-2.233E-04,1.085E-04
alpha	-2.996E-05	-9.649E-05,3.657E-05

Figure 4-19 is a plot of the raw experimental data for two wavelengths, 248 nm and 265 nm. The general decrease in intensity seen at the sample is exhibited by a general increase in the absorbance at both wavelengths over the course of the experiment. Figure 4-20 is a plot of the raw experimental data over the time period used for determining corrective fits compared to the two fits (linear and non-linear) for the wavelength of 248 nm. Both fitting equations were forced to intercept the value of relative absorbance of 0.0 at time 0 to account for the residual concentration known to be present in the latter portion of the desorption experiment. Figure 4-21 is a plot of the raw data at 248 nm and the non-linear corrective curve with zero intercept.

The raw experimental data was modified by subtracting the absorbance values obtained from the corrective fits for a given wavelength. Figure 4-22 is a plot of the raw data in comparison with the corrected data for 248 nm and 265 nm.

Finally instrument fluctuation and extraneous absorbers were accounted for by subtracting data obtained from a wavelength on the skirt of the main diuron absorbing mode (265 nm) from data obtained at the peak of the diuron absorbing mode (248 nm). This was done under the assumption that any instrument fluctuations other than the source intensity problems discussed earlier should occur similarly at both wavelengths. In addition extraneous UV absorbance

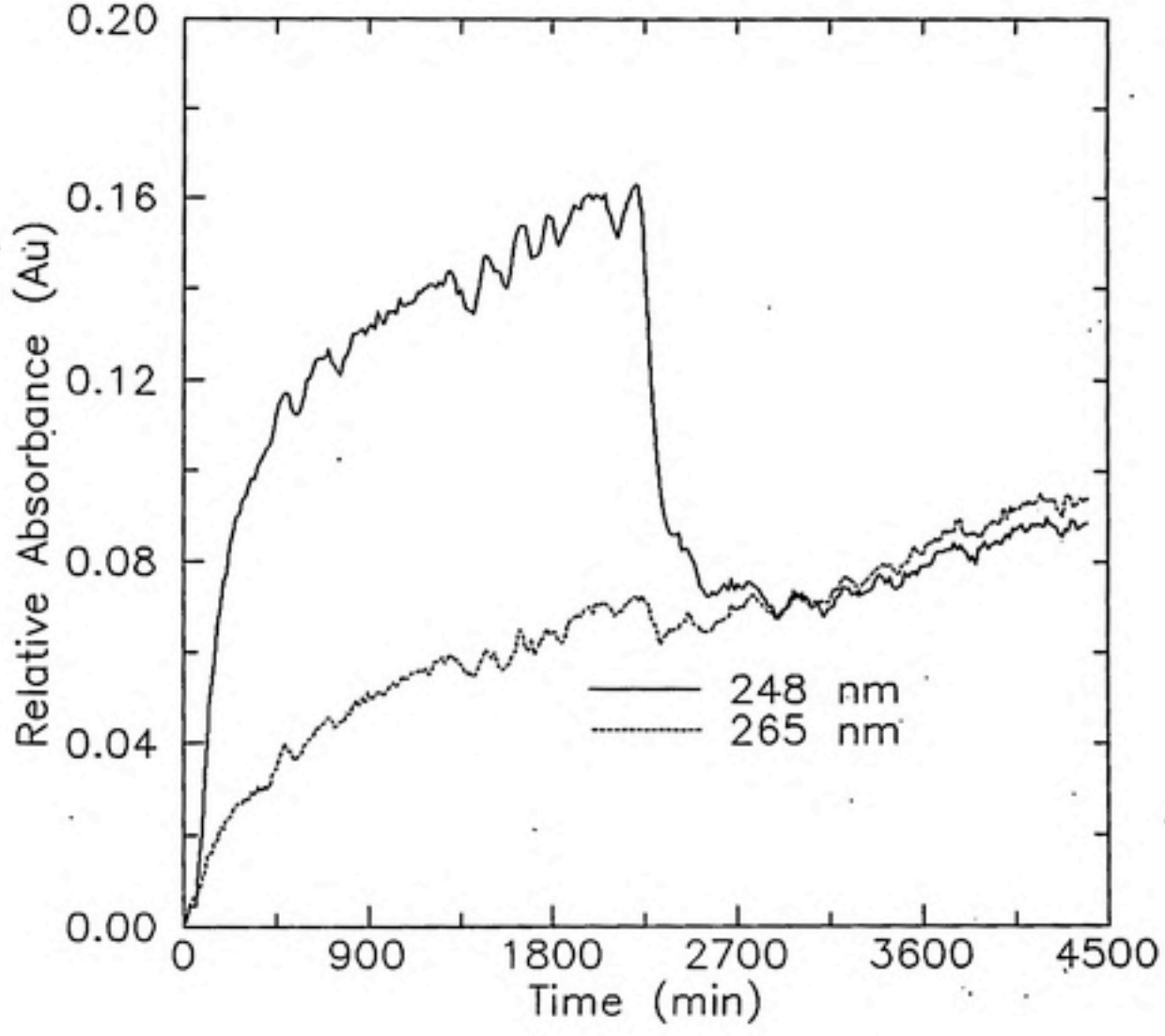

Figure 4-19 Column-1 raw fiber optic data at two wavelengths.

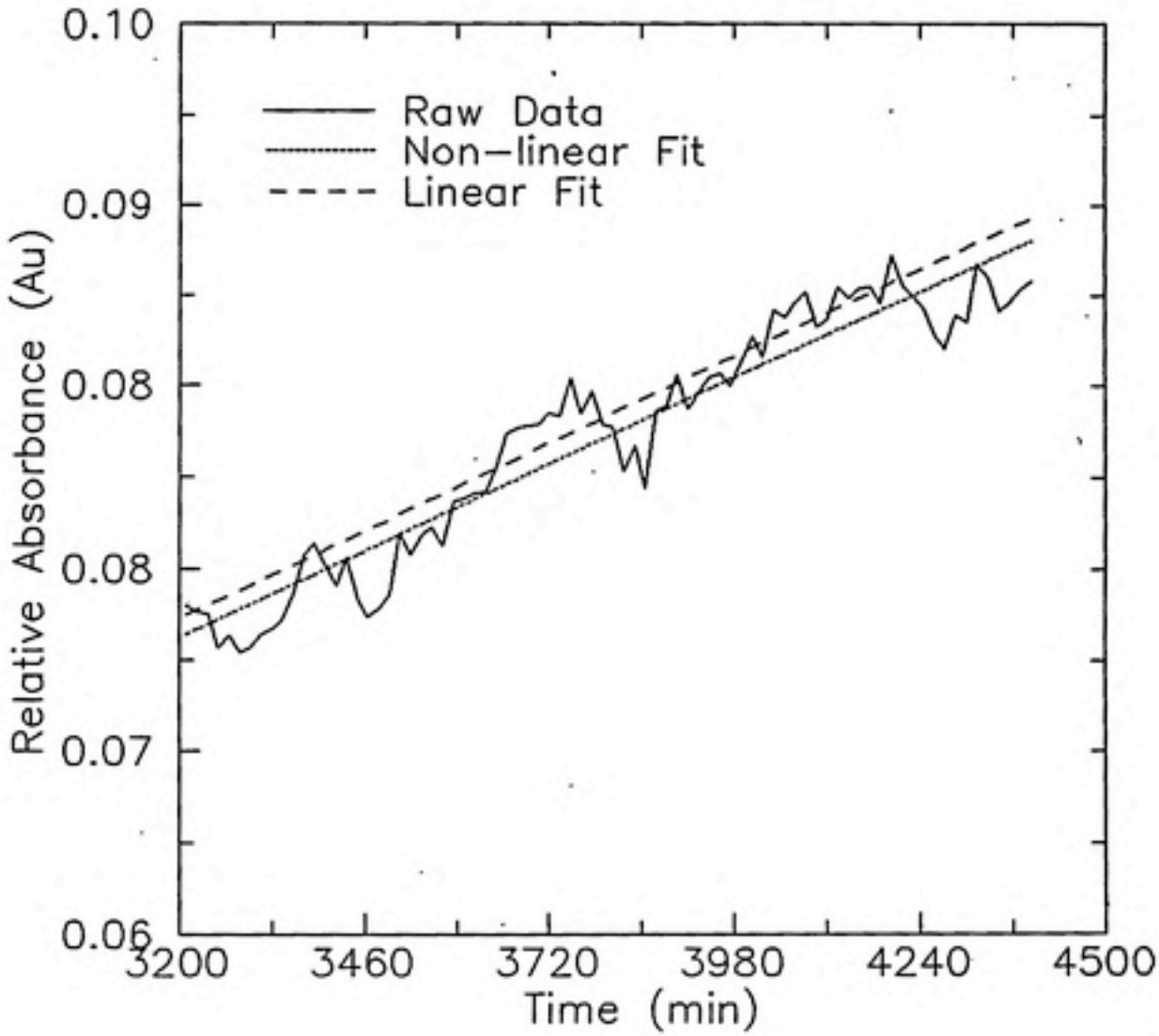

Figure 4-20 Linear and nonlinear fits to raw data.

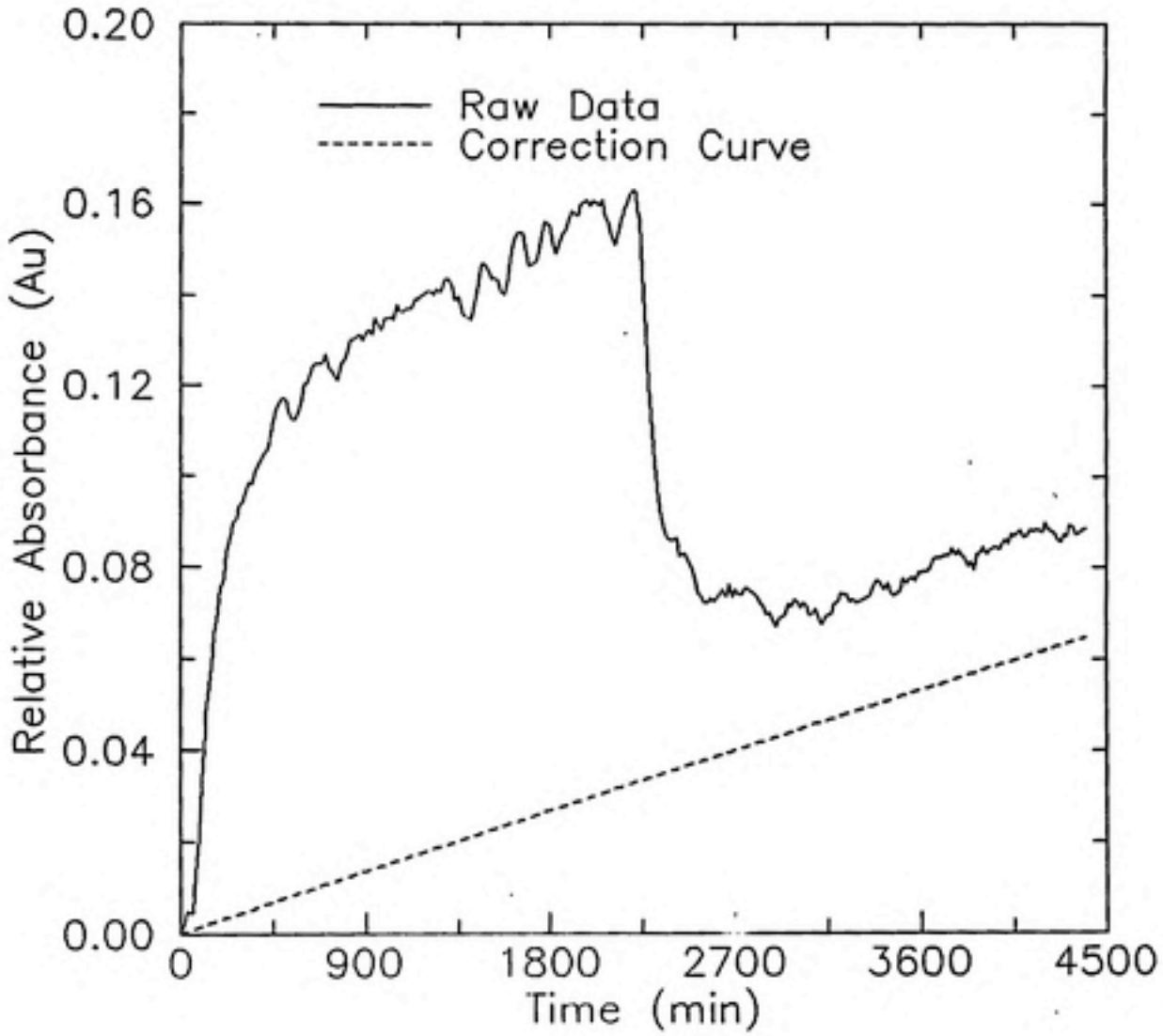

Figure 4-21 Comparison of raw data and correction curve.

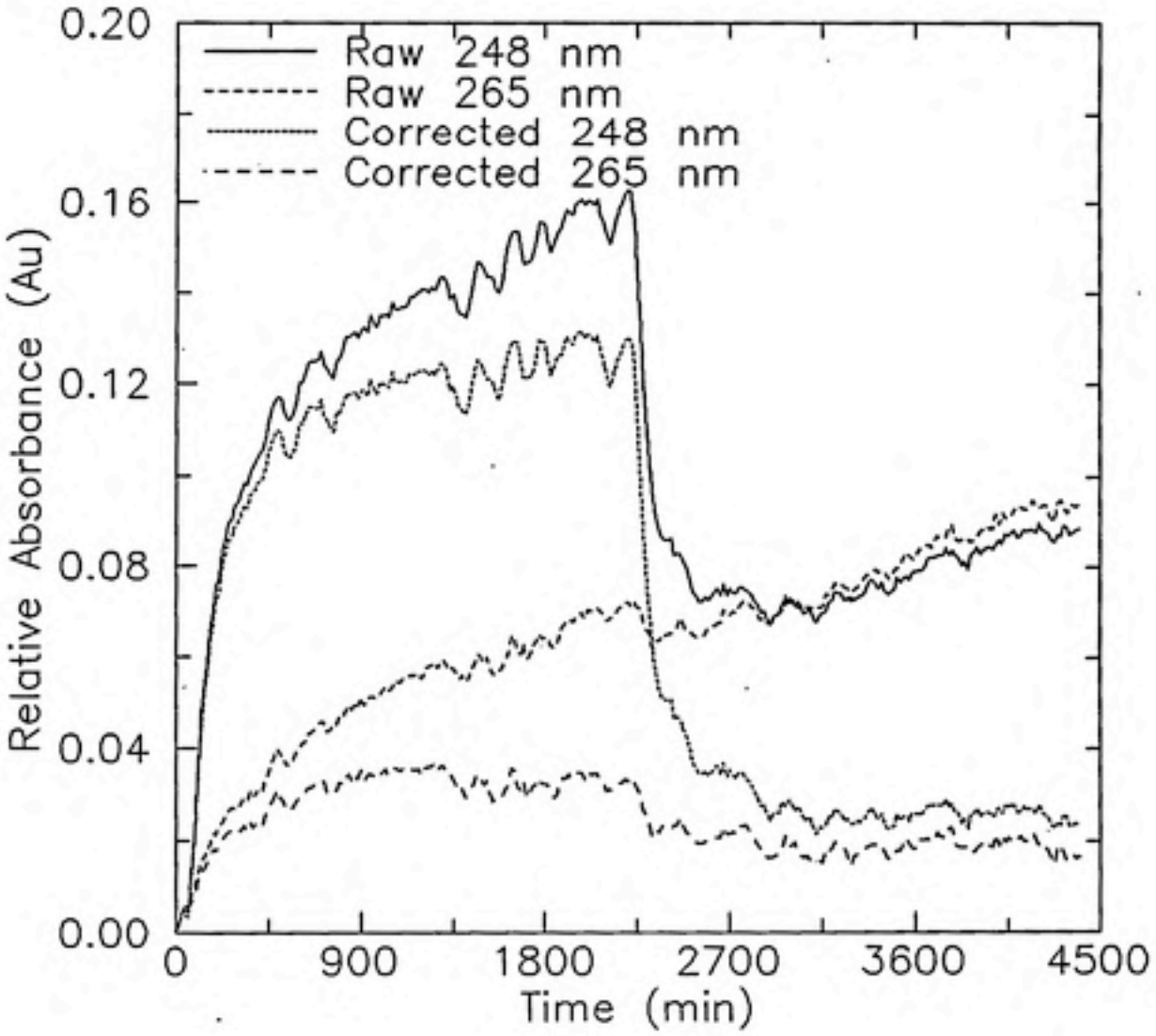

Figure 4-22 Comparison of raw data and corrected data at two wavelengths.

sources such as NOM will have similar values at these two wavelengths because these wavelengths are so far from the characteristic NOM peak occurring below 220 nm. Figure 4-23 compares the plots for the delta absorbances (Abs(248 nm) - Abs(265 nm)) for the uncorrected and corrected data. The uncorrected (raw delta) plot clearly shows that the change in source intensity is wavelength dependent by falling significantly below the relative absorbance axis in the desorption portion of the experiment.

The fiber optic absorbance data was converted to relative concentration data by assuming that the maximum absorbance value was equivalent to the maximum concentration obtained from the grab sample data. All other absorbances from the fiber optic data were referenced from that peak point.

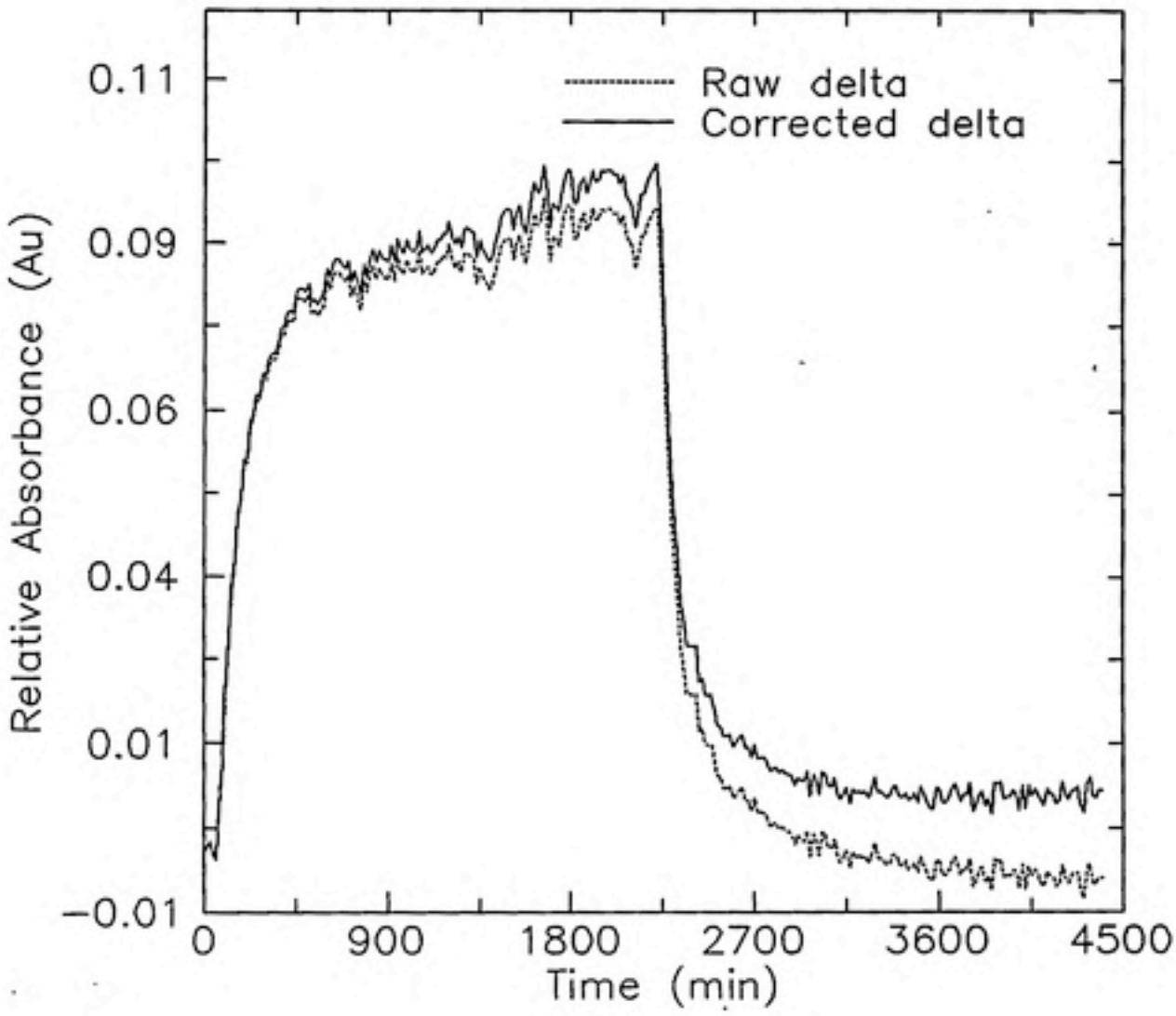

Figure 4-23 Comparison of raw delta plot and corrected delta plot at 248 nm.

4.3 Discussion of Experimental Results

4.3.1. Equilibrium distribution experiments

The Freundlich model fit the data from Eql-2 well as was shown in Figure 4-1. Chang (1989) found a more linear fit to the diuron equilibrium distribution data using similar solid materials. These experiments used much shorter equilibration times, although Pedit and Miller (1990) have shown that equilibration time is not sensitive to linearity, using a surface diffusion model. The next longest equilibration time found for diuron was performed by Chang (Chang, 1989) using unwashed Wagner media. A Freundlich fit was found with exponent 0.657 for an equilibration time of 44 days.

The equilibrium parameters determined from Eql-2 are incorrect because the system had not reached equilibrium. This conclusion is supported by the sorption kinetic data Srp-1 which showed that equilibrium was not reached in this system at 91 days and Srp-2 which had not reached equilibrium after nearly six months. In addition, significant non-singular behavior was observed in the desorption data points obtained from Eql-2. This can be an indication that sorption equilibrium has not been attained. Chang found significant nonsingular sorption/desorption as well (Chang, 1989).

4.3.2 Kinetic Experiments

Sorption and desorption batch kinetic experiments are two types of experiments that can be used to isolate sorption/desorption from other contaminant fate and transport phenomena and help predict behavior that might occur in field situations. Sorption experiments correspond to a contaminant leak into an aquifer, and desorption experiments correspond to attempts to remediate the aquifer by pumping out the aqueous phase contaminant, then repumping the aquifer at a later time. Desorption experiments can also correspond to the desorption side of a pulse or transient input.

The sorption kinetic data from Srp-1 and Srp-2, demonstrate an initial rapid sorption followed by a slower sorption period. The rapid sorption period varied from approximately 480 hours for Srp-1 to approximately 720 hours for Srp-2. The length of the slower phase was not determined because the experiments were concluded before equilibrium was reached. This behavior is consistent with a rate controlled sorption model. Further work needs to be done to elucidate the mechanism of this behavior.

The desorption kinetic data from Dsrp-2 demonstrates an initial rapid desorption period followed by a slower resorption of solute. As in the sorption rate experiments, Dsrp-2 has not reached equilibrium after over 2000 hours.

4.3.3 Suprasil™ Bottle Kinetic Experiment

The Suprasil™ bottle method was primarily developed to satisfy the requirements of an experiment with an unknown and nearly unlimited time span. It was hoped that this method would allow accurate determination of the true sorption equilibration times for particular systems. This method also had the advantage of maintaining the same sample bottles throughout the experiment rather than relying on the similarity of a large number of identically prepared bottles that were each used for only one data point. The Suprasil™ bottle method's inherent advantage was the ability to make in-bottle UV absorbance measurements because of the high UV transmission properties of Suprasil™ in comparison with normal borosilicate glass. The only problems anticipated with the method were irregular reflection and refraction losses due to possible non-uniformities in the structure of the bottles. It was thought that these problems would be relatively minor and could be corrected by an average of measurements for each bottle. Unfortunately these problems were not minor. The variations in the glass did indeed present problems as anticipated. There were large discrepancies in absorbance values between even adjacent angular orientations. In addition, repeatability was poor. This was due to the nonuniformity of the outer diameter of

the bottles and the clamping configuration of the cell holders. The standard deviations for these points were on the order of 0.1 Au. From Figure 4-3, it can be seen that a 0.1 Au variability can translate into a large difference in extrapolated concentration.

The fiber optic Suprasil™ bottle method had additional problems. It was determined that the intensity of the deuterium source of the fiber optic spectrophotometer was decreasing over time. This behavior was discovered in the latter part of the Suprasil™ sorption experiment when performing the first column experiment. The lack of a stable reference due to the variability of the light reaching the sample made the determination of the sample's concentration too time consuming to accurately solve for the degree of precision that would be achieved. Therefore the data for the fiber optic part of the batch experiment is not given here. The variability of the light source in the fiber optic spectrophotometer was discussed in Section 4.2.1.

Another problem with the Suprasil™ bottle method was the possible degradation of the subsurface media from repeated centrifugation in order to separate the supernatant for measurement. Some researchers believe that centrifugation can damage and change the solid material (Bowman and Sans, 1985). This might lead to changes in the sorption parameters of the solid/solution system although

this could not be determined from the data shown in Figure 4-8.

A practical consideration that has not been discussed yet is the time required to acquire the data points necessary for the Suprasil™ bottle method. For the conventional spectroscopic method, approximately twenty data points were required for each bottle. In addition, a standard set required an additional twenty points per concentration. The total time required for this method was approximately 150 minutes per sample period compared to approximately 15 minutes per sample period for the conventional method. The fiber optic method required approximately 240 minutes per sample period. Analysis times for the Suprasil™ methods was also an order of magnitude larger than the conventional method.

Although the use of in-bottle measurements would be useful in determining true equilibrium points of slowly sorbing solutes (assuming small subsurface media degradation effects from multiple centrifugation), the method is not practical in the configuration described here.

4.3.4 Column Experiments

Data from both column experiments Col-1 and Col-2 support the theory that a rate limited sorption process has

occurred in this system. The rapid initial process followed by a much slower one is evident from both Figure 4-13 and 4-16. One change to the column experiments in the future would be performing the column tracer studies before the column experiment. This would eliminate the presence of residual solute in the tracer experiment. The residual solute did not affect the tracer results here because the rate of change in diuron concentration due to desorption at this time was of a much longer time scale than the experimental time of the tracer test.

From Figure 4-13, it is seen that the fiber optic spectrophotometer (Guided Wave) data matches the grab sample data until the final portion of desorption. The tracer test shown in Figure 4-14 shows good correlation between the two methods as well. Figure 4-16 also supports the thesis that fiber optic spectrophotometry can be used comparably to conventional spectrophotometry. The lack of a precise match on the tail end of the desorption portion of the experiment needs to be evaluated. Possible reasons for this discrepancy and those seen in the tracer test Figure 4-17 could be the signal processing methods for the fiber optic data, data processing methods for the grab sample data, or actual physical differences. The difference could also be as a result of adsorption onto the surfaces of the fiber optic probes or instantaneous (volume averaged) versus accumulated sampling (flux averaged) . Both the adsorption

and the flux averaged versus volume averaged explanations would produce a faster rising concentration on the step-up portion, and a slower falling concentration as measured by the fiber optic system in comparison with the grab sample method. The difference between flux averaged and volume averaged concentrations were calculated (Parker and van Genuchten, 1984) for this system and determined to be minimal. The discrepancies illustrated by these plots are not enough to significantly change the dispersion and sorption parameters that would be determined from the data sets.

Based on the similarity of the results obtained from the fiber optic method and the conventional spectroscopic method, the fiber optic spectroscopic method is superior to the conventional spectroscopic method for performing column experiments. The reasons are as follows:

1. The fiber optic method has essentially no minimum volume requirement in comparison with the conventional spectrophotometers. This allows near continuous data acquisition which would enable researchers to more accurately characterize rapidly changing column concentrations.

2. The fiber optic instrument collects data automatically. This eliminates the need for round the clock sampling as required by the conventional grab sample method. This may be the most important immediate improvement over

the conventional method because it frees the researcher from a time consuming and tedious task. Although many conventional spectrophotometers have automatic data storage capabilities and flow through attachments, they are not easily portable and the additional tubing required may introduce error by increasing the apparent dispersion in the column.

3. The fiber optic instrument can collect predetermined and multiple wavelengths automatically. Many, but not all, conventional spectrophotometers provide this feature as well. This amounts to more information available to the researcher. Wavelength scanning allows modulation spectroscopy techniques such as derivative spectroscopy. Derivative spectroscopy techniques greatly increase the value of the UV absorption method because overlapping modes can often be distinguished. This allows research on the behavior of multiple solute systems using UV absorption techniques.

4. The fiber optic instrument displays data in real time. Although this data may need to be processed, trends can be identified quickly and experimental decisions may be made "on the fly". This is an advantage over the conventional spectrophotometric method particularly when there is a long lag time between sample taking and analysis because of instrument location.

5. The fiber optic instrument has multiplexing capabilities which allows in situ sampling at multiple measurement points. This feature was not exploited in these baseline experiments because control software is needed for multiplexed data acquisition in the subsurface media column configuration used here. Multiplexing capabilities would be useful in helping to illuminate the solute behavior within a column.

6. The manufacturer claims that the fiber optic instrument is field portable. No attempt was made to verify this here. Given the verity of this claim, the potential uses for this instrument would be numerous.

7. The last and perhaps most significant advantage of this instrument is that it can be configured to perform other types of spectroscopy and sensing. The instrument consists of a source and a monochromator/detector. Each of these two separate parts has a fiber optic port. The source can be replaced or reconfigured to allow wavelength control. This would enable the instrument to perform reflection and luminescence spectroscopies. For example a spectrometer may be added to select the wavelength from the deuterium source or the deuterium lamp might be replaced by a laser. In addition, the probes linked to the instrument by the fiber optic cables can be changed to accommodate measurements that might be more appropriate to a given experimental configuration. A probe might be changed to allow evanescent

sensing or porous material sensing as described in Section 2.2.

An interesting observation that has not yet been clearly discerned in other column experiments is the oscillating behavior in the slow sorption part of the experiment (450 - 2250 minutes). This behavior is clearly seen here due to the large number of data points obtainable with the in-line, fiber optic spectrophotometer. The thesis that these fluctuations are real is supported by the correlation of the minor peaks and valleys with the more discrete grab sample data. Likely explanations for this behavior might be related to the physical characteristics of the apparatus, such as the operating characteristics of the pump used in this experiment.

4.3.5 Computer Modeling of Data

Figure 4-24 depicts the data plotted with the results from a model fit using the sorption parameters obtained from a Freundlich fit to the equilibrium distribution data described in Section 4.1.1. The computer code used here numerically solved the dual resistance model and was developed by Pedit and Miller (1988). This model uses film

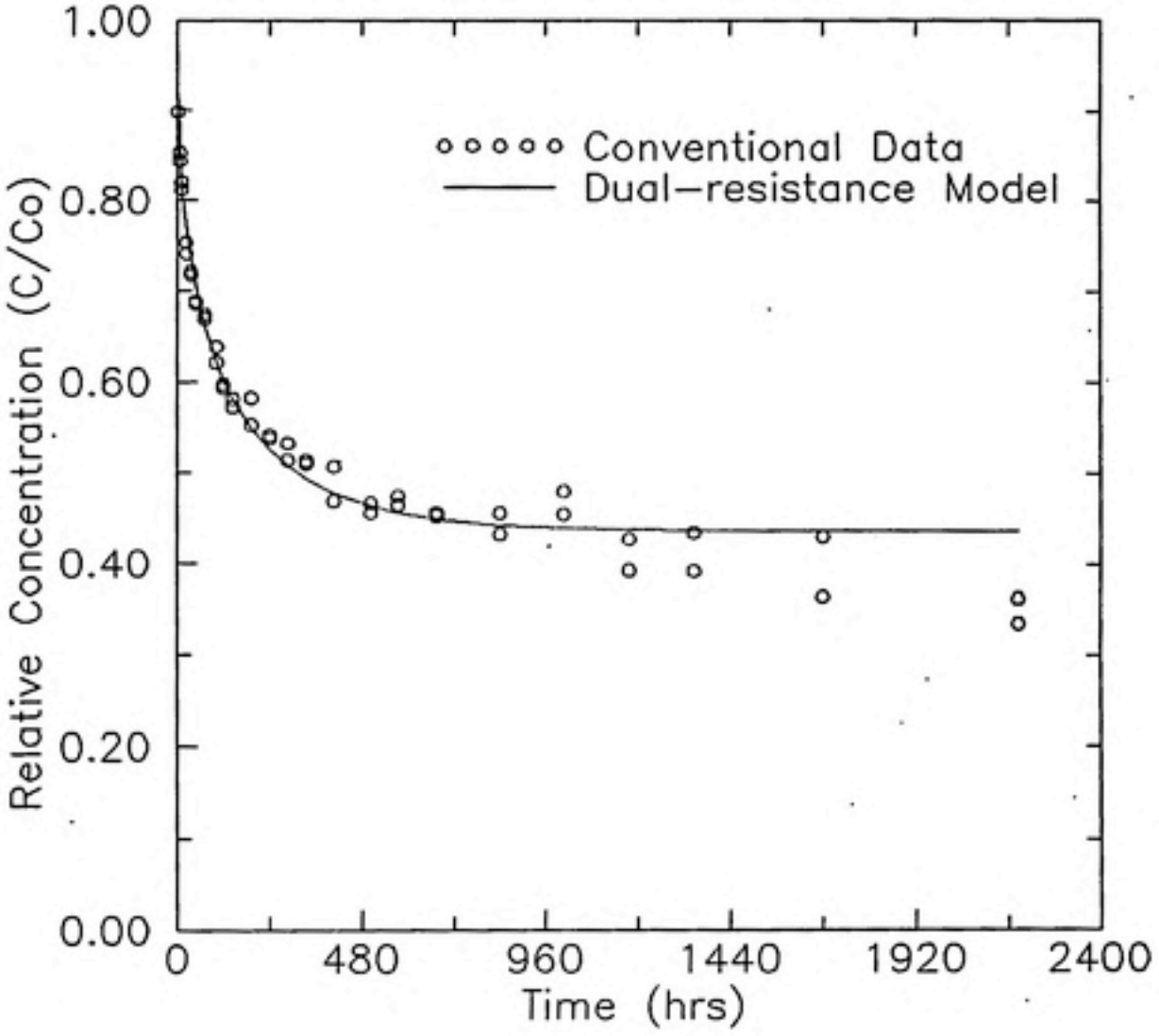

Figure 4-24 Comparison of Srp-1 data and model fit.

transfer and surface diffusion as the two impedances. For this work, surface diffusion was the rate limiting step, dominating the film transfer resistance. As can be seen in Figure 4-24, the model provides a reasonably good description of the early experimental data but not of the later data. This poor fit at later times is probably attributable to incorrect parameters supplied by the equilibrium distribution experiment, Eql-2, that was not at true equilibrium.

The Srp-2 rate study was also fit using the dual resistance model. Figure 4-25 shows the model and experimental results. Again the model fits the data well for early times but not for later times. It may be seen in this Figure that equilibrium has not been attained even after 3300 hours. This supports the findings of many researchers (Karickhoff, 1984; Coates and Elzerman, 1986; Chang, 1989; Pedit and Miller, 1990; Ball and Roberts, 1991a, 1991b; Levert, 1990) that true sorption equilibrium can take much longer to achieve than previously believed.

Figure 4-26 is a plot comparing the results of a computer simulation of the column experiment with the data obtained from the fiber optic and grab sample methods. The column experiment was simulated using a code developed by Rabideau and Miller (1990) and implemented on a Convex C240 supercomputer. The algorithm employed was based on a numerical solution for the dual resistance sorption model

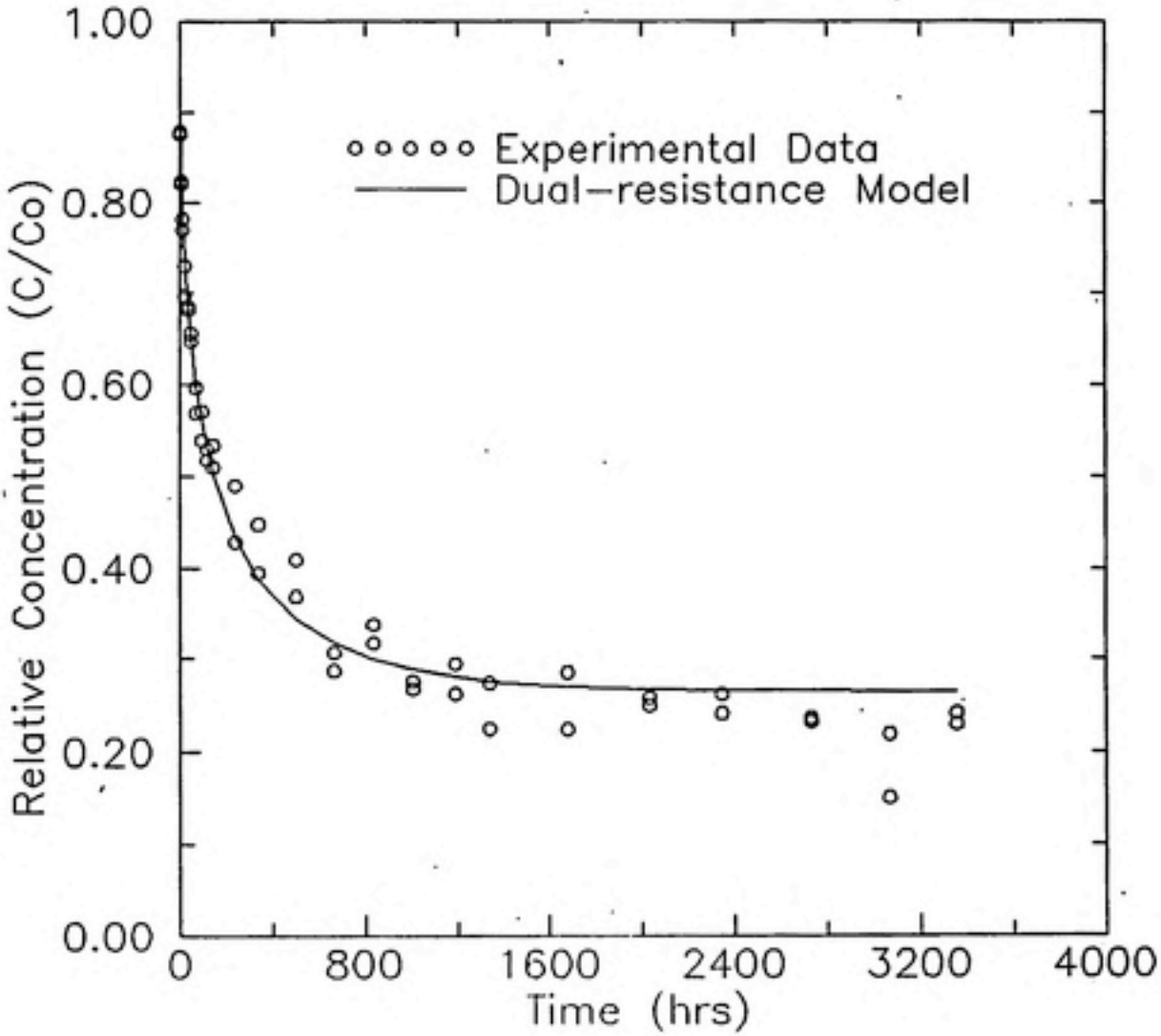

Figure 4-25 Comparison of Srp-2 data and model fit.

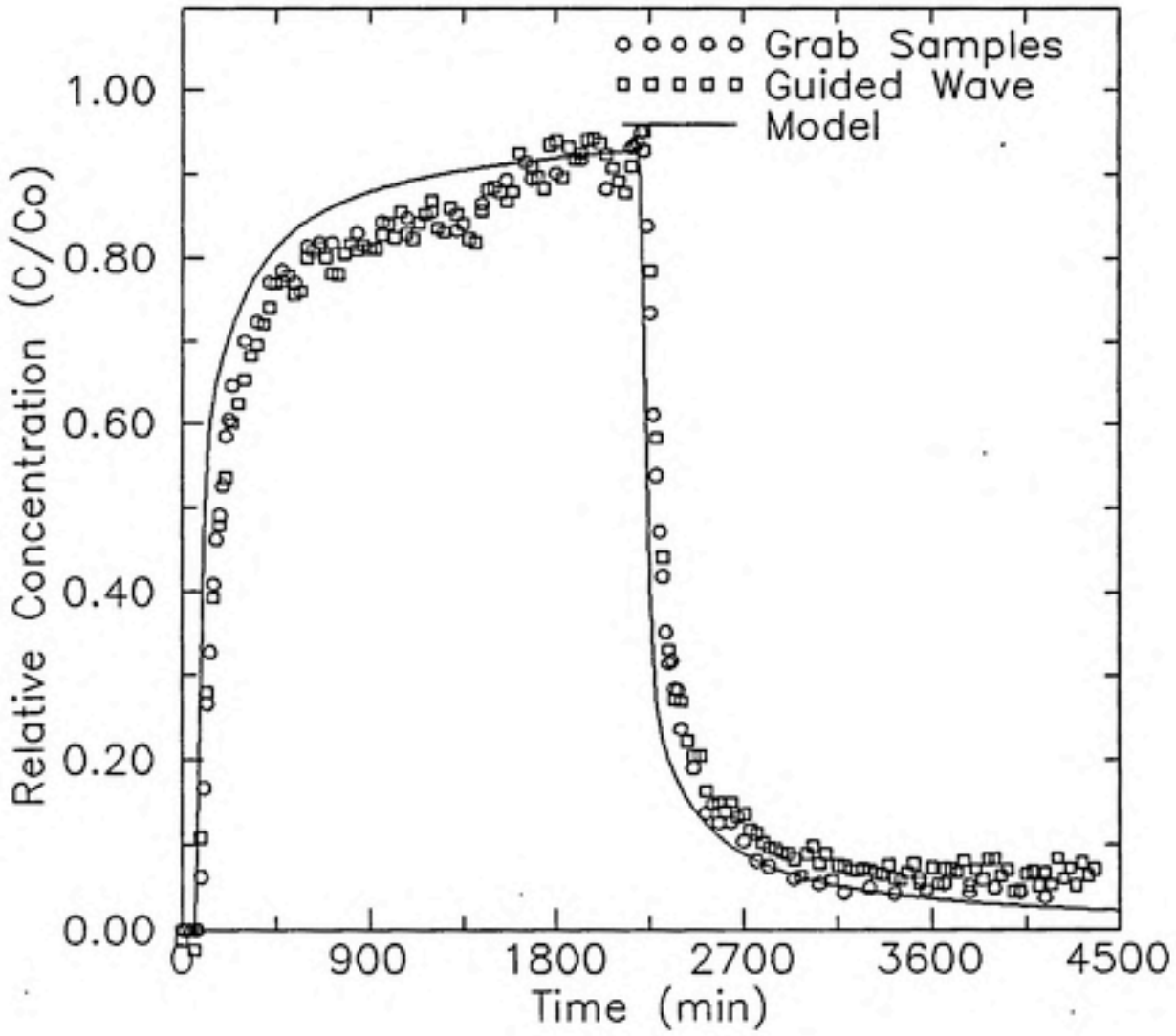

Figure 4-26 Comparison of Column-1 data with model fit.

(Miller and Weber, 1988). An operator-splitting technique was used to uncouple the fluid phase transport equations from the equations describing sorption at each spatial location. For each time increment, the transport equations were solved over half of the time step through a Petrov-Galerkin finite element scheme. The solid phase dual resistance equations were then solved over the entire time step for each spatial node, using a Galerkin finite element scheme (Pedit and Miller, 1988). The transport solution was then repeated over the second half of the time step. The model's input parameters were the Freundlich coefficient and exponent obtained from the equilibrium distribution experiment and the physical column parameters and dispersion coefficient determined from the tracer test.

From figure 4-26 it can be seen that the model does not precisely fit the data as expected given that the equilibrium distribution parameters input to the model are known to be wrong.

V CONCLUSIONS AND RECOMMENDATIONS

5.1 Conclusions

The results of this work support several conclusions regarding both the behavior of diuron in this particular subsurface media and the applicability of fiber optic spectrophotometry in experiments of this type.

5.1.1 Fiber Optic Spectrophotometry

Fiber optic spectroscopic methods used for subsurface media column sorption/desorption experiments were successful. The results from the fiber optic method matched the results from the grab sample and conventional spectroscopy method well. This is illustrated by Figures 4-13 and 4-16.

Fiber optic spectroscopic methods used for column tracer experiments were also successful as can be seen in Figures 4-14 and 4-17. The results from the fiber optic method matched the results from the grab sample method.

The two conclusions above suggest that the hypothesis that fiber optic spectrophotometry can be used to help determine some of the fate and transport parameters of

contaminants in subsurface media using a one dimensional column configuration has been proven.

5.1.2 Diuron Parameters

1. Equilibrium distribution curves obtained from not fully equilibrated experiments were more nonlinear than curves obtained by previous researchers. The Freundlich equilibrium model fit the data reasonably well.

2. Nonsingular desorption data obtained from the equilibrium distribution experiments was observed suggesting that equilibrium conditions were not met.

3. Sorption kinetic experiments support the thesis that equilibrium conditions are not attained after 140 days of equilibration.

4. Model predictions using a dual resistance model and the Freundlich parameters found from the equilibrium distribution experiments fit the early sorption kinetic data well but not the later data.

5.2 Recommendations

1. Further experimental work is necessary to evaluate the sorption/desorption parameters of diuron. Very long term equilibrium distribution experiments are required. Additional sorption/desorption batch kinetic and column work

is also required in order to help researchers determine the sorption mechanism for this and other mildly hydrophobic organic contaminants. In addition, the oscillating behavior observed in the columns should be pursued and elucidated.

2. In-bottle measurements using Suprasil™ bottles have the potential to be useful in batch experiments such as these but careful attention must be paid to the fabrication of the bottles and the physical measurement apparatus. Perhaps a Suprasil™ bottle can be fabricated which has an area with two flat, parallel sides and is still able to withstand high speed centrifugation. This would help alleviate the problems encountered with the straight cylindrical bottles.

3. Further work should be done using the fiber optic spectrophotometer. The apparatus has several operational and analytical problems, however, most of these can be defined and quantified as was demonstrated in the body of this work. Experimental work using the fiber optic spectrophotometer should include: multiple data point measurements in a column experiment using the multiplexing capabilities of the instrument; multiple solute column experiments using derivative spectroscopy techniques to discriminate overlapping modes; slower flow column experiments that more closely simulate real world ground water flows. In general, the automatic capabilities of the fiber optic spectrophotometer should be exploited to perform

more column experiments than was previously possible because of the large demand on the experimenter's time and attention that these experiments necessitated.

REFERENCES

Attaway, H. H., Camper, N. D., and Paynter, M. J. B. (1982). Anaerobic microbial degradation of diuron by pond sediment. Pesticide Biochemistry and Physiology, 17, 96-101.

Ball, W. P., and Roberts, P. V. (1991a). Long-term sorption of halogenated organic chemicals by aquifer material. 1. Equilibrium. Environmental Science and Technology, 25, 1223-1237.

Ball, W. P., and Roberts, P. V. (1991b). Long-term sorption of halogenated organic chemicals by aquifer material. 1. Intraparticle diffusion. Environmental Science and Technology, 25, 1237-1249.

Bear, J. (1979). Hydraulics of Groundwater. New York: McGraw-Hill Book Company.

Bowman, B. T., and Sans, W. W. (1985). Partitioning Behavior of Insecticides in Soil-Water Systems: II. Desorption

Hysteresis Effects. Journal of Environmental Quality, v14, 2, 270-273.

Bright, F. V., and Litwiler, K. S. (1989). Multicomponent fluorometric analysis using a fiber-optic probe. Analytical Chemistry, 61, 1510-1513.

Brusseau, M. L., Jessup, R. E., and Rao, P. S. C. (1989). Modeling the transport of solutes influenced by multiprocess nonequilibrium. Water Resources Research, 25, 1971-1988.

Brusseau, M. L., Jessup, R. E., and Rao, P. S. C. (1991). Nonequilibrium sorption of organic chemicals: Elucidation of rate-limiting processes. Environmental Science and Technology, 25, 134-142.

Brusseau, M. L., and Rao, P. S. C. (1989a). The influence of sorbate-organic matter interactions on sorption nonequilibrium. Chemosphere, 18, 1691-1706.

Brusseau, M. L., and Rao, P. S. C. (1989b). Sorption nonideality during organic contaminant transport in porous media. Critical Reviews in Environmental Control, 19, 33-99.

Butler, M. A., and Ginley, D. S. (1988). Hydrogen sensing with palladium-coated optical fibers. Journal of Applied Physics, 64, 3706-3712.

Cameron, D. R., and Klute, A. (1977). Convective-dispersive solute transport with a combined equilibrium and kinetic adsorption model. Water Resources Research, 13, 183-188.

Carey, W. P., DeGrandpre, M. D., and Jorgensen, B. S. (1989). Polymer-coated cylindrical waveguide absorption sensor for high acidities. Analytical Chemistry, 61, 1674-1678.

Carroll, M. K., Bright, F. V., and Hieftje, G. M. (1989). Fiber-optic time-resolved fluorescence sensor for the simultaneous determination of Al^{3+} and Ga^{3+} or In^{3+}. Analytical Chemistry, 61, 1768-1772.

Cavinato, A. G., Mayes, D. M., Ge, Z., and Callis, J. B. (1990). Noninvasive method for monitoring ethanol in fermentation processes using fiber-optic near-infrared spectroscopy. Analytical Chemistry, 62, 1977-1982.

Chang, R. (1971). Basic Principles of Spectroscopy. New York: McGraw-Hill Book Co..

Chang, S-L. J. (1989). Sorption-desorption of diuron in subsurface systems: An investigation of desorption hysteresis. Unpublished master's thesis. University of North Carolina, Chapel Hill.

Chen, H-L. (1987). Applications of laser absorption spectroscopy. In Radziemski, L. J., Solarz, R. W., and Paisner, J. A. (Eds.), Laser spectroscopy and its applications (pp. 261-350). New York: Marcel Dekker, Inc.

Chow, K. M., Stansfield, A. G., Carr, R. J. G., Rarity, J. G., and Brown, R. G. W. (1988). On-line photon correlation spectroscopy using fibre-optic probes. J. Phys. E: Sci. Instrum., 21, 1186-1190.

Chudyk, W., Pohlig, K., Rico, N., and Johnson, G. (1988). Ground water monitoring using laser fluorescence and fiber optics. In Lieberman, R. A., and Wlodarczyk, M. T. (Eds.), Chemical, biochemical, and environmental applications of fibers (pp.45-47). Bellingham, WA: Proceedings SPIE 990.

Chudyk, W. (1989). Field screening of hazardous waste sites. Environmental Science and Technology, 23, 504-507.

Coates, J. T., and Elzerman, A. W. (1986). Desorption kinetics for selected PCB congeners from river sediments. Journal of Contaminant Hydrology, 1, 191-200.

Conforti, G., Brenci, M., Mencaglia, A., and Mignani, A. G. (1989). Fiber-optic thermometric probe utilizing GRIN lenses. Applied Optics, 28, 577-580.

Cooney, D. O., Adesanya, B. A., and Hines, A. L. (1983). Effect of particle size distribution on adsorption kinetics in stirred batch systems. Chemical Engineering Science, 38, 1535-1541.

Curl, R. L., and Keoleian, G. A. (1984). Implicit-adsorbate model for apparent anomalies with organic adsorption on natural adsorbents. Environmental Science and Technology, 18, 916-922.

Daly, J. C. (1984). Introduction. In Daly, J. C. (Ed.), Fiber Optics (pp. 1-20). Boca Raton, Fla: CRC Press Inc.

Dickert, F. L., Schreiner, S. K., Mages, G. R., and Kimmel, H. (1989). Fiber-optic dipping sensor for organic

solvents in wastewater. Analytical Chemistry, 61, 2306-2309.

Di Toro, D. M. (1985). A particle interaction model of reversible organic chemical sorption. Chemosphere, 14, 1503-1538.

Edwards, H. O., Jedrzejewski, K. P., Laming, R. I., and Payne, D. N. (1989). Optical design of optical fibers for electrical measurement. Applied Optics, 28, 1977-1979.

Fuh, M-R. S., Burgess, L. W., and Christian, G. D.(1988). Single fiber-optic fluorescence enzyme-based sensor. analytical Chemistry, 60, 433-435.

Gabor, G., and Walt, D. R. (1991). Sensitivity enhancement of fluorescent pH indicators by inner filter effects. Analytical Chemistry, 63, 793-796.

Gilson, T. R., Hendra, P. J. (1970). Laser Raman Spectroscopy. London, U.K.: Wiley-Interscience.

Goldberg, M. C., Weiner, E. R. (1989). Introduction. In M. C. Goldberg (Ed.), Luminescence Applications in

Biological, Chemical, Environmental and Hydrological Sciences, A.C.S. Symposium Series 383 (pp. 1-22). Washington, D.C.: American Chemical Society.

Goltz, M. N., and Roberts, P. V. (1986). Interpreting organic solute transport data from a field experiment using physical nonequilibrium models. Journal of Contaminant Hydrology, 1, 77-93.

Gschwend, P. M., and Wu, S-C. (1985). On the constancy of sediment-water partition coefficients of hydrophobic organic pollutants. Environmental Science and Technology, 19, 90-96.

Gunasingham, H., Tan, C., and Seow, J. K. L. (1990). Fiber-optic glucose sensor with electrochemical generation of indicator reagent. Analytical Chemistry., 62, 755-759.

Hawthorne, A. R., Morris, S. A., Moody, R. L., and Gammage, R. B. (1984). DUVAS as a real-time, field-portable wastemonitor for phenolics. Journal of Environmental Science and Health, A19(3), 253-266.

Herron, N. R., and Whitehead, D. W. (1988). Evolution of a fiber-optic chemical fluorescence sensor for monitoring dissolved volatiles. In Lieberman, R. A., and

Wlodarczyk, M. T. (Eds.), Chemical, biochemical, and environmental applications of fibers (pp.37-44). Bellingham, WA: Proceedings SPIE 990.

Hill, G. D., McGahen, J. W., Baker, H. M., Finnerty, D. W., and Bingeman, C. W. (1955). The fate of substituted urea herbicides in agricultural soils. Agronomy Journal, 47, 93-104.

Janata, J. (1989). Principles of Chemical Sensors, New York: Plenum Press.

Jones, T. P., and Porter, M. D. (1988). Optical pH sensor based on the chemical modification of a porous polymer film. Analytical Chemistry, 60, 404-406.

Karickhoff, S. W. (1984). Organic pollutant sorption in aquatic systems. Journal of Hydraulic Engineering, 110, 707-735.

Karstang, T. V., and Kvalheim, O. M. (1991). Multivariate prediction and background correction using local modeling and derivative spectroscopy. Analytical Chemistry, 63, 767-772.

Khan, S. U., Marriage, P. B., and Saidak, W. J. (1976). Weed Science, 24, 583-586.

Kinniburgh, D. G. (1986). General purpose adsorption isotherms. Environmental Science and Technology, 20, 895-904.

Koskinen, W. C., O'Connor, G. A., and Cheng, H. H. (1979). Characterization of hysteresis in the desorption of 2,4,5-T from soils. Soil Science Society of America Journal, 43, 871-874.

Kuhn, L. S., Weber, A., and Weber, S. G. (1990). Microring electrode/optical waveguide: electrochemical characterization and application to electrogenerated chemiluminescence. Analytical Chemistry, 62, 1631-1636.

Kulp, T. J., Camins, I., Angel, S. M., Munkholm, C., and Walt, D. R. (1987). Polymer immobilized enzyme optrodes for the detection of penicillin. Analytical Chemistry, 59, 2849-2853.

Kulp, T. J., Bishop, D., and Angel, S. M. (1988). Column-profile measurements using fiber-optic spectroscopy. Soil Science Society of America Journal, 52, 624-627.

Laguesse, M. (1988). An optical fibre refractometer for liquids using two measurement channels to reject optical attenuation. J. Phys. E: Sci. Instrum., 21, 64-67.

Leugers, M. A., and McLachlan, R. D. (1988). Remote analysis by fiber optic raman spectroscopy. In Lieberman, R. A., and Wlodarczyk, M. T. (Eds.), Chemical, biochemical, and environmental applications of fibers (pp.88-95). Bellingham, WA: Proceedings SPIE 990.

Levert, A. M. (1990). Investigation of competitive sorption of hydrophobic organic contaminants on subsurface materials. Unpublished master's thesis. University of North Carolina, Chapel Hill.

Lewis, E. N., Kalasinsky, V. F., and Levin, I. W. (1988). Near-infrared fourier transform raman spectroscopy using fiber-optic assemblies. Analytical Chemistry, 60, 2658-2661.

Lieberman, R. A., and Brown, K. E. (1988). Intrinsic fiber optic chemical sensor based on two-stage fluorescence coupling. In Lieberman, R. A., and Wlodarczyk, M. T. (Eds.), Chemical, biochemical, and environmental

applications of fibers (pp.104-110). Bellingham, WA: Proceedings SPIE 990.

Louch, J., and Ingle, J. D. (1988). Experimental comparison of single- and double-fiber configurations for remote fiber-optic fluorescence sensing. Analytical Chemistry, 60, 2537-2540.

Luo S., and Walt, D. R. (1989a). Fiber-optic sensors based on reagent delivery with controlled-release polymers. Analytical Chemistry , 61, 174-177.

Luo S., and Walt, D. R. (1989b). Avidin-biotin coupling as a general method for preparing enzyme-based fiber-optic sensors. Analytical Chemistry , 61, 1069-1072.

McCarty, P. L., Reinhard, M., and Rittman, B. E. (1981). Trace organics in groundwater. Environmental Science and Technology, 15, 1, 40-51.

McCreery, R. L., Fleischmann, M., and Hendra, P. (1983). Fiber optic probe for remote raman spectroscopy. Analytical Chemistry, 55, 146-148.

Mercer, J. W., Skipp, D. C., and Giffin, D. (1990). Basics of pump-and-treat ground-water remediation technology

(Report No. EPA-600/8-90/003). Cincinnati, OH: U.S. Environmental Protection Agency, Center for Environmental Research.

Miller, C. T., and Weber, W. J., Jr. (1986). Sorption of hydrophobic organic pollutants in saturated soil systems. Journal of Contaminant Hydrology, 1, 243-261.

Miller, C. T., and Weber, W. J., Jr. (1988). Modeling the sorption of hydrophobic contaminants by aquifer materials -- II. Column reactor systems. Water Research, 22, 465-474.

Mustafa, M. A., and Gamar, Y. (1972). Adsorption and desorption of diuron as a function of soil properties. Soil Science Society of America Proceedings, 36, 561-565.

Nkedi-Kizza, P., Rao, P. S. C., Jessup, R. E., and Davidson, J. M. (1982). Ion exchange and diffusive mass transfer during miscible displacement through an aggregated Oxisol. Soil Science Society of America Journal, 46, 471-476.

Olsen, R. G., and Rogers, D. A. (1984). Propagation in optical fibers. In Daly, J. C. (Ed.), Fiber Optics (pp. 51-79). Boca Raton, Fla: CRC Press Inc.

Parker, J. C., and van Genuchten, M. Th. (1984). Flux-averaged and volume-averaged concentrations in continuum approaches to solute transport. Water Resources Research, 20, 866-872.

Patterson, C. W. (1987). Semiclassical principles of atomic and molecular spectra. In Radziemski, L. J., Solarz, R. W., and Paisner, J. A. (Eds.), Laser spectroscopy and its applications (pp. 1-90). New York: Marcel Dekker, Inc.

Pedit, J. A., and Miller, C. T. (1988). The advantage of high-order basis functions for modeling multicomponent sorption kinetics. Computational Methods in Water Resources, Vol. 1, (pp.293-298). Southampton, U.K.: Computational Mechanics Publications.

Pedit, J. A., and Miller, C. T. (1990). An investigation of apparent sorption-desorption hysteresis phenomena. EOS, Transactions, American Geophysical Union, 71, 1301.

Peterson, J. I. (1988). Fiber optic chemical sensor development. In Lieberman, R. A., and Wlodarczyk, M. T. (Eds.), Chemical, biochemical, and environmental applications of fibers (pp.2-17). Bellingham, WA: Proceedings SPIE 990.

Rabideau, A. J., and Miller, C. T. (1990). Evaluation of an operator-splitting method for approximating a diffusional sorption process. In, EOS Transactions, American Geophysical Union (pp.521). American Geophysical Union.

Rao, P. S. C., Davidson, J. M., Jessup, R. E., and Selim, H. M. (1979). Evaluation of conceptual models for describing nonequilibrium adsorption-desorption of pesticides during steady-flow in soils. Soil Science Society of America Journal, 43, 22-28.

Rasmuson, A. (1985). The effect of particles of variable size, shape, and properties on the dynamics of fixed beds. Chemical Engineering Science, 40, 621-629.

Reichert, W. M., Ives, J. T., and Suci, P. A. (1987). Emission spectroscopy utilizing an air-cooled argon laser and an optrode-based UV-Vis spectrophotometer: A scaled-down laser spectroscopy configuration for

solution-phase fiber optic sensing. Applied Spectroscopy, 41, 1347-1350.

Renn, C. N., and Synovec, R. E. (1990). Single optical fiber, position-sensitive detector-based multiwavelength absorbance spectrophotometer. Analytical Chemistry, 62, 558-564.

Ross, H. B., and McClain, W. M. (1981). Liquid core optical fibers in raman spectroscopy. Applied Spectroscopy, 35, 439-442.

Sabljić, A. (1987). On the prediction of soil sorption coefficients of organic pollutants from molecular structure: Application of molecular topology model. Environmental Science and Technology, 21, 358-366.

Schiffman, A. (1988). Ground-water contamination -- a regulatory framework. Ground Water, 26, 554-558.

Schwab, S. D., and McCreery, R. L. (1984). Versatile, efficient raman sampling with fiber optics. Analytical Chemistry, 56, 2199-2204.

Seitz, W. R. (1984). Chemical sensors based on fiber optics. Analytical Chemistry, 56, 16A-34A.

Shakhsher, Z. M., and Seitz, W. R. (1990). Optical detection of cationic surfactants based on ion pairing with an environment-sensitive fluorophor. Analytical Chemistry, 62, 1758-1762.

Silverstein, R. M., Bassler, G. C., and Morril, T. C. (1974). Spectrometric Identification of Organic Compounds (3rd ed.). New York: John Wiley and Sons.

Tenge, B., Buchanan, B. R., and Honigs, D. E. (1987). Calibration in the fiber optic region of the near-infrared. Applied Spectroscopy, 41, 779-785.

Thorne, A. P. (1988). Spectrophysics (2nd ed.). New York: Chapman and Hall.

Van Dyke, D. A., and Cheng, H-Y (1988). Fabircation and characterization of a fiber-optic-based spectroelectrochemical probe. Analytical Chemistry, 60, 1256-1260.

van Genuchten, M. Th., Wierenga, P. J., and O'Connor, G. A. (1977). Mass transfer studies in sorbing porous media: III. Experimental evaluation with 2,4,5-T. Soil Science Society of America Journal, 41, 278-285.

Walrafen, G. E., and Stone, J. (1972). Intensification of spontaneous raman spectra by use of liquid core optical fibers. Applied Spectroscopy, 26, 585-589.

Weber, J. B., and Miller, C. T. (1989). Organic chemical movement over and through soil. In B. L. Sawhney and K. Brown (Eds.), Reactions and movement of organic chemicals in soils (pp. 305-334). Madison, WI: Soil Science Society of America, Inc. and American Society of Agronomy, Inc.

Weber, W. J., and Miller, C. T. (1988). Modeling the sorption of hydrophobic contaminants by aquifer materials--I. Rates and equilibria. Water Research, 22,457-464.

Wilkinson, L. (1988). SYSTAT: The system for statistics (4th ed.) [Computer program]. Evanston, IL: SYSTAT, Inc.

Worthing, C. R., and Walker, S. B. (1983). The pesticide manual (7th ed.). Lavenham, Suffolk, England: The British Crop Protection Council.

Zhou, Q., Shahriari, M. R., Kritz, D., and Sigel, G. H. (1988). Porous fiber-optic snesor for high-sensitivity

humidity measurements. Analytical Chemistry, 60, 2317-2320.

Zhou, Q., Kritz, D., Bonnell, L., and Sigel, G. H. (1989). Porous plastic optical fiber sensor for ammonia measurement. Applied Optics, 28, 2022-2025.

Zung, J. B., Woodlee, R. L., Fuh, M-R. S., Warner, I. M. (1988). Fiber optic based multidimensional fluorometer for studies of marine pollutants. In Lieberman, R. A., and Wlodarczyk, M. T. (Eds.), Chemical, biochemical, and environmental applications of fibers (pp.49-54). Bellingham, WA: Proceedings SPIE 990.